WRIA 1 Watershed Management Project
Phase III, Task 4.1 report

Surface Water Quantity Model Development and Calibration

by David G Tarboton
(with input from Ross Woods, Irina Tcherednichenko)

Utah Water Research Laboratory
Utah State University

December 2007

Table of Contents

Abstract

This report describes the development and calibration of the surface water quantity model developed as part of the Water Resources Inventory Area (WRIA) 1 Watershed management project. An enhanced version of the TOPNET rainfall runoff model was applied to the WRIA 1 study area. TOPNET is a distributed hydrologic model with basic model elements being topographically delineated drainages that discharge into the stream network that is then used to route flow to the outlet. Within each drainage, an enhanced version of the TOPMODEL rainfall runoff model is used to compute runoff from precipitation and other weather inputs. The enhanced TOPNET includes additional processes such as irrigation, artificial drainage, and impervious areas, as well as enhanced snowmelt and evaporation calculations, and provides a means for integrated simulation of water management, including demand estimation, in-stream flow requirements, and users with differing rights to take water when it is scarce. These new features were specifically added to address the water resource management issues in the Nooksack River basin in WRIA 1 where there is significant potential and actual competition for water resources among water users, and between consumptive users and in-stream environmental requirements. In addition, human activities can significantly alter the water balance of catchments, again having significant potential effects on stream ecosystems, through changes in both water quantity (habitat availability) and water quality (nutrients, temperature). The balance between supply and demand for water in a river basin can be intricate, and may vary significantly both within and between years. Simulation modeling is one way of quantifying the likely implications of proposed water management regimes, in such complex settings. Although the project as a whole also included modeling of water quality, modeling of fish habitat, and development of a decision support system, this report covers only the water quantity modeling.

Introduction

The purpose of this project was to develop a model that could assist the watershed planning process in Water Resources Inventory Area (WRIA) 1 in the State of Washington. This project was completed in three phases:

1. Phase I, Work plan development
2. Phase II, Preliminary data collection
3. Phase III, Technical studies involving model and decision support system development

The surface water quantity component of phase III comprised two tasks:

1. Task 4.1: Develop and Implement Surface Water Quantity Model Components and Integrate into the DSS
2. Task 4.2: Validation of Model through Analyses of Scenarios

This is the final report on the development and calibration of the surface water quantity model developed under task 4.1. A separate report describes the validation and analysis of scenarios work of task 4.2.

An enhanced version of the TOPNET rainfall runoff model (Bandaragoda et al., 2004; Ibbitt and Woods, 2004) was applied to the 3600 km^2 Nooksack river basin that comprises the WRIA 1 study area. TOPNET is a distributed hydrologic model with basic model elements being topographically delineated drainages that discharge into the stream network that is then used to route flow to the outlet. Within each drainage an enhanced version of the TOPMODEL rainfall runoff model (Beven and Kirkby, 1979; Beven et al., 1995a) is used to compute runoff from precipitation and other weather inputs. The enhanced TOPNET includes additional processes such as irrigation, artificial drainage, impervious areas, snowmelt and evaporation calculations, and provides a means for integrated simulation of water management, including demand estimation, in-stream flow requirements, and users with differing rights to take water when it is scarce. The capabilities of the surface water quantity model include the ability to evaluate and compare scenarios across management options including: (a) water use changes, such as the ability to add new uses and to interchange Surface Water and Ground Water uses; (b) land use changes, such as accounting for development and the ability to adjust irrigation efficiency; (c) allow different water use rates; (d) augmentation of surface water flows in any user-defined period (of particular interest for low-flow conditions); (e) representation of trans-drainage diversions and surface storage facilities; and (f) water rights enforcement.

The TOPNET model was applied to the 3600 km^2 Nooksack basin by first assembling the datasets for climate, land use, topography and soils, and creating a model with initial estimates for all model parameters. Precipitation data in the headwaters is measured only very sparsely, and considerable effort was required to represent the observed water balance in this part of the basin. Since few management options impact the generation of runoff in the headwater areas, capability was added to the model to take measured streamflow from these upstream areas as input, focusing the modeling effort on the managed areas to address management scenarios and questions.

Substantial effort was also required to create the 172 model elements that precisely matched the drainages delineated by WRIA 1 (Figure 1). These WRIA 1 delineated drainages are the fundamental modeling elements and dictate the scale at which information is resolved in the model. The irrigated proportions of each model element were determined from GIS data, and similar information was extracted for artificially drained areas. Demand for water was estimated based on land use and population information. The model was calibrated to several subsets of the measured flow data for about 30 sites in the basin, some with records dating back to the 1940s. Once a reasonable spatially interpolation for rainfall data was obtained, the key parameter requiring calibration was the TOPMODEL *f* parameter, which controls the responsiveness of the subsurface store representing the shallow aquifer. Satisfactory to excellent calibrations were obtained for all but 5 sites, without making use of any site-specific calibration. All model calibration used simultaneous adjustment in all model elements of a given parameter (say *f*) by a parameter multiplier. This ensured that the spatial patterns in the initial GIS-derived datasets for each parameter were maintained.

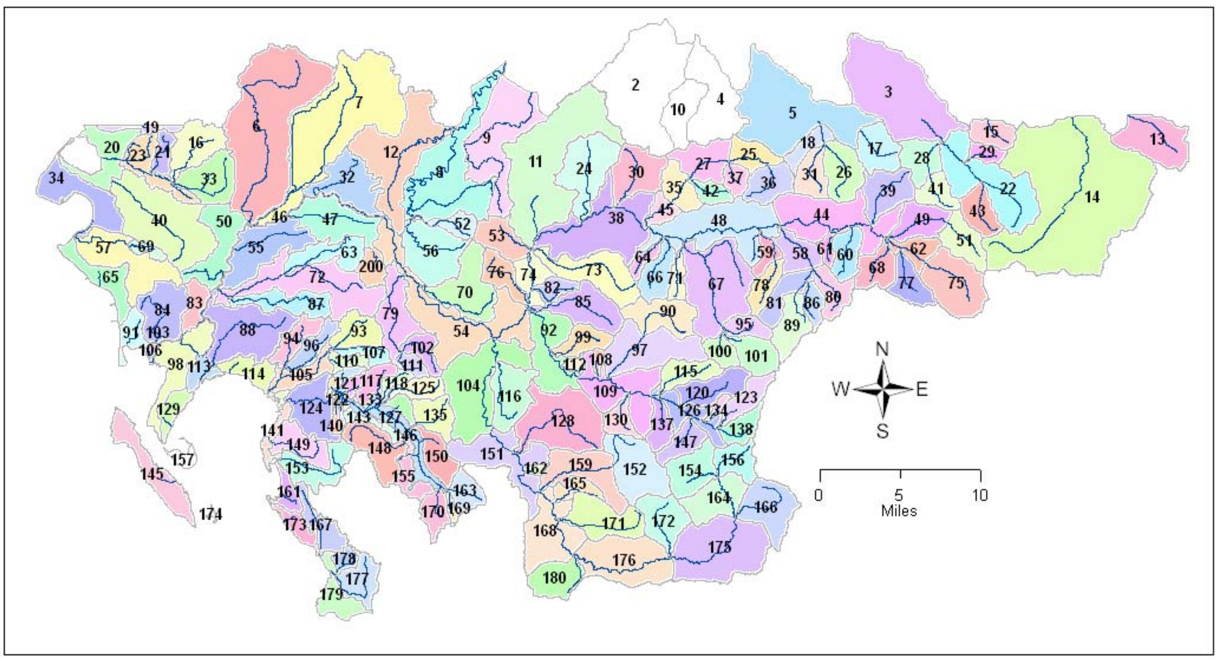

Figure 1. WRIA 1 drainages used as TOPNET Model elements. There are 177 WRIA 1 drainages, numbered according to the WRIA 1 drainage numbering system shown. Only the 172 of these that included delineated streams were modeled. These are shaded in the figure. The drainages not modeled were: Cultus (2), East Fork Luimchen (4), West Fork Luimchen (10), Portage Island (157) and Eliza Island (174)

In this report we first describe how the model and each of its components work. We then describe the model inputs and the preparation of input data. This is followed by a description of how the model was calibrated. This report ends with a section describing how to use the model.

Model Description

TOPNET was developed by combining TOPMODEL (Beven and Kirkby, 1979; Beven et al., 1995a), which is most suited to small watersheds, with channel routing so as to have a modeling system that can be applied over large watersheds using smaller subbasins within the large watershed as model elements. Enhancements that we have added include: (1) calculation of reference evapotranspiration using the Penman-Monteith method (e.g., Jensen et al., 1990); (2) calculation of snowmelt using the Utah Energy Balance Snowmelt model (Tarboton et al., 1995a); (3) the partition of model elements into separate components representing irrigated and non-irrigated areas; (4) artificial drainage to represent the effect of ditch and tile drained areas on the runoff response; (5) the partition of the model elements into pervious and impervious areas to allow representation of urban areas; (6) plumbing options for the diversion and storage of water under different management options; and (7) components to calculate water use and implement water rights rules.

Spatial Discretization

As indicated in Figure 1, the WRIA 1 drainages are the model elements that control the scale at which modeled processes are represented. The selection of these elements has fundamental impact on the model and results, because with a few exceptions, all information is represented as averages over these model elements. Input information such as model parameters, land use fractions, soil and vegetation properties, artificial drainage coefficients, water uses and other management actions are all expressed at the scale of a drainage and are modeled to occur over the drainage or at the mass balance node at the outlet of the drainage. As a result of this scale, the model can not quantify the effect of specific within drainage choices such as specific land use change or irrigation options, or the specific location of a diversion within a drainage. If quantification at a scale smaller than the input drainages is required, then the model should be re-configured and re-run with different model elements. There are two exceptions to the drainage being the smallest unit at which information is represented: (1) due to irrigation and artificial drainage, and (2) due to differences in the topographic wetness index.

Within each drainage there is a fraction of area that is irrigated, with the remaining area not irrigated. Within each drainage there is also a fraction of the area subject to artificial drainage through tile drains and a separate fraction of the area subject to artificial drainage by ditch drains. This results in six configurations (Table 1) from the combination of the two irrigation and three artificial drainage choices.

Table 1. Irrigation and Artificial Drainage configurations

	No Artificial Drainage	Tile Drained	Ditch Drained
Irrigation	1	2	3
No Irrigation	4	5	6

The fraction of area occupied by each configuration within each drainage is evaluated, and if greater than 0, the model is run separately for that configuration. Results are then combined based on an area weighting of these combinations.

The second exception to the drainage being the smallest model element is a distribution of TOPMODEL wetness index classes. TOPMODEL (Beven and Kirkby, 1979; Beven et al., 1995a) characterizes the relative saturation based on a wetness index, $\ln(a/\tan\beta)$ where 'a' is specific catchment area and β is the slope angle. The wetness index is evaluated at each digital elevation model (DEM) grid cell within each model element. The set of values obtained is grouped into on the order of 50 wetness index classes within each model element, each of which is presumed to behave similarly and the depth to water table and potential for saturation excess runoff is evaluated separately for each class.

Time Step

The basic time step for the application of TOPNET to WRIA 1 is one day. This is primarily to allow comparison to USGS streamflow data which is available at a daily time step. Input meteorological data is also available at one day time steps. Snowmelt is driven by energy inputs comprised significantly of solar radiation. The snowmelt response is threshold driven and nonlinear. For snow it is therefore important to capture the diurnal cycle. Within the snow component the time step is reduced to four hours. The diurnal temperature range, together with daily average temperature are used to specify inputs on a sine curve with daily maximum at 3 pm and daily minimum at 3 am. Other snowmelt model inputs (dew point, wind, precipitation) are held constant through the day with the model calculating solar radiation based on time of day, time of year, latitude and longitude.

Element Model

Figure 2 gives the overall flow of information in the integrated TOPNET model as applied at each model element. The functionality of the model is categorized into four major components:

1. Rainfall-Runoff Transformation
2. Potential Evapotranspiration
3. Snow
4. Water Management

Within these categories there are subcomponents as depicted in Figure 2. To understand how the model works, we will start at the top. Time series inputs are precipitation, air temperature, wind, and air humidity. On the right, precipitation is an input to the snow component and is first separated into rain or snow based upon temperature. Rain enters the Rainfall-Runoff Transformation component, while snow enters the Snow subcomponent. The Snow subcomponent keeps track of snow water equivalent and energy content, computing energy fluxes from temperature, wind and humidity producing snowmelt output that enters the Rainfall-Runoff Transformation component. Surface water input from snowmelt is treated in the Rainfall-Runoff component the same way that rainfall is treated. The other weather inputs (temperature, wind, and humidity) are also used to compute the potential evapotranspiration, which is an input to the Rainfall-Runoff Transformation. The arrow in Figure 2 is upwards from Rainfall-Runoff Transformation to potential evapotranspiration because that is the direction of the evapotranspiration water flux.

Within the Rainfall-Runoff Transformation there are five subcomponents: canopy interception store, vadose zone soil store, groundwater saturated zone, channel flow and artificial drainage. Surface water input to the canopy interception store comprises rainfall and snowmelt as well as sprinkler irrigation. Potential evapotranspiration is first satisfied from the canopy interception store. Throughfall is computed based upon the canopy interception capacity, surface water input, and water in canopy storage and is taken as input to the vadose zone soil store. Potential Evapotranspiration not satisfied from the interception store becomes potential evapotranspiration from the vadose zone soil store. Drip irrigation is also an input to the vadose zone soil store. Based on the input and storage in the vadose zone soil store recharge to groundwater and surface runoff is calculated. The vadose zone soil store also provides the facility for artificial drainage, representing ditch and tile drains that remove water directly from the vadose zone soil store to channels. The vadose zone soil store calculation also accounts for potential upwelling from groundwater where the water table is shallow. The groundwater saturated zone calculations account for recharge, upwelling and groundwater pumping and produce baseflow as an output. Baseflow and surface runoff from the vadose zone soil store are combined to calculate channel flow.

The Water Management component depicted on the right of Figure 2 is comprised of subcomponents for irrigation, withdrawals, non-irrigation users and return flows. Irrigation may be either sprinkler or drip. Sprinkler irrigation enters the Rainfall-Runoff Transformation above the canopy interception store because it is subject to interception, while drip irrigation directly enters the vadose zone soil store. Withdrawals are either from surface water, taken from channel flow, or groundwater, taken from the groundwater saturated zone. Return flows from non-irrigation users may be to surface channels or groundwater.

The following subsections give details of how the processes are modeled in each component and sub-component.

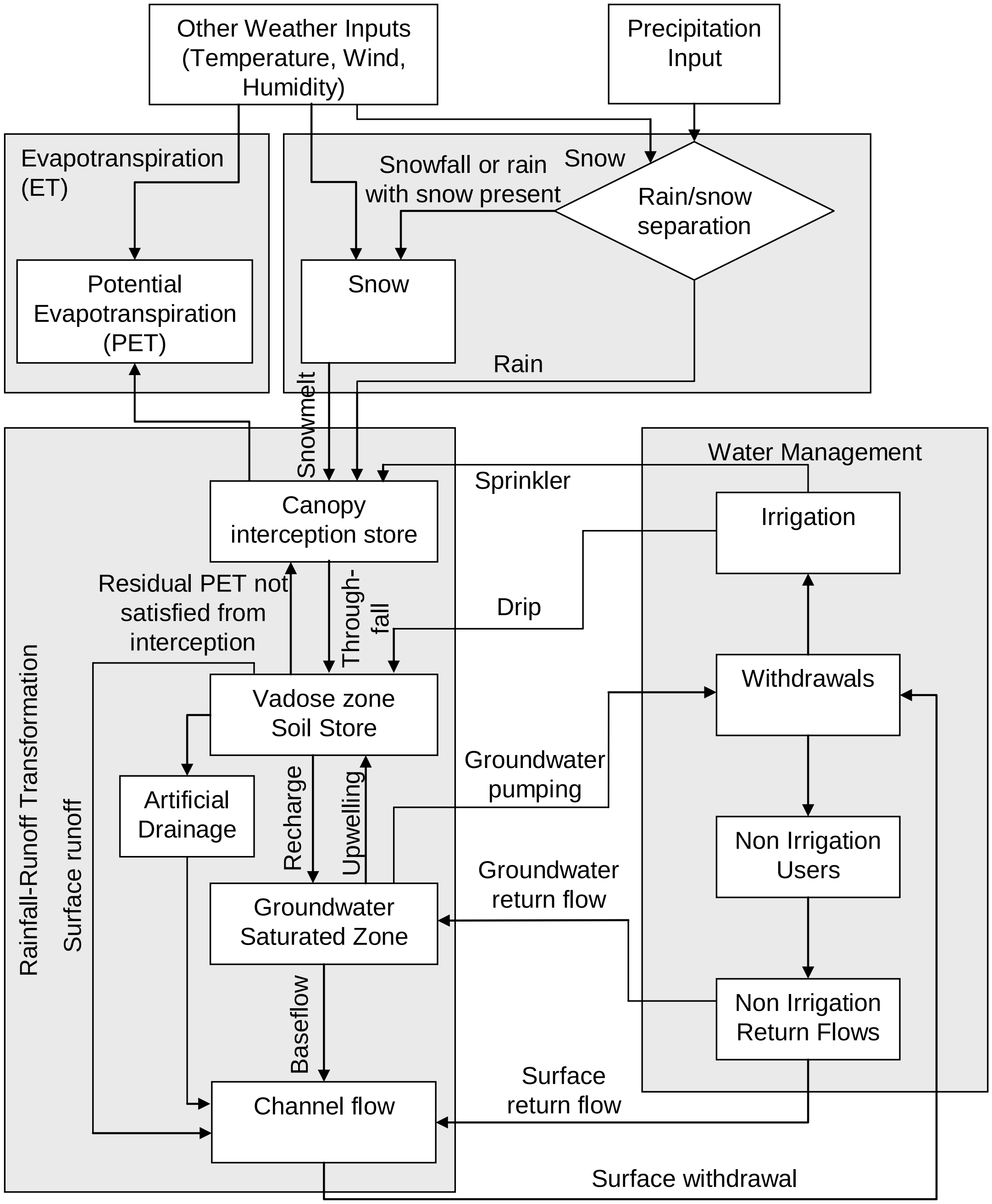

Figure 2. Overall Model Schematic

Precipitation-Runoff Transformation

The Precipitation-Runoff Transformation component of TOPNET used here was based largely upon the version of TOPNET that we used in the Distributed Model Intercomparison Project (Bandaragoda et al., 2004) with the addition of the capability for the representation of artificial drainage and with the coupling to snow and water management components. Much of the description that follows is excerpted from Bandaragoda et al. (2004).

A key contribution of TOPMODEL is the parameterization of the soil moisture deficit (depth to water table) using a topographic index to model the dynamics of variable source areas contributing to saturation excess runoff. Beven et al. (1995a) indicate that "TOPMODEL is not a hydrological modeling package. It is rather a set of conceptual tools that can be used to reproduce the hydrological behavior of catchments in a distributed or semi-distributed way, in particular the dynamics of surface or subsurface contributing areas." The Precipitation-Runoff Transformation component of TOPNET uses TOPMODEL concepts for the representation of subsurface storage controlling the dynamics of the saturated contributing area and baseflow recession.

Canopy Interception Component

The canopy interception component is a simpler approach, requiring fewer difficult to obtain parameters, than standard interception models (e.g. Rutter et al., 1972). It was developed based on the work of Ibbitt (1971) and requires only two parameters: canopy interception capacity, CC, and interception evaporation adjustment factor, C_r. These are assigned from the GIS land cover data based upon the vegetation. Driving inputs to the canopy interception component are potential evapotranspiration and surface water input comprising a combination of rainfall, snowmelt and sprinkler irrigation. The state variable quantifying the amount of water held in interception storage, S_i, is used in a function $f(S_i)$ to quantify the proportion of surface water input (precipitation+snowmelt+sprinkler irrigation) that is throughfall (Ibbitt, 1971). The remainder $P(1-f(S_i))$, where P is surface water input rate, is added to interception storage. The same function $f(S_i)$ is used to quantify the exposure of water held in interception storage to potential evapotranspiration. Physically, $f(S_i)$ could be interpreted to express the fraction of leaf area that is wet, relative to its maximum. Higher rates of evaporation from interception than transpiration under the same conditions, have been suggested (Stewart, 1977; Dingman, 1994). Here we represent this effect using a factor C_r quantifying the increase in evaporation losses from interception relative to the potential evapotranspiration rate (Ibbitt, 1971; Stewart, 1977). The evaporation outflux from the interception store is written as $E \cdot C_r \cdot f(S_i)$ where E is the potential evapotranspiration rate. The rate of change for interception storage is therefore given by:

$$\frac{dS_i}{dt} = P(1 - f(S_i)) - E \cdot C_r f(S_i) \qquad (1)$$

where $f(S_i)$, the function giving throughfall as a function of interception storage, S_i, and canopy interception capacity, CC, is given by:

$$f(S_i) = \frac{S_i}{CC} \cdot \left(2 - \frac{S_i}{CC} \right) \qquad (2)$$

Analytic integrals of equation (1) using (2) are used to solve for S_i at the end of each time step to obtain the cumulative throughfall and cumulative evaporation of intercepted water. C_r applies only to intercepted water, not soil water available for transpiration. Unsatisfied potential evapotranspiration is calculated as potential evapotranspiration minus cumulative evaporation of intercepted water divided by the interception enhancement factor C_r.

Vadose Zone Soil Store Component

Throughfall, T, and unsatisfied potential evapotranspiration, E_p, from the interception component serve as the forcing for the soil component, which represents the upper layer of soil to the depth below which roots can no longer extract water. Beven et al. (1995a) indicate that two formulations that have been adopted in past TOPMODEL applications have assumed that the unsaturated flows are essentially vertical and have been expressed in terms of drainage flux from the unsaturated zone. Neither of the formulations presented by Beven et al. (1995a) limit the infiltration capacity, possibly due to the historical association of TOPMODEL with the saturation excess rather than the infiltration excess runoff generation mechanism. Bandaragoda et al. (2004) felt it important to accommodate both saturation and infiltration excess runoff generation mechanisms and, therefore, developed a soil component that combines gravity drainage and Green-Ampt infiltration excess concepts to control the generation of surface runoff by infiltration excess as well as the drainage to the saturated zone and evapotranspiration.

Parameters describing the soil store processes are depth (*d*), saturated hydraulic conductivity (*K*), Green-Ampt wetting front suction (ψ_f), pore disconnectedness index soil drainage parameter (*c*), drainable porosity ($\Delta\theta_1$), and plant available porosity ($\Delta\theta_2$). The soil parameters are estimated from GIS soils data.

To simulate the effect of urbanization, the impervious fraction (I_f) has been added as a parameter. The fraction of surface water input over impervious areas is immediately added to runoff. Over the remaining fraction of the area, $1-I_f$, the following calculations are used to determine infiltration, changes in soil water storage, recharge to groundwater and runoff. Over the pervious area of each model element the state variable S_r quantifies the depth of water held in the soil zone. This is calculated according to:

$$\frac{dS_r}{dt} = I - E_s - R \qquad (3)$$

where I is the infiltration rate, E_s is soil evaporation rate and R the drainage rate or recharge to the saturated zone store from the soil store. The infiltration rate, I, is limited to be less than the infiltration capacity, I_c, modeled with a Green-Ampt formulation where we use the soil zone storage as infiltrated depth for the purposes of calculating I_c.

Unsatisfied potential evapotranspiration is given first call upon available surface water so the forcing to the soil zone is $T\text{-}E_p$. When this quantity is negative it represents potential evapotranspiration from the soil component. When this quantity is positive it represents net surface water input that may infiltrate or become infiltration or saturation excess surface runoff. Soil evapotranspiration is assumed to be at the potential rate when the soil moisture content is in excess of field capacity, but between field capacity and permanent wilting point, evapotranspiration is assumed to reduce linearly to zero as wilting point is approached. Soil evapotranspiration is modeled as:

$$E_s = Min\left(1, \frac{S_r}{d\Delta\theta_2}\right)(E_p - T) \quad \text{for } \mathrm{E_p} > T \text{ and 0 otherwise} \qquad (4)$$

where $E_p - T$ is the unsatisfied potential evapotranspiration.

We assume the soil zone is comprised of two parts, the drainable part in excess of field capacity, characterized by $\Delta\theta_1$, and the plant available moisture, characterized by $\Delta\theta_2$. Drainage is estimated as gravity drainage and is modeled to only occur when the moisture content is greater than field capacity. The relative drainable saturation, S_{rd}, is defined as:

$$S_{rd} = \frac{Max(0, S_r - d\Delta\theta_2)}{d\Delta\theta_1} \tag{5}$$

The drainage from the soil store and recharge to the saturated zone occurs at a rate (m/hr) given by:

$$R = K\, S_{rd}^{c} \tag{6}$$

This is based upon a Brooks and Corey (1966) parameterization of the unsaturated hydraulic conductivity controlling the rate of drainage.

For locations with large wetness index values, the water table evaluated in the saturated zone component described below may upwell into and influence the soil moisture content of the soil zone. This occurs when depth to the water table, z, is less than depth of the soil zone, d. We model the supplementary moisture in the soil zone in these cases by assuming uniform soil moisture deficit from the surface to the water table and saturated conditions from the water table to the root zone. Thus the shallow water table ($z<d$) increases the soil storage to:

$$S_r^{'} = S_r + (d \cdot \theta_e - S_r) \cdot \left(\frac{d - z}{d} \right) \tag{7}$$

where θ_e is effective porosity, defined as $\Delta\theta_1 + \Delta\theta_2$.

Groundwater Saturated Zone Component

The saturated zone component is constructed using the classical TOPMODEL assumptions of 1) saturated hydraulic conductivity decreasing exponentially with depth and 2) saturated lateral flow driven by topographic gradients at 3) steady state (Beven et al., 1995a; Beven and Kirkby, 1979). With these assumptions the local depth to the water table, z, is the following function of the wetness index $\ln(a/\tan\beta)$:

$$z = \bar{z} + (\lambda - \ln(a / \tan\beta)) / f \tag{8}$$

where λ is the spatial average of $\ln(a/\tan\beta)$ and $\bar{z}$ the spatial average of the depth to the water table quantifying the basin average soil moisture deficit and serving as a state variable for the saturated zone component. The parameter f quantifies the assumed decrease of hydraulic conductivity with depth. A histogram of wetness index values over each subbasin is used to record the proportion of each subbasin falling within each wetness index class. Locations, or wetness index classes, where z is less than 0 as calculated using equation (8) are interpreted to be saturated and represent the variable source area where surface water input (T-E_p) becomes saturation excess runoff.

The saturated zone state equation is:

$$\frac{d(\Delta\theta_1 \bar{z})}{dt} = -r_{is} + T_o e^{-\lambda} e^{-f\bar{z}} \tag{9}$$

where r_{is} is the recharge, R, to the saturated zone averaged across wetness index classes, recognizing that for classes where the water table impacts the soil zone S_r, and hence R, are impacted by z through equation (7). The last term in this equation represents the per unit area baseflow, Q_b, draining the saturated zone derived using the exponential decrease in hydraulic conductivity with depth assumed by TOPMODEL, with T_o being transmissivity:

$$Q_b = T_o e^{-\lambda} e^{-f\bar{z}} \tag{10}$$

In solving the model we do not save a state variable either for the saturated zone or soil zone for each wetness index class. Rather we only save state variables $\bar{z}$ and S_r for each subbasin. At each time step, equation (8) gives the depth to the water table for a specific wetness index class within a subbasin, and equation (7) gives the modification of S_r for wetness index classes impacted by a shallow water table. This approach is different from the Beven version of TOPMODEL (Beven et al., 1995b) where a separate soil zone is modeled for each wetness index class. Bandaragoda et al. (2004) felt that keeping track of state variables at scales smaller than the basic subbasin model element introduces unnecessary complexity and is unwarranted. If smaller spatial resolution is required to provide more explicit resolution of spatial variability, then smaller subbasins can be delineated.

Channel Flow Component

There are three sources of runoff from each subbasin; 1) saturation-excess runoff from excess precipitation on variable source saturated areas as determined from the topographic wetness index, 2) infiltration-excess runoff as determined from the Green-Ampt parameterization that is based upon soil zone storage, and 3) base flow representing saturated zone drainage according to equation (10). This runoff is delayed in reaching the outlet due to the time taken by within subbasin travel, as well as travel in the stream network to the overall watershed outlet. Within subbasin travel is modeled assuming a constant hillslope velocity, V, which is a calibrated input parameter. A histogram of the down slope flow distances from each grid cell in each subbasin to the first stream encountered is derived from the GIS and used to perform this routing.
In the WRIA 1 implementation we neglect time delays associated with flow in streams. The model is being run at a daily time step for the purposes of water resources management scenario analysis and for these purposes it was deemed unnecessary to use detailed channel routing.

Artificial Drainage

The facility to represent artificial drainage has been incorporated into the model because of the assumption that agricultural drainage installed during development of agriculture in WRIA 1 has altered the runoff processes and these alterations should be simulated. The capacity for artificial drainage is represented by an empirical "drainage coefficient" established for each drainage model element[1]. This empirical coefficient quantifies the depth of water removed per day when soils contain excess water. Excess water in the vadose zone soil store is defined as $S_r\text{-}d\Delta\theta_2$. The vadose zone soil store already has a function that represents natural gravity drainage from the vadose zone into the deeper groundwater when there is excess water in the vadose zone soil store. The empirical drainage coefficient quantifies the rate of extra artificial drainage from the vadose zone soil store. This extra artificial drainage is added directly to streamflow, bypassing the groundwater saturated zone. The following four parameters are specified for each drainage model element:

1. Tile drained fraction
2. Ditch drained fraction
3. Tile coefficient
4. Ditch coefficient

[1] The model elements being used in WRIA 1 are usually simply referred to as "drainages". However in this section, the more specific term "drainage model element" is used to avoid confusion with the artificial drainage process that is being modeled.

Separate instances of the Rainfall-Runoff Transformation component are run for the fraction of each model element that is tile and ditch drained and the artificial drainage rate is set to the corresponding coefficient while there is excess water in the vadose zone soil store (S_r-$d\Delta\theta_2 > 0$) or 0 otherwise. Accuracy of the model simulations of artificial drainage depend directly upon the reliability of the empirically determined and WRIA 1 provided drainage coefficients.

Evapotranspiration Calculation

There are many methods for the calculation of evapotranspiration (Jensen et al., 1990; Shuttleworth, 1993; Allen et al., 1998). This reflects the complexity of the evapotranspiration (ET) process, where ET depends upon soil moisture and plant environmental conditions as well as atmospheric conditions. The concept of potential evapotranspiration (PET) was advanced to quantify the evaporation from a surface with an unlimited supply of soil moisture and to thereby quantify the potential of the atmosphere to absorb evaporation. However, PET was found to depend upon surface conditions (vegetation type, height, etc.) as well as the actual evaporation that occurs, because over dry surfaces where the evaporative flux is less the atmosphere tends to be hotter and dryer with higher PET. To avoid these difficulties the concept of reference evapotranspiration was developed. Reference ET is defined for a very specific surface condition (e.g., specific crop or vegetation type at a specific height). As a consequence, there are a number of different reference ET definitions that pertain to different surfaces.

Although it is widely understood that the dynamics of vegetation interaction with the atmosphere plays a role in the quantity of ET from a surface, a common approach to the calculation of ET in models is to use a two step approach (Shuttleworth, 1993): (1) Calculate reference ET; (2) estimate actual ET as reference ET multiplied by a vegetation or crop coefficient (K_c) and a function to quantify the reduction in ET below potential due to limitations in soil moisture. This is the approach taken in TOPNET. We first compute reference ET using a standard method. We then multiply this by a vegetation or crop coefficient determined based on the vegetation over the WRIA 1 drainage model element. This defines the PET from that drainage for that specific time step. This is used as input first to the canopy interception store with PET not satisfied from the evaporation of interception being imposed as an input residual PET for the vadose zone soil moisture store.

Reference ET is calculated using a standardized form of the ASCE Penman-Monteith equation recommended by the ASCE Standardization of Reference ET Task Committee (Walter et al., 2000; Allen et al., 2005). This committee recommended using a single standardized reference ET equation with appropriate constants and standardized computational procedures. Two reference surfaces were defined : (1) a short crop with an approximate height of 0.12 m similar to clipped, cool-season grass; and (2) a tall crop with an approximate height of 0.50 m similar to full-cover alfalfa. Both were coded into TOPNET, but all results were generated using the tall crop reference surface.

The ASCE standard reference equation as used here is:

$$(\rho_w)ET_{sz} = \frac{\frac{1}{\lambda}\Delta(R_n - G) + C_n \cdot \gamma \frac{u_2}{T}(e_s - e_a)}{\Delta + \gamma(1 + C_d \cdot u_2)} \qquad (11)$$

where:

ET_{sz} = standardized reference crop ET (mm/h)

R_n = calculated net radiation at the crop surface (kJ m^{-2} h^{-1})

G = soil heat flux density at the soil surface (kJ m^{-2} h^{-1}). Following Allen (2001 equation 28 in Appendix 1) we set G=0 since TOPNET calculations here are at a daily time step

T = mean daily air temperature (Kelvin)

u_2 = mean daily wind speed at 2 m height (m/s)

e_s = saturation vapor pressure (kPa) calculated for daily time steps as the average of the saturation vapor pressure at maximum and minimum air temperature

e_a = mean actual vapor pressure (kPa)

Δ = slope of the saturation vapor pressure-temperature curve (kPa $^oC^{-1}$)

γ = psychrometric constant (kPa $^oC^{-1}$)

C_n = numerator constant that changes with reference type and time units (kg K kJ^{-1} s h^{-1})

C_d = denominator constant that changes with reference type and time units (s m^{-1})

λ = Latent heat of vaporization (kJ/kg)

ρ_w = Density of water (kg/m^3). A value of 1000 kg/m^3 is used

This equation as written differs from the usual way the ASCE reference equation (see e.g., Allen et al., 2005) is written in that the density of water has been included on the left, 1/λ has been included in the first term in the numerator, and the second term of the numerator has T, rather than T+273 in the denominator. Including the density of water on the left makes explicit the implicit units conversion between ET_{sz} expressed in mm/h and the right hand side that has units kg m^{-2} h^{-1}. Numerically these are equivalent because the m to mm conversion factor cancels with the water density of 1000 kg/m^3. In the ASCE way of writing this equation, the 1/λ is expressed as a value of 0.408 which results from using a standard value for λ = 2.45 MJ/kg. The T+273 written in the ASCE way of writing the equation is a conversion from ^{o}C to Kelvin.

The following relationships are used in the evaluation of this equation:

1. Latent heat of vaporization (Shuttleworth, 1993 equation 4.2.1 page 4.2):

$$\lambda = 2501 - 2.361\,T \quad \text{kJ/kg} \tag{12}$$

   where T is temperature (^{o}C).

2. Saturation vapor pressure-temperature gradient (Shuttleworth, 1993 equation 4.2.3 page 4.3):

$$\Delta = \frac{4098\,e_s}{(237.3+T)^2} \quad \text{kPa } ^oC^{-1} \tag{13}$$

   where e_s is saturation vapor pressure. A polynomial provided by Lowe (1977) was used to compute saturation vapor pressure as a function of temperature.

3. Psychrometric constant (Shuttleworth, 1993 equation 4.2.28 page 4.13):

$$\gamma = \frac{c_p P}{0.622\lambda} \tag{14}$$

   where P is atmospheric pressure and c_p is the specific heat of moist air (1.013 kJ kg^{-1} $^oC^{-1}$).

4. Atmospheric pressure derived from elevation using a standard atmosphere approximation (Shuttleworth, 1993 equation 4.4.12 page 4.37):

$$P = 101.3\left(\frac{293-0.0065z}{293}\right)^{5.256} \quad \text{kPa} \tag{15}$$

   where z is elevation in meters.

The inputs for the calculation of ET_{sz} are air temperature, dew point, wind speed, surface albedo, date, elevation and location (latitude and longitude). Net radiation (R_n) is calculated as the sum of net short (S_n) and longwave (L_n) radiation:

$$R_n = S_n + L_n \tag{16}$$

Net shortwave radiation is calculated from:

$$S_n = (1-\alpha)\, T_f\, S_o \tag{17}$$

where S_o is extraterrestrial radiation at the top of the atmosphere calculated based on sun angles from the date, α is the surface albedo which is derived from surface vegetation, and T_f is the atmospheric transmissivity. We approximate atmospheric transmissivity using a procedure given by Bristow and Campbell (1984) based on the diurnal temperature range:

$$T_f = a\,[1-\exp(-b\Delta T^{c})] \tag{18}$$

where ΔT is the diurnal temperature range and a (=0.8) and c (=2.4) are parameters that Bristow and Campbell calibrated. b is a parameter dependent on the monthly mean diurnal temperature range $\overline{\Delta T}$:

$$\mathrm{b} = 0.036\exp(-0.154\overline{\Delta \mathrm{T}}) \tag{19}$$

Net longwave radiation is calculated from (Shuttleworth, 1993; Allen et al., 2005):

$$L_n = -c_f \varepsilon' \sigma (T_{\max}^4 + T_{\min}^4)/2 \tag{20}$$

where c_f is a cloudiness factor, ε' is net emissivity and σ is the Stefan-Boltzmann constant (2.0747×10^{-7} kJ K^{-4} m^{-2} h^{-1}). T_{max} and T_{min} are daily maximum and minimum temperatures expressed in Kelvin. The cloudiness factor is calculated as:

$$c_f = T_f / 0.8 \tag{21}$$

This is based on (Shuttleworth, 1993 equation 4.2.10) with parameters for humid conditions. Net emissivity is calculated as (Shuttleworth, 1993 equation 4.2.8):

$$\varepsilon' = a_e + b_e\sqrt{e_d} \tag{22}$$

where a_e=0.34 and b_e = -0.14 are coefficients and e_d is vapor pressure (kPa). Vapor pressure is determined from the dew point temperature using the polynomial provided by Lowe (1977) that gives saturation vapor pressure as a function of temperature.

For the ASCE Penman-Monteith tall crop reference *ET*, the constants C_n = 66 and C_d = 0.38 are used.

The above provides all the information needed to compute ET_{sz}. Potential evapotranspiration (*PET*) is obtained from this using:

$$PET = K_c\, ET_{sz} \tag{23}$$

where K_c is a vegetation crop coefficient that varies by month to represent growing seasons, is determined based upon land cover, and is averaged over each WRIA 1 drainage. This *PET* is used as input to the Rainfall-Runoff Transformation component.

Snow Component

For the WRIA 1 implementation of TOPNET, the Utah Energy Balance (UEB) snowmelt model (Tarboton et al., 1995a; Tarboton and Luce, 1996b; Luce et al., 1998; 1999; Luce, 2000; You, 2004) was added as the Snow component. Previous implementations of TOPNET had not included a snow component because they had been in regions not subject to snow (Bandaragoda et al., 2004). The following description of the UEB TOPNET Snow component is excerpted from the publications listed above. The core of the UEB Snow component is a physically-based point energy and mass balance model for snow accumulation and melt. The snowpack is characterized using two primary state variables, namely, snow water equivalent, W, (m) and the internal energy of the snowpack and top layer of soil, U, (kJ m^{-2}). The physical basis of the model is the conservation of mass and energy. Snow surface temperature, a key variable in calculating latent and sensible heat fluxes and outgoing longwave radiation, is modeled using a modified force-restore approach (Deardorff, 1978; Dickinson et al., 1993; Hu and Islam, 1995; Luce, 2000; Luce and Tarboton, 2001) to represent the key physical dynamics of surface temperature without requiring the introduction of multiple snowpack layers. Luce (1998) showed that basin average snowmelt (for example at the scale of WRIA 1 drainages) cannot be described using point scale equations with basin-averaged parameters. To overcome this limitation, Luce et al., (1999) suggested a depletion curve approach to quantify the variability of snow accumulation across model elements. This approach allows the snowmelt model to be used with larger model elements and still provide reasonable aggregate surface water input values for each model element. The depletion curve approach has been used with the UEB snowmelt model component within TOPNET using WRIA 1 drainages as model elements.

Mass and Energy Balance State Variables

In the UEB model (Tarboton et al., 1995b; Tarboton and Luce, 1996a), the time evolution of the snowpack is driven by the energy exchange between the snowpack, the air above, and the soil below according to the following mass and energy balance equations:

$$\frac{dU}{dt} = Q_{sn} + Q_{li} - Q_{le} + Q_p + Q_g + Q_h + Q_e - Q_m, \quad (\text{kJ m}^{-2}\text{ h}^{-1}) \tag{24}$$

$$\frac{dW}{dt} = P_r + P_s - M_r - E, \quad (\text{m h}^{-1}) \tag{25}$$

where Q_{sn} is the net shortwave energy received by the snowpack, Q_{li} is the incoming longwave radiation, Q_{le} is outgoing longwave radiation, Q_p is the energy advected by precipitation into the snow, Q_g is the ground heat flux to the snow, Q_h is the sensible heat flux to/from the snow with sign convention that flux to the snow is positive, Q_e is the latent heat flux to/from the snow with sign convention that flux to the snow is positive, and Q_m is the advected heat removed by meltwater. P_r is the rate of precipitation as rain; P_s is the rate of precipitation as snow; M_r is the melt rate; and E is the sublimation rate; t is time (h). Internal energy U is defined relative to the melting point and is taken as 0 kJ m^{-2} when the snowpack is frozen at 0 ^{o}C and contains no liquid water. With this definition negative internal energies correspond to the cold content (e.g., Dingman, 1994, page 182) and positive internal energies reflect change in phase of some fraction of snow from frozen to liquid. The model requires inputs of air temperature, wind speed and incident radiation that are used to drive the energy balance, and precipitation that is used to drive the mass balance. Precipitation is partitioned into snowfall or rainfall based upon air temperature (U.S. Army Corps of Engineers, 1956). The use of energy content as a state variable means that the model does not explicitly prognose snowpack temperature. Since snowpack temperature is important for energy fluxes into the snow, it needs to be obtained diagnostically from internal energy and snow water equivalent as follows:

If $U < 0$ $\qquad T_{ave} = U/\left(\rho_w W C_i + \rho_g D_e C_g\right)$ $\qquad$ All solid phase (26 a)

If $0<U<\rho_w W h_f$ $\qquad T_{ave} = 0°C$ with L_f=U/($\rho_w h_f W$) $\qquad$ Solid and liquid mixture (26 b)

If $U>\rho_w W h_f$ $\qquad T_{ave} = \dfrac{U - \rho_w W h_f}{\rho_g D_e C_g + \rho_w W C_w}$ $\qquad$ All liquid (26 c)

In the equations above, T_{ave} denotes snowpack average temperature (^oC), h_f denotes the heat of fusion (333.5 kJ kg^{-1}), ρ_w the density of water (1000 kg m^{-3}), C_i the specific heat of ice (2.09 kJ kg^{-1} °C^{-1}), ρ_g the soil density, C_g the specific heat of soil, C_w the specific heat of water (4.18 kJ kg^{-1} °C^{-1}), D_e the depth of soil that interacts thermally with the snowpack and L_f the liquid fraction by mass. The basis for equations (26 a) to (26 c) is that the heat required to melt the entire snow water equivalent at 0 °C is $\rho_w W h_f$ (kJ m^{-2}). Where U is between 0 and this quantity, the liquid fraction is determined by proportioning, i.e., $L_f=U/(\rho_w h_f W)$. The heat capacity of the snow combined with thermally interacting soil layer is $\rho_w W C_i + \rho_g D_e C_g$ (kJ °C^{-1}m^{-2}), so in the case that U<0, dividing U by this combined heat capacity gives T_{ave}. Where $U> \rho_w W h_f$ the snow contains sufficient energy to melt completely and the temperature of the remaining liquid phase is given by (26 c). Practically, the condition in equation (26 c) only occurs when W is zero since a completely liquid snowpack cannot exist; it becomes melt runoff. Nevertheless, this equation is included for completeness to keep track of the energy content during periods of intermittent snow cover, with T_{ave} representing the temperature of the ground, with the possibility of snowfall melting immediately due to coming in contact with warm ground.

Radiative Fluxes

The net shortwave radiation is calculated from incident shortwave radiation and albedo calculated as a function of snow age and solar illumination angle following Dickinson et al. (1993). The incident shortwave radiation is estimated using the same procedure described above for ET that estimates atmospheric transmissivity from the diurnal temperature range (Bristow and Campbell, 1984).

In the albedo model, which follows Dickinson et al. (1993), the dimensionless age of the snow surface, τ, is retained as a state variable, and is updated with each time step, dependent on snow surface temperature and snowfall. Reflectance is computed for two bands; visible (< 0.7 µm) and near infrared (> 0.7 µm) with adjustments for illumination angle and snow age. Then albedo is taken as the average of the two reflectances. A parameter d_{NewS} (m) represents the depth of snowfall that is assumed to restore the snow surface to new conditions (τ = 0). With snowfall, P_s, less than d_{NewS} in a time step the dimensionless age is reduced by a factor (1-P_s/d_{NewS}). When the snowpack is shallow (depth $D < h$ = 0.1 m) the albedo, α, is taken as $r_\alpha \alpha_{bg}+(1-r_\alpha)\alpha_s$, where $r_\alpha=(1-D/h)e^{-z/2h}$. This interpolates between the snow albedo, α_s, and bare ground albedo, α_{bg}, with the exponential term approximating the exponential extinction of radiation penetration of snow.

The incident longwave radiation is estimated based on air temperature, T_a (K) using the Stefan-Boltzmann equation. The emissivity of air is estimated using Satterlund's (1979) equation for clear conditions. The presence of clouds increases downward longwave radiation. This is modeled by estimating the cloud cover fraction based on the Bristow and Campbell (1984) atmospheric transmission factor. The outgoing longwave radiation is calculated from the snow surface temperature using the Stefan-Boltzmann equation, with emissivity of snow, ε_s, taken as 0.99.

Turbulent Fluxes

The latent heat flux, Q_e and sensible heat flux, Q_h are modeled using bulk aerodynamic formulae (Anderson, 1976):

$$Q_h = \rho_a C_p (T_a - T_s) K_h \tag{27}$$

and

$$Q_e = \rho_a h_v (q_s - q_a) K_e \tag{28}$$

where ρ_a is the density of air, C_p is the specific heat of air at constant pressure (1.005 kJkg^{-1}°C^{-1}), h_v is the latent heat of vaporization (sublimation) of ice (2834 kJ kg^{-1}), q_a is the air specific humidity, q_s is the specific humidity at the snow surface which is assumed to be saturated relative to the vapor pressure over ice (e.g., Lowe, 1977), and K_h and K_e are turbulent transfer conductances for sensible and latent heat respectively. Under neutral atmospheric conditions K_e and K_h are given by:

$$K_n = \frac{k_v^2 u}{\left[\ln(z_m / z_0)\right]^2} \tag{29}$$

where z_m is the measurement height for wind speed, air temperature, and humidity, u is the wind speed, k_v is von Kármán's constant (0.4), and z_0 is the aerodynamic roughness. When there is a temperature gradient near the surface, buoyancy effects may enhance or dampen the turbulent transfers, necessitating adjustments to K_n. We use:

$$K_h = K_n \frac{1}{\Phi_M \Phi_H} \tag{30}$$

and

$$K_e = K_n \frac{1}{\Phi_M \Phi_E} \tag{31}$$

where Φ_M, Φ_H, Φ_E are the stability functions for momentum, sensible heat, and water vapor, respectively. The stability functions are estimated using the bulk Richardson number:

$$R_i = \frac{g z_m (T_a - T_s)}{\frac{1}{2}(T_a + T_s) u^2} \tag{32}$$

where g is gravity acceleration (9.8 m s^{-2}). For stable conditions (R_i>0), we use the approximation of Price and Dunne (1976):

$$\frac{1}{\Phi_M \Phi_H} = \frac{1}{\Phi_M \Phi_E} = \frac{1}{1 + 10 R_i} \tag{33}$$

For unstable conditions (R_i<0) we use (Dyer and Hicks, 1970; Anderson, 1976; Jordan, 1991):

$$\frac{1}{\Phi_M \Phi_H} = \frac{1}{\Phi_M \Phi_E} = (1 - 16 R_i)^{0.75} \tag{34}$$

Because information for estimating turbulence under extremely unstable conditions is poor, we capped the value of $1/\Phi_M \Phi_H$ at 3, which occurs near R_i = -0.2. Anderson (1976) shows that iterative solutions of Deardorff's (1968) empirical equations begin to level off for more strongly unstable situations as the value of 3 is approached. These approximations assume that K_h=K_e.

Snow Surface Temperature

A unique characteristic of the UEB model is its separate representation of surface temperature and average snowpack temperature. This facilitates good modeling of surface energy exchanges that depend on snow surface temperature, while retaining a parsimonious single layer model. The model includes parameterizations for the snow surface temperature described by You (2004). The sum of energy fluxes in equation (24) from above the snowpack are referred to as the surface energy forcing:

$$Q_{forcing}(T) = Q_{sn} + Q_{li} + Q_h(T_s) + Q_e(T_s) + Q_p - Q_{le}(T_s) \tag{35}$$

The sensible heat, latent heat, and outgoing longwave radiation are functionally dependent on the surface temperature, T_s. In the UEB model, the heat conducted into the snow, Q_{cs}, is calculated as a function of the snow surface temperature, T_s, and average snowpack temperature, T_{ave}, using a modified force-restore approach (Luce, 2000; Luce and Tarboton, 2001):

$$Q_{cs} = \frac{\lambda}{d_1}\frac{1}{\omega_1 \Delta t}\left(T_s - T_{s_{lag1}}\right) + \frac{\lambda}{rd_1}\left(T_s - \overline{T}_s\right) + \frac{\lambda}{d_{lf}}\left(T_s - \overline{T}_{ave}\right), \tag{36}$$

Here Δt is the time step, T_{slag1} is the surface temperature of snow in the previous time step, $\overline{T}$ is the average surface temperature estimated for the previous 24 hours, and $\overline{T}_{ave}$ is the 24 hour time average of the depth average snowpack temperature. The parameters in equation (36) are:

λ, the thermal conductivity of snow (kJ m^{-1} K^{-1} h^{-1})

ω_1=2π/24 h^{-1}, the diurnal frequency

$d_1 = \sqrt{\frac{2k_s}{\omega_1}}$, the damping depth corresponding to frequency ω_1

r, damping depth scaling factor

$d_{lf} = \sqrt{\frac{2k_g}{\omega_{lf}}}$, the damping depth associated with longer time scale fluctuation

ω_{lf}, frequency corresponding to longer time scale temperature fluctuation

$k_s = \frac{\lambda}{C_i \rho_s}$, snow thermal diffusivity

$k_g = \frac{\lambda_g}{C_g \rho_g}$, ground thermal diffusivity

This modified force-restore approach superimposes a lower frequency gradient term (the third term) onto the diurnal force-restore approach represented by the first two terms. The choice of appropriate low frequency parameter (ω_{lf}) is discussed by Luce (2000) and Luce and Tarboton (Luce and Tarboton, 2001). Here ω_{lf} was set to 1/4 ω_1 to represent approximate four day fluctuations as the next most important time scale for snowmelt following diurnal fluctuations.

Meltwater Refreezing

The approaches described above solve for surface temperature based upon a balance between surface forcing and the capacity of the snow near the surface to conduct heat into or out of the snowpack. However, during a cooling period following melting where there is liquid water present in the snow, the depression of snow surface temperature is inhibited by the energy required to refreeze liquid water near the surface before a temperature gradient can be established and conduction can occur. The net effect of this is that when there is liquid water present the snow surface stays warmer longer and heat loss at night and in cooling periods is more rapid. To accommodate this effect You (2004) developed a parameterization for the penetration of a refreezing front and conduction of heat between the surface and refreezing front while there is liquid water present in the snow.

When snow energy content, *U,* is greater than 0, liquid water exists in the snowpack. The snowpack is assumed to be isothermal at 0 °C. Using the relationship between energy content and liquid fraction (Equation 26 b), the equivalent depth of liquid water in the snowpack w_m(m) is calculated as:

$$w_m = L_f W = \frac{U}{\rho_w h_f} \tag{37}$$

The capillary holding capacity of the snow is defined as mass fraction liquid holding capacity L_c times snow water equivalent L_cW, which implies that the maximum density of capillary water:

(ρ_m) is $\rho_m = \dfrac{L_c W}{D} = L_c \rho_s$

where *D* is the depth of snowpack. We assume that prior to melt outflow, when the liquid water content is less than the capillary holding capacity, the meltwater is held at the maximum density of capillary water in the upper portion of the snowpack. With this assumption the depth to which meltwater has penetrated is:

$$d_w = \frac{w_m \rho_w}{\rho_m} = \frac{U}{\rho_w h_f}\frac{\rho_w}{\rho_m} = \frac{U}{\rho_m h_f} \tag{38}$$

This describes the state of the snowpack prior to the onset of a refreezing episode during which $Q_{forcing}$ is negative. The negative forcing will result in refreezing that penetrates down from the surface as illustrated in Figure 3. The rate of increase of the depth to the refreezing front, d_r, is given by:

$$\frac{dd_r}{dt} = -\frac{Q(T_s)}{\rho_m h_f} \tag{39}$$

where $Q(T_s)$ is the heat flux just above the refreezing front, here indicated to be a function of surface temperature, T_s. The sign convention is that heat flux is positive into the snow which is why there is a negative sign in Equation (39).

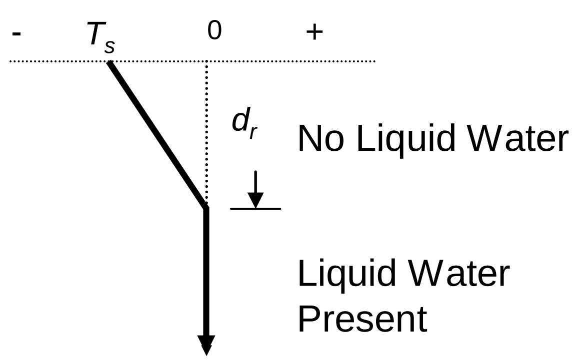

Figure 3. Schematic illustration of temperature profile during the downward propagation of a refreezing front.

We assume a linear temperature gradient above the refreezing front with $Q(T_s)$ given by:

$$Q(T_s) = \lambda \frac{T_s}{d_r} \tag{40}$$

We use an equilibrium approach for surface temperature that balances the surface forcing with the conduction into the snow above the refreezing front, neglecting any heat stored in the snow between the refreezing front and the surface (as this will be small because the heat capacity of snow is less than the latent heat of fusion). This is written:

$$Q(T_s) = Q_{forcing}(T_s) \tag{41}$$

To solve for $d_r(t)$ the dependence of $Q_{forcing}(T_s)$ on T_s is linearized:

$$Q_{forcing}(T_s) = a - bT_s \tag{42}$$

Here a is the forcing surface energy flux when the surface temperature of snow is 0 ^{o}C. b is the slope of surface forcing flux to surface temperature function. This is a positive value since $Q(T_s)$ decreases with T_s. a is obtained by putting T_s=0 into $Q_{forcing}(T_s)$. b is obtained by putting a small negative (below freezing) T_s into $Q_{forcing}(T_s)$ and solving (42). If a is greater than 0, then the surface forcing is positive and meltwater is being generated at the surface so d_r is set to 0. When a becomes less than 0, the snowpack starts refreezing. Combining Equations (40) and (42) gives:

$$\frac{\lambda}{d_r} T_s = a - bT_s \tag{43}$$

T_s can then be expressed as:

$$T_s = \frac{a}{\frac{\lambda}{d_r} + b} \tag{44}$$

Substituting this T_s into (26) we have:

$$\frac{dd_r}{dt} = -\frac{Q(T_s)}{\rho_m h_f} = -\frac{a - \frac{abd_r}{\lambda + bd_r}}{\rho_m h_f} = -\frac{\lambda a}{\rho_m h_f (\lambda + bd_r)} \tag{43}$$

Integrating equation (43) starting from the initial refreezing depth d_{r1} during a time step, we get:

$$\lambda d_r + \frac{b}{2} d_r{}^2 - (\lambda d_{r1} + \frac{b}{2} d_{r1}{}^2) = -\frac{a\lambda}{\rho_m h_f} \Delta t \tag{44}$$

This has the solution:

$$d_r = \frac{-\lambda + \sqrt{\lambda^2 + 2b(\lambda d_{r1} + \frac{b}{2} d_{r1}{}^2 - \frac{a\lambda \Delta t}{\rho_m h_f})}}{b} \tag{45}$$

Only the positive root has been retained since only positive values of d_r are physically interpretable and b is a value greater than 0. When d_r is greater than rd_1, the effective depth associated with diurnal temperature fluctuations, or all meltwater is refrozen, the model reverts back to the surface temperature parameterization without refreezing of meltwater as described above.

Adjustment of Thermal Conductivity, λ, for Shallow Snowpack

In equation (36) the temperature gradient is calculated over an effective depth ($Z_e = rd_1$) estimated from the depth of penetration of surface temperature forcing at a diurnal frequency. When the snow is shallow this depth may extend into the ground below the snow cover. In such cases the thermal conductivity used in the surface temperature parameterizations above needs to reflect the combined conductivity of snow and soil below. We therefore, take the effective thermal conductivity of the snowpack, λ_e, as the harmonic mean to the effective depth, Z_e, where the amplitude is damped by the same factor as it would be for deep snow (see Figure 4). In deep snow the amplitude of diurnal temperature fluctuations at depth Z_e is damped by $e^{-Z_e/d_1} = e^{-r}$. In the combined snow/soil system, given r, we first solve for the depth into the soil z_2 at which the amplitude of diurnal temperature fluctuations is damped by this same factor e^{-r}. Then λ_e is obtained by taking the harmonic mean to this depth. The thermal diffusivity of the ground below the snow, k_g, is related to the thermal conductivity, λ_g, heat capacity, C_g, and density, ρ_g, of the ground through:

$$k_g = \frac{\lambda_g}{C_g \rho_g} \tag{46}$$

The diurnal damping depth, d_g, associated with this ground thermal diffusivity is:

$$d_g = \sqrt{\frac{2k_g}{\omega_1}} \tag{47}$$

The amplitude of diurnal temperature fluctuation at depth z_2 into the ground, relative to the surface temperature fluctuation is therefore damped by $e^{-z_s/d_1} e^{-z_2/d_g}$. Equating this to e^{-r} we obtain:

$$\frac{z_s}{d_1} + \frac{z_2}{d_g} = r \tag{48}$$

Thus z_2 is:

$$z_2 = d_g \left(r - \frac{z_s}{d_1}\right) \tag{49}$$

The effective thermal conductivity, λ_e, and the effective depth, Z_e, for the shallow snowpack are then estimated through:

$$Z_e = z_s + z_2 = z_s + d_g \left(r - \frac{z_s}{d_1}\right) \tag{50}$$

$$\frac{1}{\lambda_e} = \frac{\frac{z_s}{\lambda} + \frac{z_2}{\lambda_g}}{Z_e} \tag{51}$$

Equation (51) is used to obtain the effective thermal conductivity near the surface when the snow is shallow. This is used in the parameterizations for surface temperature that calculate the surface heat flux between the snowpack and the atmosphere as well as conduction into the snow.

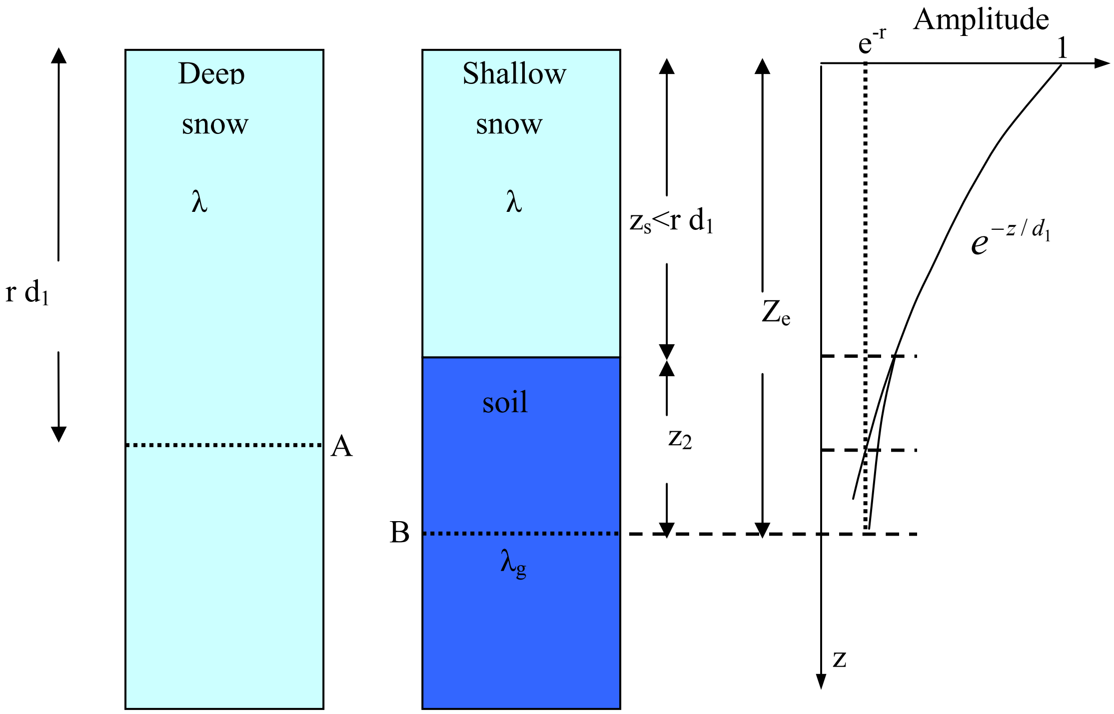

Figure 4. Heat conduction scheme for combined snow/soil system. The dashed lines at depths A and B indicate the depths at which temperature fluctuation amplitude is damped by e^{-r} in the deep snow and combined snow/soil system respectively.

Depletion Curve Parameterization

Figure 5 depicts schematically the area snowmelt model with subgrid parameterization using depletion curves described by Luce et al. (1999) that was used to extend the point snowmelt model over WRIA 1 drainages.

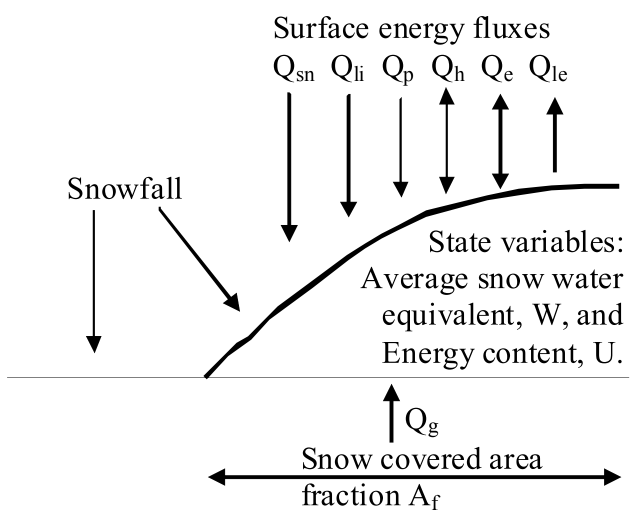

Figure 5. Schematic diagram of the area snowmelt model

The snow-covered area fraction, A_f, is introduced as a new state variable, and the basin or element average snow water equivalence, $W_a = W_s A_f$, is used as the mass state variable. The point snowmelt model is driven by basin averaged climate inputs to calculate fluxes to and from this fractional area. During accumulation A_f increases to full cover quickly with initial snowfall, and stays at full cover until melt begins. During melt, as W_a decreases, A_f is decreased following a depletion curve (Figure 6), $A_f(W_a)$, starting from a point of maximum accumulation, A towards B.

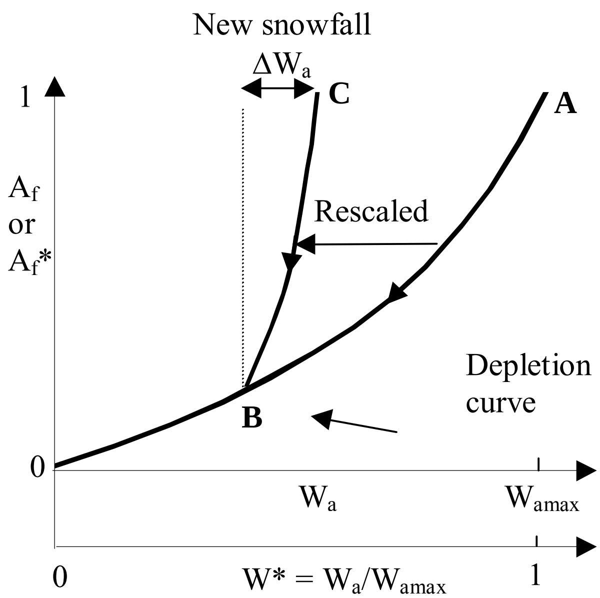

Figure 6. Schematic of depletion curve in area snowmelt model

When there is new snowfall part of the way along, for example at point B, W_a is incremented by the new snowfall water equivalent ΔW (taken over the whole area) and A_f goes to one (point C in Figure 6). The new snowfall (covering the whole element) will be subjected to the same processes that led to spatial variability in the old snow, and the new snow will melt first. Therefore, we assume the system returns along a rescaled depletion curve to the point of original departure, B. In this fashion multiple accumulation and ablation periods can be accommodated.

Luce et al (1999) found that the spatial pattern of snow accumulation in the areas that they studied is relatively consistent. This justifies the use of a single dimensionless depletion curve, scaled by the maximum snow water equivalent (W_{amax}) since W_a was last 0 (generally the beginning of the snow season). This provides scaling of the depletion curve, letting the onset of melt be determined naturally from the modeling of physical processes, rather than using parameters determining the 'beginning' of the melt season. It allows for melt episodes during the accumulation season and accumulation episodes during the melt season. The following equation gives a particular depletion curve, $A_f(W_a)$, in terms of the dimensionless depletion curve, $A_f^*(W^*)$:

$$A_f(W_a) = A_f^*(W_a/W_{amax}) \qquad (52)$$

There is no data available to determine a specific dimensionless depletion curve for WRIA 1. Given this, we used a depletion curve that was derived from our earlier work (Luce et al., 1999) at Upper Sheep Creek. Although this is not ideal, it is a pragmatic approach. Our work has shown that the difference in simulations between different depletion curves is a lot less than the difference between simulation with and without a parameterization for subgrid variability (Luce et al., 1998). Figure 7 shows the dimensionless depletion curve that was used.

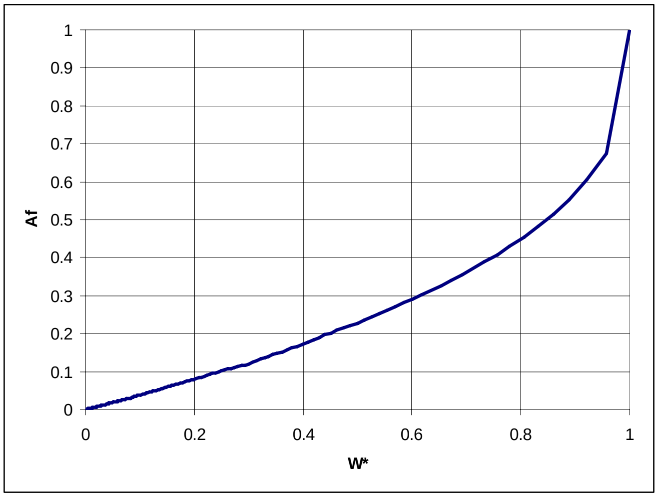

Figure 7. Dimensionless depletion curve used with the WRIA 1 snow component

Water Management

The Water Management component of TOPNET for WRIA 1 has been designed to provide the capability to compare scenarios across management options including: (a) water use changes, e.g., ability to add new uses and to interchange surface water and groundwater uses; (b) land use changes, e.g., account for development; (c) different water use rates; (d) augmentation of surface water flows in any user-defined period (of particular interest for low-flow conditions); (e) representation of trans-drainage diversions and surface storage facilities; (f) water rights enforcement.

Broadly, water use is separated into irrigation and non irrigation use because these are fundamentally different in terms of both demand and the behavior of return flows. The water management component is organized around two important concepts: (1) users and (2) drainages. Input includes a list of users and specifications of the drainage(s) that are the source, place of use and return flow location for each use. The model may be run in water rights enforcement mode, or demand driven mode, or water management may be turned off. When being run in water rights enforcement mode the water right priority date is also specified.

The Water Management component of TOPNET for WRIA is comprised of subcomponents for irrigation, withdrawals, non-irrigation users and return flows. Irrigation may be either sprinkler or drip, sprinkler irrigation entering the Rainfall-Runoff Transformation above the canopy interception store because it is subject to interception, while drip irrigation directly enters the vadose zone soil store. Withdrawals are either from surface water, taken from channel flow, or groundwater, taken from the groundwater saturated zone. Return flows from non-irrigation users may be to surface channels or groundwater.

There are three input modes for water management

0. No Water Management

1. Water Rights Allocation
2. Demand Allocation

With mode 0, No Water Management, the simulation of water management is bypassed. This means that there will be no simulation of withdrawals from surface or groundwater for irrigation or non-irrigation users. As a consequence, there will also be no return flows simulated.

With mode 1, Water Rights Allocation each user source is associated with a water right that specifies the allowable quantity and priority date. Withdrawal requests to these sources, up to the allowable quantity, are processed in priority date order to ensure that higher priority sources get allocated water first.

With mode 2, Demand Allocation, each user, either irrigation or non-irrigation, generates a demand based on simulated conditions, such as soil moisture, in the case of irrigation users, or population and time of year in the case of urban users. This translates into a withdrawal request from a set of sources, which may include surface water and groundwater sources. Requests are processed in an upstream to downstream order and within the same drainage in an arbitrary order.

Referring to the water management component of Figure 2, the simulation of water management proceeds as follows. A user, either irrigation or non-irrigation generates a demand. This translates into a withdrawal request from a set of sources, which may include surface water and groundwater sources. Withdrawal requests are at the level of WRIA 1 drainages. Surface withdrawal requests are taken from the streamflow at the outlet (downstream end) of the associated drainage. Groundwater withdrawal requests are taken from the groundwater saturated zone of the associated drainage. Requests are processed in water right priority order if water rights are being enforced; otherwise requests are processed in an upstream to downstream order and within the same drainage in an arbitrary order. Requests are limited by allowable water rights when these are being enforced. Requests are also limited by physical capacity constraints associated with each source. All surface water requests are granted to the point where the flow is 0. If there is a minimum instream flow requirement this needs to be specified as an instream water user. The model will then treat this as a request, just like all other use requests, and attempt to grant it based on the availability of water according to the input priority date if water rights enforcement is being used. Groundwater requests are always granted (subject to right and physical constraint limitations) because the TOPNET groundwater saturated zone store is a depletion store and does not have a physical capacity limit. This is one of the drawbacks of using this modeling approach as compared to a more formal groundwater modeling approach.

The calculated withdrawal is then allocated to the corresponding user, either an irrigation or non-irrigation user. In the case of irrigation users the fraction of irrigation that is sprinkler is applied as surface water input above the canopy over the fraction of the drainage that is irrigated. Sprinkler irrigation is subject to interception as simulated by the Canopy Interception store. The non-sprinkler (drip) irrigation fraction is used to supplement throughfall surface water input. The Rainfall-Runoff Transformation component then simulates the disposition of irrigation water among infiltration, ET, percolation to groundwater, artificial drainage and runoff.

In the case of a non-irrigation user, the calculated withdrawal may generate a return flow to a designated return flow point that may be surface or subsurface. Surface return flows are added to the flow at the outlet of the corresponding drainage, while subsurface return flows are added to the groundwater saturated zone. Diversions, inter-basin transfers and storages are all implemented as specific types of users. For example an inter-basin transfer from drainage A to drainage B would be specified to the model as a withdrawal from drainage A, with 100% return flow to drainage B. A storage facility maintains a record of the volume of water in storage and has separate users for filling the storage, using water from the storage and releasing water from the storage.

The following subsections give details of the subcomponents of the water management component.

Users, Sources and Rights

Each water user is specified through a record in the users table in the file user.txt. Figure 8 gives the schema showing the relationships between records in user.txt and associated tables.

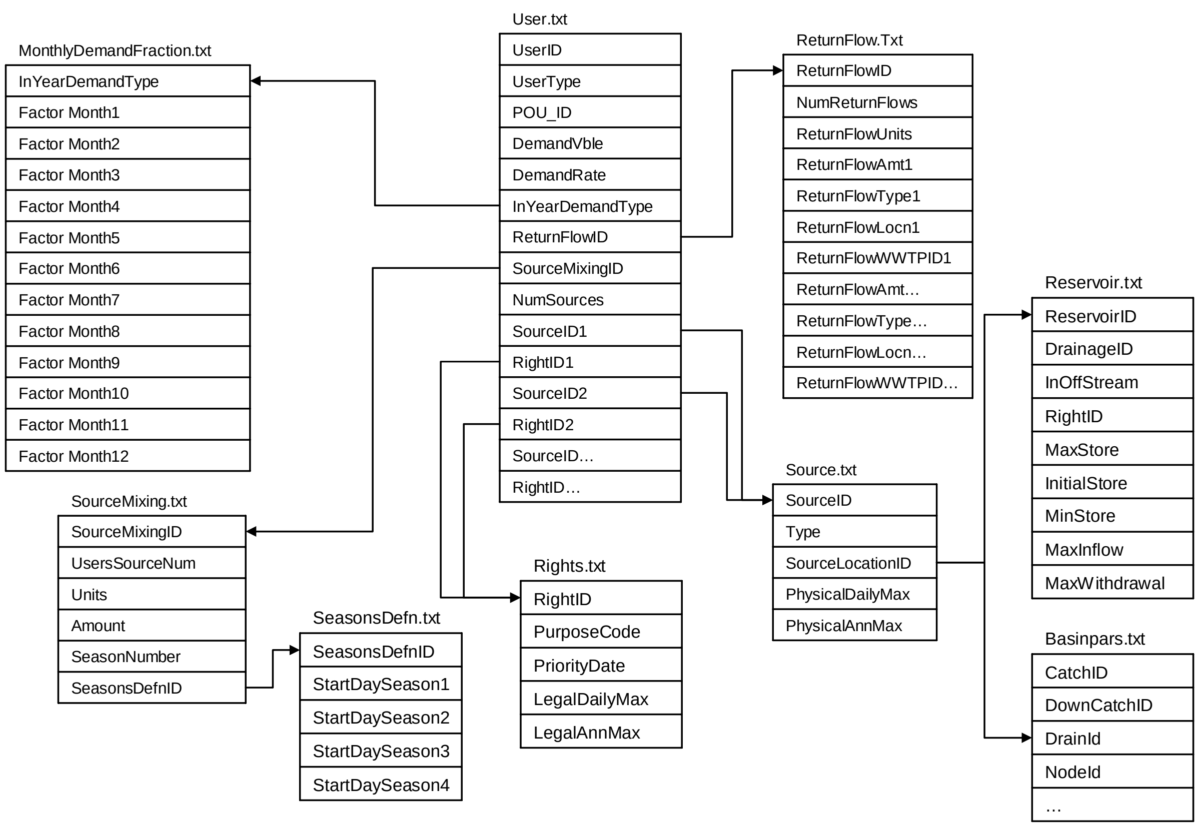

Figure 8. Schema of Inter-relationships between files specifying users for the Water Management component of WRIA 1 Topnet surface water quantity model

Table 2 gives the contents of the users table.

Table 2. Fields in Water Management Users Table (user.txt)

Information	Description
UserID	User sequential identifier
UserType	One of 14 user types – see table below
POU_ID	Place of Use. The WRIA1 Identifier for the drainage where the use occurs
DemandVble	Number of quantifiable user units (e.g. people or cows) used to calculate demand
DemandRate	The number of units of water per unit time for one quantifiable user unit (m^3/day/unit)
InYearDemandType	Identifier specifying the monthly use pattern
ReturnFlowID	Return flow identifier that serves as index to table specifying return flow quantities and locations
SourceMixingID	Source mixing identifier that serves as index to table specifying the proportioning of demand between sources
NumSources	Number of sources that a user can draw water from
SourceIdentifiers	Identifier for sources
RightIDs	Identifier for water rights for each source

Although users fall into two broad categories, irrigation and non irrigation, there are fourteen specific types of users that may be designated (Table 3).

Table 3. Water Management User Types

ID	Type	Description
1	SoilMoistureIrrigation	Irrigation where the demand is driven by soil moisture
2	FixedDemandIrrigation	Irrigation where the demand is fixed
3	DownstreamReservoirRelease	Release from a reservoir at the downstream end of a drainage
4	PWS	Public Water Supply
5	NonPWSMandI	Non Public Water Supply Municipal and Industrial
6	Dairy	Dairy
7	Ranch	Ranch
8	Poultry	Poultry
9	ParkGolfCemetery	Park, Golf Course and Cemetery
10	InstreamFlow	Instream flow
11	Diversion	Diversion
12	ReservoirFill	Reservoir fill
13	InStreamReservoirRelease	In stream reservoir release
14	OffStreamReservoirRelease	Off stream reservoir release

The majority of these user types are for information purposes and use by the water quality model and do not have any specific impact on the water quantity model. However, the water management component does use types 1 and 2 to identify irrigation users and types 3, 10, 12, 13 and 14 control the location of sources and return flows.

User type 1 is an irrigation user with demand calculated from soil moisture. The method used is given in the Irrigation Water Use section below. User type 2 is an irrigation user with demand fixed. Fixed here means independent of conditions in the model. A seasonal cycle of fixed demands may still be specified. User type 3 is release from a reservoir at the downstream end of a drainage. Such release is not available for use in the drainage, but is available for use in the downstream drainage. Lake Whatcom fish hatchery releases are implemented as user type 3. Users type 4-9 and 11 are all handled exactly the same in TOPNET, the different types being for information and use by other models, such as the water quality model. For these users, a demand is requested from a source at a specified location, with a designated return flow to a specified return flow location. User type 10 specifies an instream flow in the stream at the outlet of a drainage. Return flow is to the downstream drainage. User type 12 is used to designate the withdrawals to an off stream reservoir. An instream reservoir automatically has the streamflow entering the drainage, as well as runoff from the drainage as input. Users types 13 and 14 specify releases from instream and offstream reservoirs respectively.

Each user is designated as taking water from up to 10 sources. Each source is designated as one of the following types:

- Surface water
- Groundwater
- Reservoir

Each surface and groundwater source has a drainage designated as the location, together with the physical daily and annual maximum volume of water that can be supplied from that source. These are intended to represent infrastructure capacities. Each source may also have a designated water right that specifies the associated priority date and legal daily and annual maximum amounts that the source can supply. When run in Water Rights Allocation mode, the model will assign water to users from sources in priority date order and enforce water right daily and annual total amounts. When run in demand allocation mode, water rights information is ignored.

Unless the user is an irrigation user, the demand is calculated as the product of the demand variable and demand rate. The demand variable should be a unit quantity such as the population or head of cattle for the calculation of demand. The demand rate is then the per unit (e.g., per capita) demand. A monthly demand pattern may be specified for each user.

Irrigation Water Use

Irrigation water use is modeled for surface water quantity using soil-moisture content to derive irrigation demand amounts. Irrigation demand can also be specified as a fixed seasonal pattern, similar to the approach used for non-irrigation demand. This demand is passed to specified sources which may or may not meet the demand depending on the limitations specified by the user in the water management and rights part of the model.

The model calculates reference ET using the ASCE Penman-Monteith method as described in the Evapotranspiration section above. This reference ET together with specific crop coefficients, averaged at the WRIA 1 drainage level drives the simulation of actual evapotranspiration from the vadose zone soil moisture component of the model. Irrigation demand is calculated based upon the simulated soil moisture content. This accounts for weather variability (through ET and effective precipitation), soil properties (through their effects on root zone moisture dynamics), and irrigation efficiency (with losses of irrigation water to interception or runoff being simulated by the Rainfall-Runoff Transformation model component).

The irrigation demand calculations depend upon three input parameters that need to be specified for each WRIA 1 drainage that has irrigation (i.e., irrigated fraction greater than 0):

- Field capacity fraction threshold, T (e.g., 0.5)
- Field capacity fraction goal, G (e.g., 0.9)
- Maximum irrigation rate, R (e.g., 1 in/day, converted and specified to the model as 0.025 m/day)

The soil moisture content in the vadose zone soil store, which represents the root zone over irrigated areas is:

$$\theta = S_r / d \tag{53}$$

where S_r is the depth of water held in the soil zone and d is the depth of the soil zone. Refer to the section above on the vadose zone soil store for how these are defined and calculated. The drainable part of the soil zone, in excess of field capacity is characterized by parameter $\Delta\theta_1$, while the plant available moisture is characterized by $\Delta\theta_2$. These are model parameters that are determined from soil properties. The irrigation goal soil moisture content is defined as:

$$\theta_G = G \cdot \Delta\theta_2 \tag{54}$$

The irrigation threshold soil moisture content is defined as:

$$\theta_T = T \cdot \Delta\theta_2 \tag{55}$$

Irrigation demand is defined, on a sliding scale as varying from 0 when soil moisture content is at or above the goal moisture content and at maximum when soil moisture content is at or below the irrigation threshold. The irrigation demand is thus:

$$D = \begin{cases} R & \text{if } \theta \le \theta_T \\ \dfrac{\theta_G - \theta}{\theta_G - \theta_T} R & \text{if } \theta_T < \theta < \theta_G \\ 0 & \text{if } \theta_G \le \theta \end{cases} \tag{56}$$

Recall that these calculations are done at the scale of a drainage. This sliding scale approach thus reflects the fact that when moisture content over the entire drainage is above the goal (e.g., following rain) that irrigation is likely to be 0, but as moisture content drops (in response to ET drying the soil) irrigation will increase and at the point where moisture content is at the threshold, irrigation will be applied at the maximum rate, if there is water available.

The sequence of model components is such that the Rainfall-Runoff Transformation that performs soil moisture calculations is run before the Water Management component that allocates water to user demands. On a particular day the soil moisture is therefore used to calculate irrigation demand for irrigation that is applied the next day.

Input Data Preparation

Preparation of the complete input data to set up and run TOPNET for WRIA 1 is complex and involved the following broad steps:

1. Geographic Information System (GIS) information comprised of a Digital Elevation Model (DEM), watershed boundaries, stream network and points of interest were combined to establish the topological configuration of the model representing the spatial connectivity between model elements. The WRIA 1 drainages were used as model elements.
2. Spatial information from a number of GIS layers such as soils, land use, mean annual precipitation, and artificially drained areas was used to estimate model parameters for each drainage.
3. Information on users and management options was used to prepare the water management input files.
4. Climate input data comprised of precipitation, temperature, wind, humidity, etc. was assembled into the time series input files
5. Streamflow data was assembled for use in calibration and to drive upstream boundary inputs.

Spatial Inputs

The spatial inputs to the model comprise steps 1 and 2 above. The Universal Transverse Mercator zone 10 projection with North American Datum of 1983 (NAD_1983_UTM_Zone_10N) was used as the spatial reference system for all data for this project.

Topologic configuration

The surface water quantity model is designed to simulate streamflow originating from two dimensional area features referred to as "drainages" routed along the linear channel network and accumulated at points of interest. These three types of input are illustrated in Figure 8 for four drainages in the WRIA 1 tenmile area.

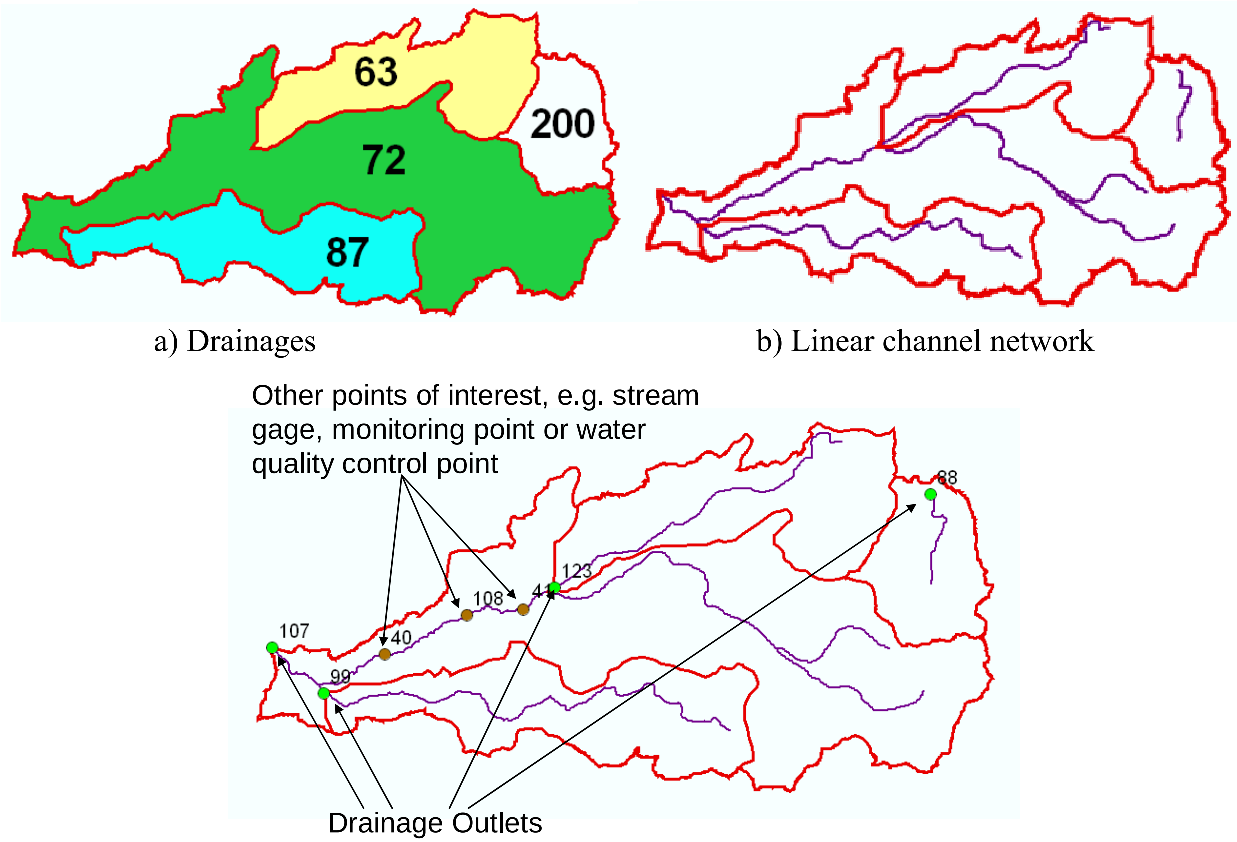

a) Drainages
b) Linear channel network
c) Nodes that define points of interest

Figure 9. Surface Water Quantity Model Configuration.

The drainage labeled with drainage identifier (drainID) 72 is the Ten Mile drainage. This receives inflow from drainage 87 (Deer) and 63 (Four Mile). The drainage to the right (drainID=200) is the internally draining Fazon drainage. There are drainage outlet points of interest at the outlet of each drainage. There are also internal monitoring points along Ten Mile Creek.

The model calculates a single per unit area runoff generated over each drainage. The flow entering the stream network at each node is then this per unit area runoff times the direct drainage area to that node. Within drainage spatial variability resulting in per unit area runoff generation that varies among subareas within drainages is ignored. This assumption is consistent with the level of spatial detail in the model being defined by drainages. Drainages are the finest scale of granularity for which runoff is calculated. If within drainage detail on runoff generation is required, this should be achieved by recalculating or redefining the drainages at a finer scale.

Table 4 lists the initial spatial data used to establish this model configuration.

Table 4. Spatial Input Data

Spatial Input	File information
Digital Elevation Model (DEM)	Dem, 2005 rows, 4491 columns
WRIA 1 Drainages	bsnwria1_v7.shp, 177 polygons
WRIA 1 Points of interest	points_of_interest_v8.shp, 337 points
WRIA 1 Stream network	Net1104.shp, 629 lines

The digital elevation model (DEM) was used as the starting point for a sequence of Geographic Information System (GIS) processing steps, which together with the drainages, points of interest and stream network are used to establish the model spatial configuration. These steps use a number of tools, some of which were customized and adapted for the purpose. TauDEM is a set of terrain analysis tools used for delineation of streams and watersheds (http://www.engineering.usu.edu/dtarb/taudem). Topsetup is the program that prepares inputs for Topnet from streams and watersheds delineated by TauDEM. Nooknet is a program that was developed to consolidate short stream reaches into single reaches to accommodate water quality modeling needs.

Nodes

Nodes are points on the stream network where streamflow is of interest. These comprise streamflow measurement locations, Department of Ecology control points, points of water withdrawal and pour points at the outlet of each drainage. The points of interest are specified as a shape file: Points_of_interest.shp. This contains an attribute table illustrated in Figure 10**Error! Reference source not found.**.

FID	Shape*	ID
0	Point	40
1	Point	41
2	Point	88
3	Point	99
4	Point	107
5	Point	108
6	Point	123

Figure 10. Excerpt from points of interest shape file attribute table. The field headed ID in this shapefile is referred to as Project Node Identifier (ProjNodeID) in this report to distinguish it from other identifiers used for other purposes.

The key field in this shape file attribute table is ID. This ID value is referred to as the Project Node Identifier, ProjNodeID, a unique integer number that identifies this node within the WRIA 1 project. Other fields in the points of interest shapefile are informational and are not used by the surface water quantity model.

Stream network

TauDEM is used to delineate a stream network taking the points of interest as inputs to define nodes on the stream network. Stream network delineation involves the following steps:

1. Calculation of flow directions over the DEM, burning in the stream network and walling the drainage boundaries so that flow directions are calculated consistent with the given stream network and basin boundaries.
2. Specify points of interest shapefile as outlets.

3. Run TauDEM River Network Raster upstream of outlets using the option to use existing streams.
4. Run TauDEM Stream order grid and network files.

The output from this sequence consists of the stream network tree file and stream coordinate file. These are used as input to Topsetup. The stream network tree file defines the topological linkage of the stream network. Columns are as follows:

1. Link Number (Indexed from 0)
2. Start Point Number in Coord.dat (Indexed from 0)
3. End Point Number in Coord.dat (Indexed from 0)
4. Next (Downstream) Link Number (-1 indicates no links downstream, i.e., a terminal link)
5. First Upstream Link Number. 0 indicates no upstream links. Because of this choice the first link with link number 0 must be a terminal link, i.e., not have any links downstream of it. Where only one of these is 0, it indicates an internal monitoring point where the reach is logically split, but does not bifurcate.
6. Second Upstream Link Numbers. See 5 above.
7. Strahler Order of Link
8. Monitoring point identifier at downstream end of link. This inherits its value from the ID field in the outlets shape file so contains ProjNodeID. -1 indicates downstream end is not a monitoring point in the outlets shape file.

<u>Drainages</u>

The "drainage" is the principal spatial element of the model. These have been delineated by WRIA participants, based on topography, local knowledge and areas relevant for management. Drainage identifiers referred to as DrainID are identified by the field header BSNSWRIA1 in the bsnwria1_v7.shp file.

Shape*	OBJECTID	AREA	PERIMETER	BSNSWRIA1
Polygon	68	47941181.675	59772.105	72
Polygon	82	17699646.001	29164.317	87
Polygon	170	17406744.355	27033.877	63
Polygon	171	8695315.54	14339.659	200

Figure 11. Excerpt from attribute table of shape file defining drainages.

A drainage grid was derived from this shape file using an ArcGIS Vector to Raster function. This was used as input to Topsetup, together with the stream network definition files. The drainage grid has the following attribute table.

ObjectID	Value
0	63
1	72
2	87
3	200

Figure 12. Excerpt from drainage grid attribute table

<u>Nodelinks and Basinpars tables</u>

The Topsetup program was used to define the input files for Topnet. These include the Node linkages 'Nodelinks.txt' and basin parameters, 'basinpars.txt' tables.

Table 5. Partial listing of Node links table

NodeId	DownNodeId	DrainId	ProjNodeId	DOutFlag	ReachId	Area	AreaTotal
1	-1	72	107	1	26	3.65E+06	8.31E+07
2	1	72	40	0	30	2.94E+06	6.17E+07
3	2	72	108	0	32	5.49E+06	5.88E+07
4	3	72	41	0	34	3.59E+07	5.33E+07
5	4	63	123	1	42	1.74E+07	1.74E+07
6	1	87	99	1	45	1.77E+07	1.77E+07
7	-1	200	88	1	46	6.52E+06	6.52E+06

Table 6. Nodelinks table field definitions

NodeID	An internally defined node number in a sequence starting at 1.
DownNodeID	The NodeID of the Downstream node. This defines the flow connectivity between nodes determined by the stream network.
DrainID	The drainage containing the node.
ProjNodeID	The point of interest identifier used in the project from the node point of interest file via the stream network tree file .
DOutFlag	A flag to indicate whether this is the most downstream node (outlet) within a drainage (1=Most downstream, 0=not).
ReachId	Ignore this for WRIA. Topnet defines another network topology comprising two reaches for each physical reach. This is the identifier of the topnet reach that ends at this node.
Area	The area (in m^2) draining directly to that node without flowing to another node first .
Areatotal	The total area (in m^2) draining to each node.

Table 7. Partial listing of basin parameters table

CatchID	DownCatchID	DrainID	ProjNodeID	Reach_number	direct_area
1	-1	72	107	26	4.80E+07
2	1	63	123	42	1.74E+07
3	1	87	99	45	1.77E+07
4	-1	200	88	46	8.68E+06

Table 8. Basin parameters table field definitions

CatchID	An internally defined number in a sequence starting at 1 for each drainage (referred to here as catchment).
DownCatchID	The CatchID of the Downstream drainage. This defines the flow connectivity between drainages.
DrainID	The drainage identifier from the drainage grid.
ProjNodeID	The point of interest identifier used in the project from the node point of interest file via the stream network tree file.
Reach_number	Ignore this for WRIA. Topnet defines another network topology comprising two reaches for each physical reach. This is the identifier of the topnet reach that ends at the drainage outlet. This topology was surpassed with the inclusion of water management, but still remains in the code and input.
Direct_area	The area (in m^2) of the drainage.

Figure 13 and Figure 14 illustrate the relationships between identifiers in the drainage and node shapefiles and their connections to basinpars and nodelinks that specify the model configuration.

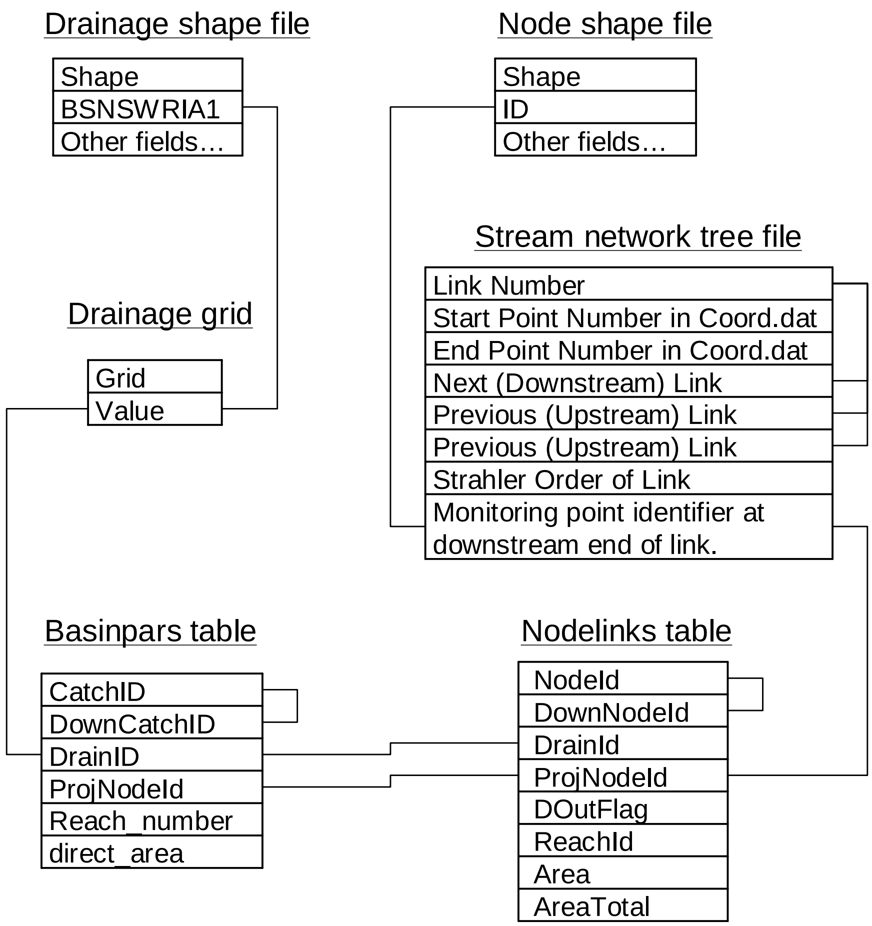

Figure 13. Schema showing node and drainage identifier relationships

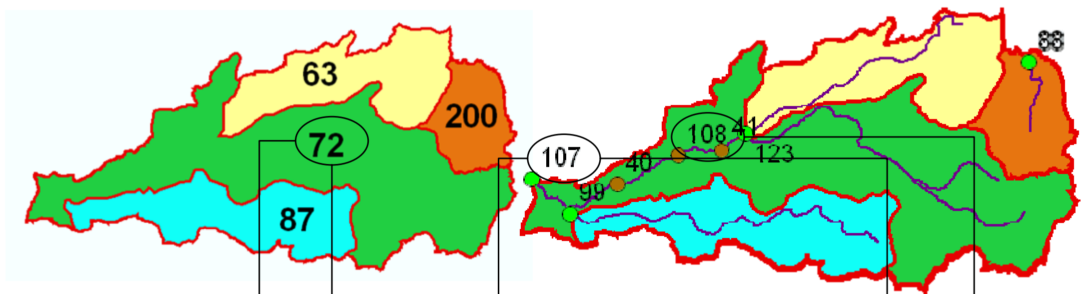

Catch-ID	Down-CatchID	Drain-ID	Proj-Node-Id
1	-1	72	107
2	1	63	123
3	1	87	99
4	-1	200	88

Basin parameters table

Node-Id	Down-Node-Id	Drain-Id	Proj-Node-Id	DOut-Flag
1	-1	72	107	1
2	1	72	40	0
3	2	72	108	0
4	3	72	41	0
5	4	63	123	1
6	1	87	99	1
7	-1	200	88	1

Node links table

Figure 14. Example of node and drainage identifier relationships

<u>Consolidation of short stream reaches to accommodate Water Quality Modeling Needs</u>

The program nooknet has been developed to consolidate short stream reaches into single reaches for water quality modeling. This takes as input the tree.dat and coord.dat produced by TauDEM. Also input is a maximum length parameter indicating the maximum length segment that can be consolidated into a downstream segment. Output comprises a table of <u>junctions</u>, <u>nodes</u> and <u>reaches</u>, as well as a reach shapefile (Figure 15).

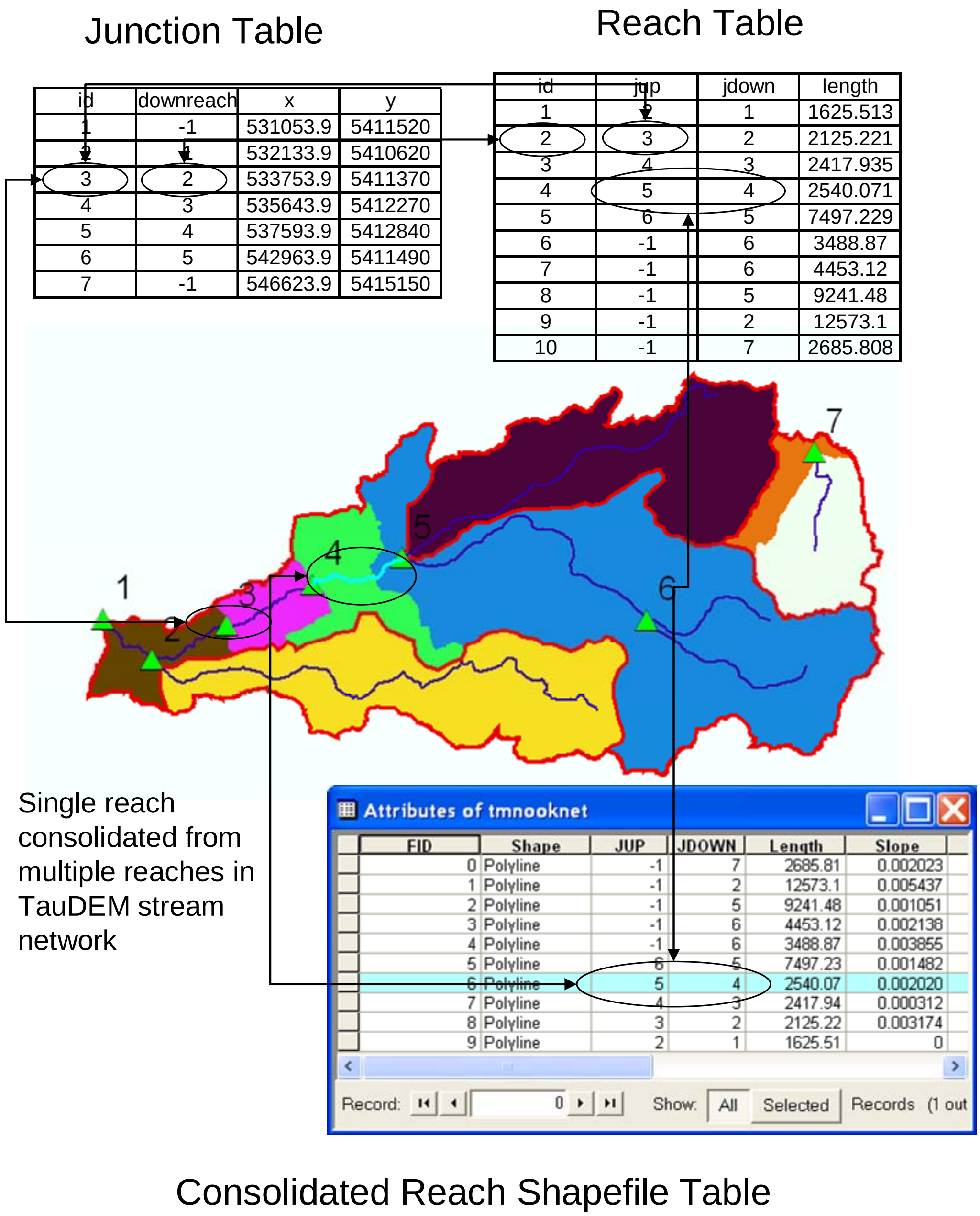

Figure 15. Illustration of consolidated connectivity defined through junction and reach tables

Network connectivity is defined through the junction table and reach table. The junction table has for each junction an '**id**' (identifier) and '**downreach**' field pointing to the outflow reach from this junction. Junctions are where water quality mixing should occur. The reach table has for each reach an '**id**' (identifier) and '**jup**' and '**jdown**' field pointing to the junction at the upstream and downstream end of the reach respectively. Where junctions were previously closer together than the maximum length parameter, they are removed and a single reach formed.

Nodes and Junctions

Each point of interest is associated with a junction. If the point of interest has a junction within the threshold distance downstream it is associated with that junction, otherwise a junction is created at the point of interest. Multiple point of interest nodes may be associated with the same junction. Each point of interest has a direct watershed, referred to as a 'node catchment' and is identified by the nodeID. This is illustrated in Figure 16.

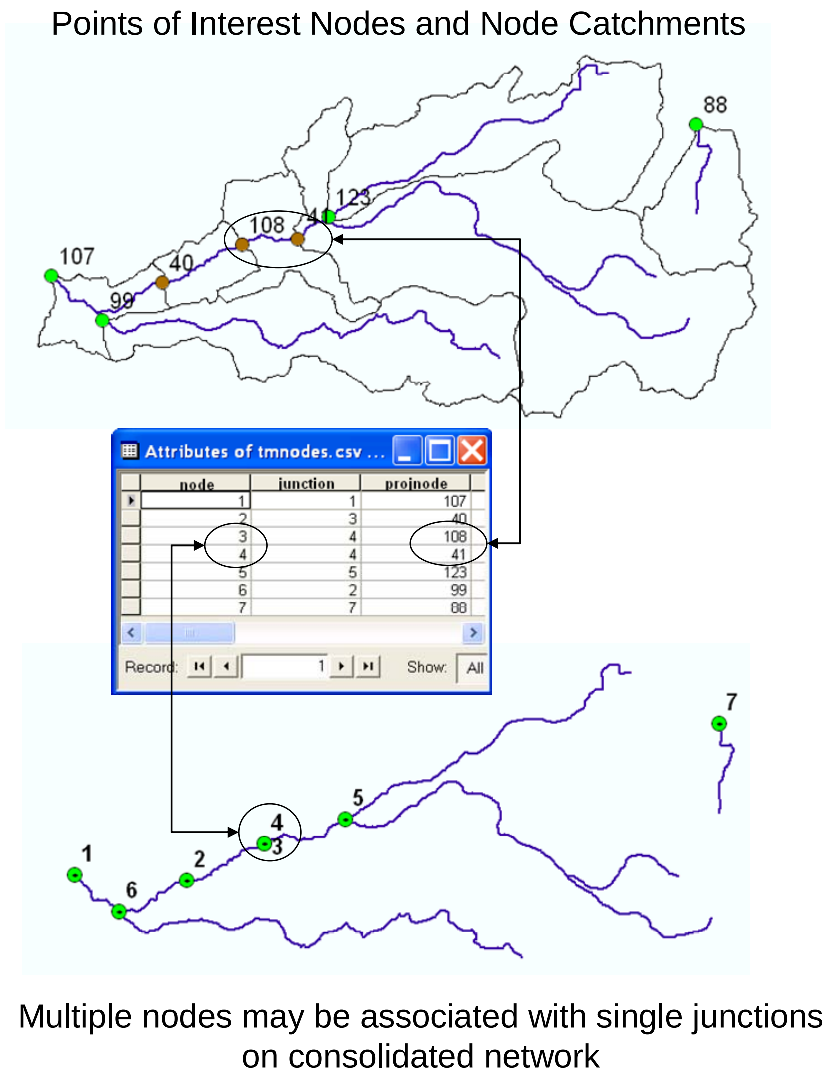

Figure 16. Example of consolidation of nearby points of interest onto a single junction

Nodes, Node Catchment and Drainages

The association between nodes and node catchments is defined in the nodelinks table. NodeId corresponds to the ID of the node catchments grid and shapefile. ProjnodeId corresponds to the ID of the node from the points of interest shapefile. This is illustrated in Figure 17.

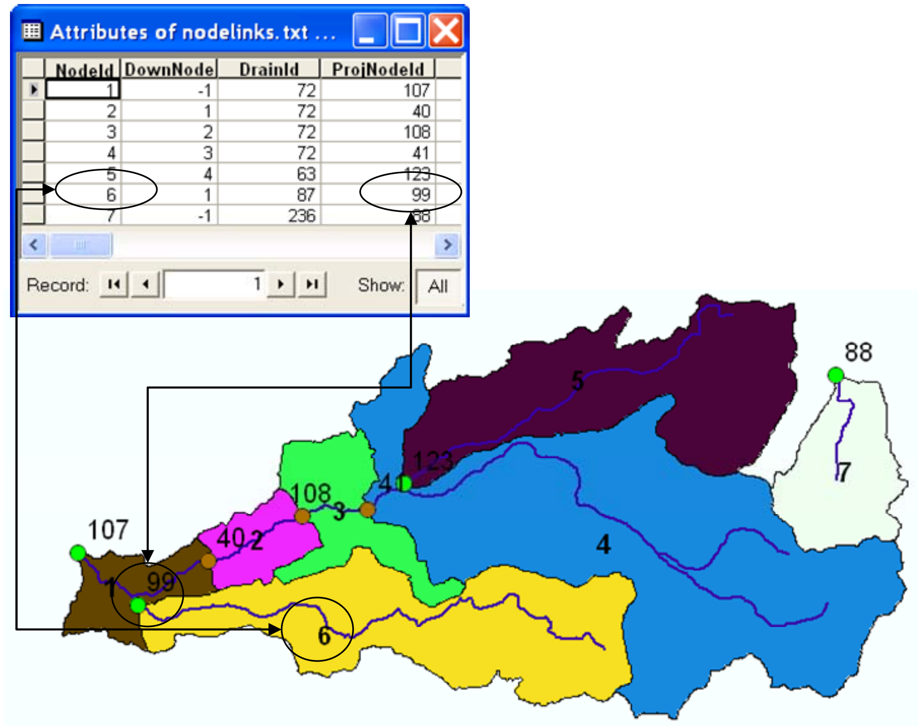

Figure 17. Example of association between nodes and node catchments

Drainage Parameters

Following topologic configuration, parameters for each drainage model element were calculated. Most parameters are computed for each 30 m DEM grid cell then averaged spatially to obtain aggregate values for each drainage. Table 9 lists the spatial data used to estimate model element parameters.

Table 9. Spatial Input Data used for model element parameter estimation

Spatial Input	File information
Topographic wetness index grid	dematanb, 2005 rows, 4491 columns. This stores the ratio tanβ/a which is the inverse of wetness index so as to avoid the divide by 0 error that occurs when slope, tanβ is 0. a, the specific catchment area is never 0.
Distance to stream grid	demdist, 2005 rows, 4491 columns
Soils grid	soils_wqty.asc, 2005 rows, 4491 columns. Associated lookup table lut_soils.xls
Land use and land cover for each scenario	lulc_hist.asc, lulc_fbo.asc, lulc_exist.asc, 2005 rows, 4491 columns
Artificial drainage	ddr_wqty.asc, tdr_wqty.asc, , 2005 rows, 4491 columns
PRISM Annual Rainfall grid	Prism_wqty, 2005 rows, 4491 columns

Topographic Index

The D∞ multiple flow direction approach (Tarboton, 1997) implemented in TauDEM was used to calculate topographic slope (S), specific catchment area (a) and the topographic wetness index ln(a/tanβ) from the DEM. The Topsetup program was then used group the values of topographic index into bins for each drainage, tabulating the lower and upper bound of each bin and the proportion of area within each bin. Topsetup was configured to have no more than 5% of the area in each bin, resulting on average in just over 20 wetness index classes for each drainage. The data giving the proportion of area in each wetness index class for each drainage was written to the input file modelspc.dat.

Distance to streams

A stream raster grid was defined from the initial stream network shapefile (Table 4). TauDEM was used to compute D8 flow directions from the DEM. The TauDEM distance to stream function was then used to compute the overland flow distance from each grid cell to the streams along the DEM derived flow directions. The Topsetup program was then used to group the values of distance to stream into bins for each drainage, tabulating the lower and upper bound in each bin and the proportion of area with distance less than each bin upper bound, thereby providing a cumulative distribution of distances to the stream. Topsetup was configured to have no more than 20% of the area in each bin, resulting on average in just over 5 distance to stream classes for each drainage. The data giving the distributions of distance to stream for each drainage was written to the input file modelspc.dat.

Soils Grid

The soils grid was prepared using a combination of SSURGO and STATSGO data from the following sources.

- SSURGO Pre-release obtained from Mike Pelela (Whatcom County Planning Dept)
- STATSGO data from NRCS (1:250,000 scale)

A search for soils data for Canada was completed, but no adequate data available in electronic form was found. For drainages that include Canada, the soils data for the area-weighted parameters on the U.S. side will be applied to the whole drainage.

STATSGO data is available for the whole U.S. area, while SSURGO covers only the lowlands. Since the SSURGO information represents a finer resolution, we used STATSGO only where SSURGO was not available. The STATSGO polygon coverage was converted to a grid using the numeric portion of the MUID (less the “WA” prefix) as the grid value. The SSURGO polygon coverage was converted to a grid using the “minor 1” field. The soils grid was created to have the same extents and cell size as the DEM.

Table 10 gives the model parameters that were derived from soil data.

Table 10. Model parameters derived from soil data

Model Parameter	Method
$\Delta\theta_1$ (dimensionless)	Equivalent to Available Water Capacity (AWC) parameter in soil databases. Depth weighted average over soil layers to depth of 24 inches.
$\Delta\theta_2$ (dimensionless)	Porosity n derived from n=1-BD/PD where BD is bulk density from soil databases and PD is particle density assumed to be 2.65 g/cm^3. $\Delta\theta_2$=n-$\Delta\theta_1$. Depth weighted average over soil layers to depth of 24 inches.
K_o (m/hr)	Harmonic mean of database saturated hydraulic conductivity to depth of 24 inches. Impermeable layers omitted from this averaging.[1]
d (m)	The sum of layer depths to a maximum of 24 inches (0.61 m).
ψ_f (m)	Derived from clay percentage reported in database – see below.
T_o (m^2/hr)	Integral of hydraulic conductivity over complete soil profile for each map component averaged across map components.

Notes:

1. The harmonic mean is used to average hydraulic conductivity because this hydraulic conductivity parameterizes flow across the layers.

Dingman (1994, page 222) presents a table giving wetting front suction ψ_f, based on soil texture. The STATSGO and SSURGO datasets used provided only the clay percentage so soil texture could not be determined. ψ_f, was therefore estimated based on a weighted average of all possible soil textures for a given range of clay percentage. The averaging weights and resulting estimates of ψ_f for each percent clay class are given in Table 11.

Table 11. Weights used to estimate wetting front suction (ψ_f) from percent clay values with resulting estimates.

Soil Texture	ψ_f Value	Weights of texture based on Percent Clay Values									
		0-10	10-20	20-30	30-40	40-50	50-60	60-70	70-80	80-90	90-100
sand	12.1	0.025	0.015	0.010	0.000	0.000	0.000	0.000	0.000	0.000	0.000
loamy sand	9	0.020	0.020	0.000	0.000	0.000	0.000	0.000	0.000	0.000	0.000
sandy loam	21.8	0.125	0.126	0.125	0.099	0.060	0.013	0.000	0.000	0.000	0.000
silt loam	78.6	0.210	0.212	0.219	0.231	0.250	0.280	0.328	0.353	0.333	0.316
loam	47.8	0.070	0.071	0.073	0.077	0.083	0.093	0.047	0.000	0.000	0.000
sandy clay loam	29.9	0.085	0.086	0.089	0.082	0.054	0.013	0.000	0.000	0.000	0.000
silty clay loam	35.6	0.040	0.040	0.042	0.044	0.048	0.053	0.063	0.078	0.111	0.105
clay loam	63	0.050	0.051	0.052	0.055	0.060	0.067	0.063	0.039	0.000	0.000
sandy clay	15.3	0.045	0.045	0.047	0.049	0.054	0.040	0.000	0.000	0.000	0.000
silty clay	49	0.040	0.040	0.042	0.044	0.048	0.053	0.063	0.078	0.111	0.158
clay	40.5	0.290	0.293	0.302	0.319	0.345	0.387	0.438	0.451	0.444	0.421
ψ_f Value for this class of clay percentage		44.6	44.9	45.9	47.3	49.1	52.1	55.0	55.1	53.6	53.4

Note: ψ_f values shown here in cm. Value converted to meters for use in model.

The model parameters in Table 10 each drainage (model element) were derived by averaging over the grid cells within the drainage. The soils grid and corresponding parameter lookup table are included in the electronic appendix to this report. Aggregate parameter values for each drainage were written to the model input file basinpars.txt.

Land use and land cover

Three land use and land cover scenarios were provided to the surface water quality modeling team as the outcome of other work on this project. Grids of land use and land cover for each scenario were used to determine the following model parameters with values for each land cover class tabulated in the corresponding files in the electronic appendix:

From file lut_lulc.xls

- Canopy Capacity, *CC* (m)
- Evaporation adjustment factor, C_r
- Albedo, α

From file lut_impervious.xls

- Impervious fraction, I_f

From file lut_irrigation.xls

- Fraction irrigated
- Fraction of irrigation that is by sprinklers
- Field capacity fraction threshold for irrigation demand, *T*
- Field capacity fraction goal for irrigation demand, *G*
- Maximum irrigation rate, *R*

Aggregate parameter values for each drainage were written to the model input file basinpars.txt.

Land use and land cover data was also used to obtain the aggregate crop coefficient, K_c, for use in the evapotransipration calculations for each drainage. A K_c value for each land use land cover class for each month was determined following guidance in FAO-56 (Allen et al., 1998). Initial, mid and end K_c values were aligned with estimated planting dates in WRIA 1. The classes in the land use land cover datasets do not distinguish individual crops, so we estimated K_c values for each class based on an assessment of the crop and vegetation types likely in each land use class. The crop coefficient lookup table for each month and land use class are included in the electronic appendix. Aggregate K_c coefficients for each month that average across the land use classes in each drainage were written to the model input file basinpars.txt.

Artificial Drainage

Shapefiles specifying the areas with ditch and tile drainage were provided by WRIA (John Gillies) and converted to grids consistent with the DEM. For the existing and full buildout scenarios these were used to determine the tile drained and ditch drained fraction of each drainage model element as well as assign drainage coefficients (Table 12).

Table 12. Artificial Drainage Coefficients

Type	Coefficient (in/day)	Coefficient (m/hr)
Tile	0.25	0.000257
Ditch	0.075	0.000079375

Aggregate parameter values giving the fraction of each drainage subject to ditch or tile drainage and these drainage coefficients were written to the model input file basinpars.txt.

Precipitation and Climate Interpolation

TOPNET is configured to derive aggregated drainage precipitation inputs as a weighted sum of point precipitation measurements. The weights associated with each gauge for each drainage were calculated as part of the preprocessing by Topsetup using linear interpolation based upon Delauney triangles, adjusted using an annual rainfall surface to account for topographic effects. Let $A(\underline{x})$ denote the normal annual precipitation at location $\underline{x}$. Let P_i denote time step (hourly or daily) precipitation at gauge location $\underline{x}_i$. Let $P(\underline{x})$ denote time step precipitation at a non gauge location $\underline{x}$. We define the normalized time step precipitation at gauge i as:

$$N_i = P_i/A(\underline{x}_i) \tag{57}$$

This is then used to interpolate a normalized precipitation field at any location $\underline{x}$:

$$N(\underline{x}) = \sum_{gauges\ i} \phi_i(\underline{x}) N_i \tag{58}$$

where $\phi_i(\underline{x})$ is a weight function for linear interpolation of normalized precipitation at location $\underline{x}$ from gauges at nodes of the encompassing Delauney triangle. The precipitation estimate for location $\underline{x}$ is then defined, adjusting for the annual rainfall surface, as:

$$P(\underline{x}) = N(\underline{x})\, A(\underline{x}) \tag{59}$$

This can be expanded to:

$$P(\underline{x}) = \sum_{gauges\ i} \phi_i(\underline{x}) A(\underline{x}) N_i = \sum_{gauges\ i} \left\{ \phi_i(\underline{x}) \frac{A(\underline{x})}{A(\underline{x}_i)} \right\} P_i = \sum_{gauges\ i} w_i(\underline{x}) P_i \tag{60}$$

where the term in {} defines the weight associated with each gauge, $w_i(\underline{x})$, for estimating the precipitation at location $\underline{x}$. This is integrated over each drainage to obtain:

$$Pb = \sum_{gauges\ i} \frac{1}{A} \int w_i(\underline{x})\, dx\ P_i = \sum_{gauges\ i} wb_i\ P_i \tag{61}$$

where Pb is the drainage average precipitation at each time step represented as a weighted linear combination of the gauge precipitation values. The weights associated with each gauge do not depend upon time and are given by:

$$wb_i = \frac{1}{A} \int w_i(\underline{x})\, dx \tag{62}$$

Topsetup evaluates these weights and writes them to the modelspc.dat file for input to TOPNET.

This procedure provides a way to estimate precipitation as a smooth surface based on nearby surrounding gauges while at the same time adjusting point gauge values, which are often recorded at low elevation, for topographic effects that are represented by the annual precipitation surface $A(\underline{x})$. Here the annual precipitation surface was obtained from Oregon State University Climate Center (http://www.prism.oregonstate.edu/) produced using the PRISM method (Daly et al., 1994). PRISM estimates precipitation (and other climate variables) based on regression using nearby stations and topographic attributes such as slope and aspect. The PRISM Annual Rainfall Grid file (Table 4) was produced by merging a high resolution PRISM dataset that provided cross Canadian border coverage, but just within the WRIA 1 boundary, with a lower resolution dataset for the State of Washington to extend the coverage to the location of some precipitation and climate stations that are nearby, but outside the WRIA 1 watershed boundary that we used to drive the model.

In addition to precipitation, TOPNET is also driven by inputs of daily maximum and minimum temperature and dew point. These are input at the same locations as precipitation and need to be interpolated to obtain appropriate values for each drainage model element. A similar weighting scheme is used for these variables, but without the annual surface adjustments. The annual surface for temperature is taken as 1, so that in equation (60) we have $\phi_i(\underline{x})=w_i(\underline{x})$. A set of weights from equation (62) are obtained for each basin and written to the input file interpweight.dat that is used by TOPNET. Temperature in TOPNET is then calculated using

$$Tb = \sum_{gauges\ i} wb_i\ (T_i + (z_i - z_b)\cdot\lambda) \qquad (63)$$

where T_i is temperature at gauge i at elevation z_i, z_b is the average elevation for the drainage and λ is the lapse rate giving the decrease of temperature with elevation.

The lapse rate of 5.3 C/km was used for all drainages in WRIA 1. This was derived from the National Weather Service (NWS) and SNOTEL stations. Figure 18 shows the linear regression of mean annual temperature versus station elevation that was used to determine this lapse rate.

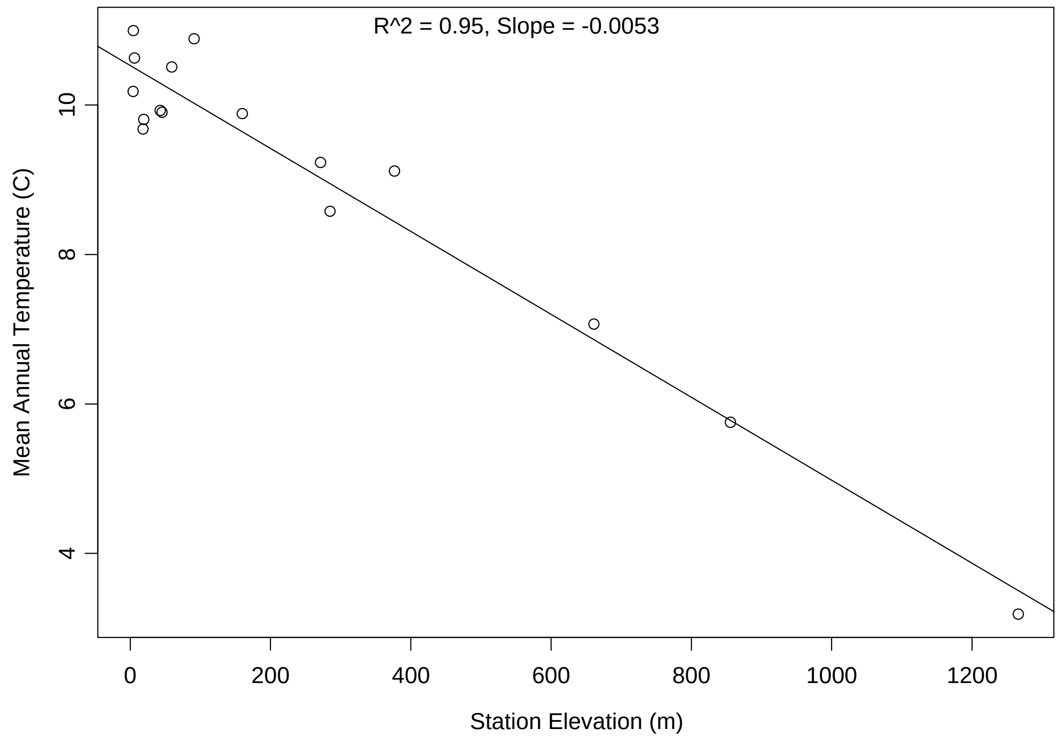

Figure 18. Empirical lapse rate determination.

The same lapse rate was used for maximum, minimum and dew point temperatures.

Management Inputs

In preparing the water management inputs information from a number of data sources was examined and combined. These sources included:

- Whatcom County
- Washington Department of Ecology (Wastewater treatment plant information)
- Washington Department of Health (Public Water Supply Information)
- City of Bellingham (Information on Lake Whatcom releases)
- US Environmental Protection Agency

The following information has been assembled to model water use aggregated at the drainage scale:

- Public water supply GIS grid (pws.asc). This contains the public water supply identifier (equivalent to department of health identifier) at each grid cell so that the part of each drainage served by a specific public water supplier can be identified. 32 public water supplies are identified.
- Table of public water supply sources (PWS_existing_sources.xls). This identifies the source location (drainage) and source type (surface or groundwater) for each of the 32 public water supplies. In the case of the City of Ferndale, there are two sources representing surface water from the Nooksack river and groundwater from drainage 83 (Schell).

- Drainage population table (population_data.xls). This spreadsheet contains population for each drainage in 2000 and projected for 2022 used for the full buildout scenario.
- Return flows table (ReturnFlow.xls). This spreadsheet identifies the wastewater treatment plants associated with some public water supplies for return flows, and includes additional return flow information.
- Dairy users spreadsheet (additional_users.xls). This spreadsheet contains estimates of the number of cows per drainage used to estimate dairy water use. The demand rate per cow is from Water System Design Manual Chapter 5 (http://www.doh.wa.gov/ehp/dw).
- Middle fork diversion: 42277 m^3/day. Cubic meter per day equivalent of total gallons withdrawn in 1999 and 2000.
- Fish Hatchery instream flow 25689 m^3/day from year round flow requirement of 10.5 cfs.

The computer files listed above are included in the electronic appendix to this report.

Table 13 lists the water management files needed to run TOPNET. The relationships between these files was shown in Figure 8.

Table 13. TOPNET Water Management Files

File	Description
User.txt	Provides information about users to water accounting model.
Source.txt	Specifies location, type and physical limits associated with each water source.
SourceMixing.txt	Specifies the proportioning between sources providing water to users.
SeasonsDefn.txt	Specifies the days that define seasons for changing the proportions among user sources.
Reservoir.txt	Specifies information on reservoirs .
MonthlyDemandFraction.txt	Specifies how user demand varies over the year.
ReturnFlow.txt	Specifies the location and quantity of return flows.
Rights.txt	Specifies water right information for data sources.

The User.txt file is the principle file water use model input file. Because it is linked to many of the other files, it was necessary to prepare the other file first.

Source.txt

Each drainage is a potential source of the surface water (from stream) or a groundwater. Sources of surface water are identified as type 1, while sources of groundwater are of type 2. Sources identifiers were generated as sequential numbers for all Source Location Ids represented by WRIA 1 drainages (identified by DrainID) regardless of whether they were actually used as a source for withdrawal or not. This then guaranteed that when a DrainID was specified as a source location that there would be a corresponding source. The physical daily maximum and physical annual maximum threshold for each of these sources was set to a large number because we did not have information on physical limits to source withdrawals from each drainage. The 172 drainages modeled resulted in 344 sources. Lake Whatcom was added as source number 345 with type 3, indicating its use as a reservoir.

SourceMixing.txt

A user may draw water from multiple sources. When this is the case the source mixing table is used to specify the proportion drawn from each source. Four source mixing categories have been configured in Sourcemixing.txt:

1. 20% from source 1 and 80% from source 2. This is used to represent the combined use of surface (20%) and groundwater (80%) for self supplied commercial/industrial/transportation users based on annual water use data from the USGS for Whatcom County.
2. 20% from source 1 and 80% from source 2. This is used to represent the combined use of surface (20%) and groundwater (80%) for Dairies.
3. 70% from source 1 and 30% from source 2. This is used for dairies and irrigation with the 70% corresponding to groundwater sources and 30% corresponding to surface water sources.
4. Equal distribution between two sources (50%:50%). This is used for the City of Ferndale distribution between ground and surface water sources because the City buys water from the City of Bellingham while completing the demand with groundwater withdrawals.

SeasonsDdfn.txt

The model provides the capability for the proportions of water taken from sources to vary seasonally as specified in the seasons definitions table linked to each source mixing record. This capability has not been exploited and a single season starting on day 1 and ending on day 366 of the year has been used.

MonthlyDemandFraction.txt

The monthly demand fraction table defines the variation in demand associated with each user by month over the year. Five monthly demand fractions have been set up and assigned as follows:

1. Residential. Varies from 0.8 in winter to 1 in summer.
2. Commercial, Industrial and Transportation. Held constant.
3. Dairy. Held constant.
4. Diversions and instream flows. Held constant.
5. Irrigation. Varies from 0 in winter to 1 in summer. Only used when irrigation demand is fixed, rather than driven by soil moisture.

ReturnFlow.txt

The return flow table is used to specify for the model the portion of water use that converted to return flow and the final destination of return flow. The following return flow proportions were specified in the return flow table:

- Public water supplied residential water users: 0.1
- Self-supplied residential water users: 0.05
- Public water supplied commercial/industrial/transportation users: 0.2
- Self-supplied commercial/industrial/transportation users: 0.1
- Dairies: 0.1

- Middle Fork Diversion: 1 to represent the interbasin transfer of water.

Return flow is not specified for irrigation users because the model accounts for what happens to irrigation based on its modeling of evapotranspiration (crop water use), runoff generation, infiltration, and drainage.

Return flow may go either to surface or groundwater. For self-supplied users and dairies return flow was assumed to return to the groundwater of the drainage where it is used. For public water supplies serving residential areas return flow may be through a wastewater treatment plant, or if a wastewater treatment plant is not identified return flow is to groundwater in the same drainage.

ReturnFlow.xls in the electronic appendix gives return flow details.

Reservoir.txt

Lake Whatcom is the single reservoir that has been implemented in the system. An active storage capacity of 18 x 10^6 m^3 has been specified. This was calculated as the volume between the levels of 311.5 ft and 314.5 ft. The 311.5 ft level is the target level to which the lake is drawn down at the end of summer. The 314.5 ft level is the target level to which the lake is filled at the beginning of summer.

Rights.txt

The water rights table specifies the priority date as well as legal daily and annual allowable takes from each water source. This is used to determine the priority order in which water use is assigned when the model is run in water rights mode. The water rights table has not been populated.

User.txt

A matlab script was used to generate the users table from the information above according to the following rules:

- A single residential water user was created for each public water supply source (PWS_existing_sources.xls) with return flow to a wastewater treatment plant (as specified in ReturnFlow.xls). The demand variable was population. This was estimated for each drainage and summed. The population density was calculated by dividing drainage population by the area that is in land cover land use class residential (both low and high intensity). The area of this residential land cover class that intersects the public water supply service area and was then multiplied by population density to obtain the population served by the public water supply. A per person demand rate of 0.3785 m^3/day is specified (equivalent to 100 gal/day).
- A single commercial, industrial and transportation water user was created for each public water supply source (PWS_existing_sources.xls) with return flow to a wastewater treatment plant (as specified in ReturnFlow.xls). The demand variable was area in acres of land with land cover land use class =23 representing commercial, industrial and transportation intersecting the public water supply service area. A per acre demand rate of 13.4 m^3/day was specified. This is equivalent to 3540 gal/day per acre. This rate was obtained by dividing the USGS 2000 Industrial water use reported for Whatcom County

(38.8 Mgd) by the area in acres of Commercial, Industrial and Transportation land use (49,273 acres).

- For public water supply systems that to not discharge to a wastewater treatment plant a separate residential user was created for each drainage. The return flow was specified as to groundwater in the drainage of use. The demand variable was population. This was estimated for each drainage by dividing drainage population by the area that is in land cover land use class residential (both low and high intensity) then multiplying by the residential area within the service area of the public water supply system. A per person demand rate of 0.3785 m^3/day is specified (equivalent to 100 gal/day).
- For public water supply systems that do not discharge to a wastewater treatment plant a separate commercial, industrial and transportation user was created for each drainage. The demand variable was area in acres of land with land cover land use class = 23 representing commercial, industrial and transportation intersecting the public water supply service area. A per acre demand rate of 13.4 m^3/day was specified as for 2 above.
- A residential user was created for the area that is residential within each drainage but is not served by a public water supply in each drainage. The population and demand rate is estimated as for 3 above. The source location is specified as groundwater.
- A commercial, industrial and transportation water user was created for the area that is land use class = 23 but is not served by a public water supply in each drainage. The acreage and demand rate is estimated as for 4 above. The source location is specified as 20% groundwater, 80% surface water.
- An irrigation user was created for each drainage that has irrigated fraction greater than 0. The demand variable is the irrigated area in m^2, determined from the area of the drainage and the irrigated fraction. The source location is specified as 70% groundwater, 30% surface water. The usertype was set as 1 to indicate soil moisture driven irrigation.
- The dairy users spreadsheet (additional_users.xls) was used to create dairy water users for each drainage based on the number of cows.
- A user was created to represent the middle fork diversion of 42277 m^3/day.
- A user was created to represent the Fish Hatchery instream flow of 25689 m^3/day.

Climate Input Data

The model was driven by precipitation, maximum and minimum temperature and dew point inputs from 16 NCDC weather stations, two SNOTEL stations and the Abbotsford, BC, Canada weather station (Table 14, Figure 19).

Table 14. Climate Stations used to drive the TOPNET model over WRIA 1

Station ID	Name	Source	Number of days in precipitation record	Start	End
71108	ABBOSTFORD AIRPORT	CANADA	22383	10/1/1944	9/29/2005
2131	WELLS CREEK SNOTEL	SNOTEL	3643	10/1/1995	9/29/2005
2132	ELBOW LAKE SNOTEL	SNOTEL	3643	10/1/1995	5/31/2006
450176	ANACORTES	NCDC	26864	1/1/1931	5/31/2006
450564	BELLINGHAM 2 N	NCDC	19167	1/1/1931	4/30/1985
450566	BELLINGHAM KVOS	NCDC	2852	4/1/1998	5/31/2006

450574	BELLINGHAM INTL AP	NCDC	18191	1/1/1949	6/30/2001
450587	BELLINGHAM 3 SSW	NCDC	7593	8/1/1985	5/31/2006
450729	BLAINE	NCDC	26142	1/1/1931	5/31/2006
451484	CLEARBROOK	NCDC	27310	1/2/1931	5/31/2006
451679	CONCRETE PPL FISH STN	NCDC	26931	1/1/1931	5/31/2006
452157	DIABLO DAM	NCDC	26722	1/1/1931	5/31/2006
453160	GLACIER R S	NCDC	14171	7/1/1934	7/31/1983
455663	MOUNT BAKER LODGE	NCDC	3759	1/1/1931	12/31/1952
455678	MOUNT VERNON 3 WNW	NCDC	17529	1/1/1956	1/31/2005
455840	NEWHALEM	NCDC	17032	1/1/1959	5/31/2006
457185	ROSS DAM	NCDC	16620	9/1/1960	5/31/2006
457507	SEDRO WOOLLEY	NCDC	26877	1/2/1931	5/31/2006
458715	UPPER BAKER DAM	NCDC	14672	10/1/1965	5/31/2006

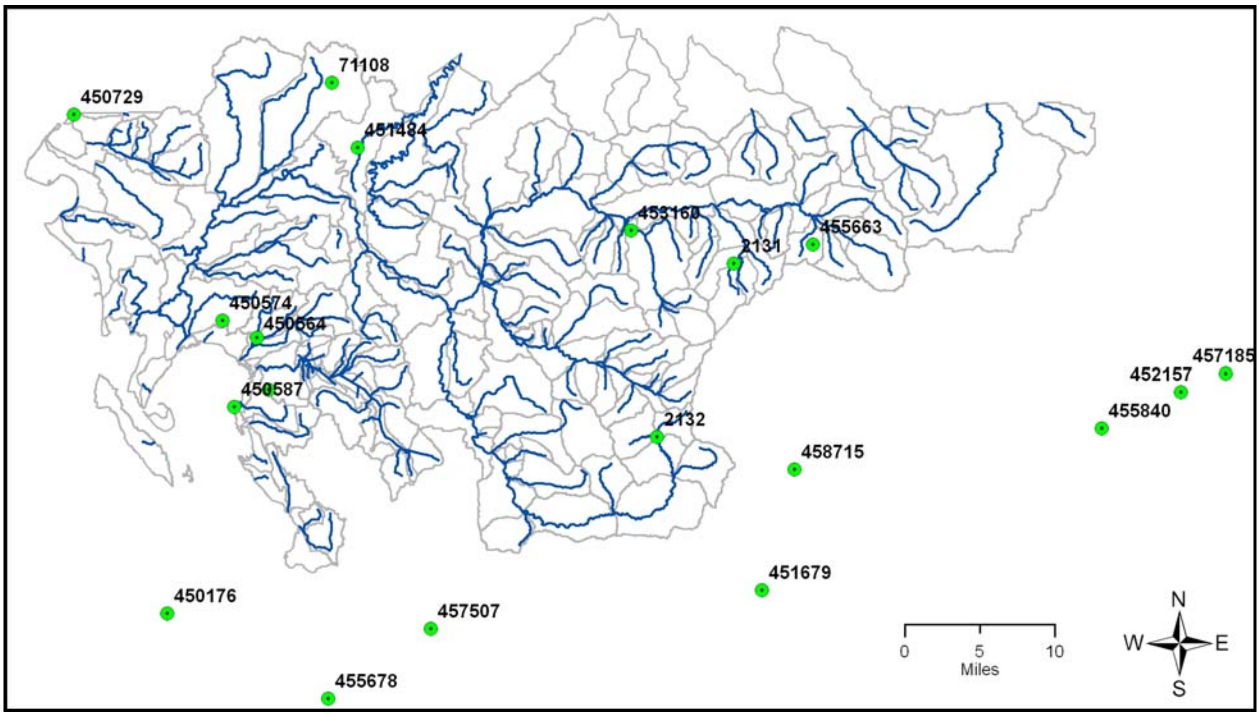

Figure 19. Climate Stations used to drive the TOPNET Model over WRIA 1

Missing climate data was filled in using regression. For each series (precipitation, maximum and minimum temperature and dew point) we computed the correlation between all stations for the periods of overlapping record. When data at a station was missing the highest correlated station in the dataset for which data was not missing was used to fill in the missing data. Precipitation data was filled in used linear regression constrained to go through the origin, so that if the nearby highest correlation station did not have precipitation, the filled in value would also be zero. Temperature and dew point were filled in using standard regression. On rare occasions this infilling procedure resulted in maximum temperatures that were less than minimum temperatures. When this occurred the maximum and minimum temperatures were switched.

Streamflow Data

Upstream boundary streamflow inputs

Many of the streams draining the Mt Baker region within WRIA 1 receive input from glacial melt. In modeling the streamflow from highland areas with substantial glacial melt the following considerations apply:

- The estimates of precipitation inputs in the highland areas is uncertain due to orographic effects not fully captured by the PRISM and Delauney triangle interpolation approach.
- The surface water quantity model does not include a detailed glacier melt model. Modeling glacial melt requires surface temperature and energy inputs which are not available for the glacial areas and would have to be extrapolated from available climate data, introducing uncertainty.
- There are no management options that will modify glacial melt.
- There are no management options that will impact the natural stream flow originating in these highland areas.

In light of these considerations, rather than trying to model glacial melt and thereby introduce unwarranted uncertainty into the streamflow we deemed it better to use streamflow measurements directly. We therefore used measured streamflow at four locations as upstream boundary streamflow inputs. Table 15 lists the stream gauges used as upstream boundary streamflow inputs.

Table 15. Gauges used for Upstream Boundary Stream flow Inputs

Node	Station number	Station name	Drainage area (square miles)	Period of record	Years of record	Daily mean discharge cfs
8	12205000	NF Nooksack River blw Cascade Creek near Glacier	105	1938-present	62	809.3
21	12208000	MF Nooksack River near Deming	73.3	1910-11; 1920-21; 1934-35; 1954*; 1965-70; 1992-present	20	499.1
18	HNW-2052	Glacier Creek near Glacier	13.5	1984-88	5	112.1
25	12209000	SF Nooksack River near Wickersham	103	1935-77;1980-present	63	741.3

The locations of these gages are shown in Figure 21 together with stream gauges used for calibration.

<u>Filling Missing Data and Extending the Period of Record of Daily Flows for Boundary Streamflow Inputs</u>

The target simulation period of record is 1961-1990. This period was chosen to be sufficiently long and representative of both phases of Pacific inter-decadal climate oscillation (PDO), to provide meaningful evaluation between management alternatives. However, calibration used time periods chosen based upon data availability that started as early as 1948 and ended in 2001. Input data was prepared to cover this full period. Observed streamflow was not available for this full period of interest at two of the upstream boundary gage locations. The missing data was filled using regression with nearby stream gages with similar characteristics. Log transformed streamflow was used in these regressions because this streamflow data is better approximated by a log-normal rather than a normal distribution. Also a log-transform avoids the introduction of negative values that can occur with untransformed data. Figure 20 shows the scatter plot of daily flow values and linear regression results for two of the gages that were extended. The Y-axis in each plot is the gage that was extended, and the NF Nooskack gage used to extend it is on the X-axis. The title of each plot shows the coefficient of determination (R^2) and the slope of the least-squares regression line. The coefficient of determination indicates the goodness-of-fit, and the slope indicates the relationship between the two gages.

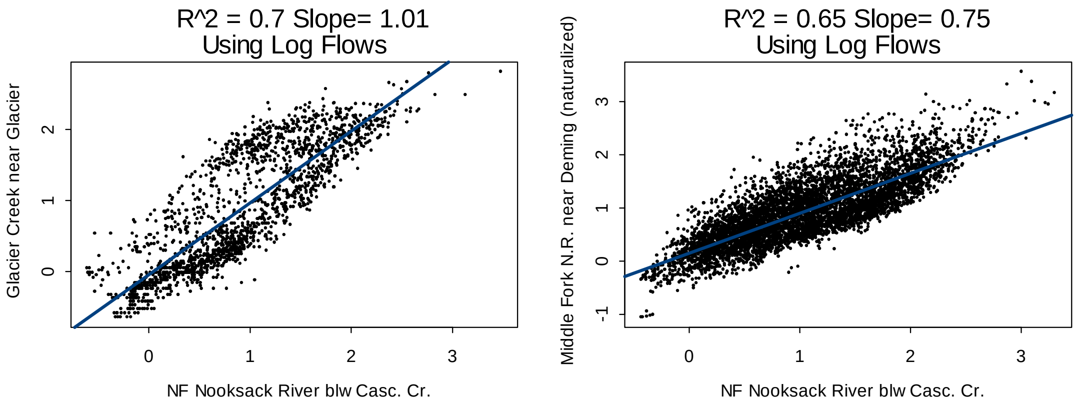

Figure 20. Scatter-plots of daily flow per unit area (log-transformed) with least squares-regression line for the highlands flow boundary condition control points that were extended.

Streamflow Data Used for Model Calibration

Daily streamflow data was used for calibration. Table 16 gives the streamflow gauges used for model calibration. These gauges were selected based on the availability of streamflow data for common calibration periods. The calibration periods were selected as periods where there was generally more data available and representative of differing climate inputs (i.e., wet and dry years). Figure 21 shows the locations of streamflow gauges used.

Table 16. Streamflow Data Used in Surface Water Quantity Model Calibration

Node	Station number	Station name	Drainage area (square miles)	Period of record	Years of record	Daily mean discharge cfs
Highland collector						
14	12207200	NF Nooksack River near Deming	282	1964-75	11	1648.0
Highland drainage						
13	12206900	Racehorse Creek at North Fork Road near Kendall	10.8	1999-present	2	51.5
12	12207000	Coal Creek near Kendall	4.6	1948*;1954*	<1	7.9
27	12209500	Skookum Creek near Wickersham (see note 1)	23.1	1948-69, 1993-present	29	137.5
Lowland Drainage						
32	12202050	Smith Creek near Bellingham	5.12	1968-69	2	14.4
34	12202300	Olsen Creek near Bellingham	3.8	1968-69	2	10.7
35	12204000	Squalicum Creek at Bellingham	12	1948*;1954*	<1	7.2
11	12206000	Kendall Creek at Kendall	24	1948-50	3	25.9
15	12206500	Kendall Creek at mouth at Kendall	29.2	1954*	<1	18.4
3	12212000	Fishtrap Creek at Lynden	22.3	1948-71	24	37.5
4	12212050	Fishtrap Creek at Front Road at Lynden	27.7	1999-present	3	67.7
7	12212500	Bertrand Creek near Lynden	40.3	1948*;1954*	<1	15.5
40	12212900	Tenmile Creek near Laurel	23.6	1968-72	5	30.6
39	12213000	Tenmile Creek near Ferndale	22.7	1948*;1954*	<1	8.1
6	12213500	California Creek near Custer	6.8	1954*	<1	1.4
5	12214000	Dakota Creek near Blaine	18.4	1948-55	8	28.1
16	12214500	Sumas River near Sumas	33	1948-	<4	60.9
46	12215000	Johnson Creek at Sumas	23	1954*	<1	19.4
47	12215100	Sumas River near Huntington BC	57.6	1952-59 (EC); 1960-78 (USGS); 1979-present (EC)	19	115.9
44	08MH152	Bertrand Creek at International Boundary BC	16.9	1984-86*;1987-	13	11.4
45	08MH153	Fishtrap Creek at International Boundary BC	8.1	1984-86*;1987-	16	25.6
43	08MH156	Pepin Creek at International Boundary BC	2.8	1985-present*	15	8.2
MAINSTEM COLLECTOR						
23	12210500	Nooksack River at Deming	584	1936-57;1958-present	64	3501.3
42	12211500	Nooksack River near Lynden	648	1945-67	23	3698.0
38	12213100	Nooksack River at Ferndale	786	1967-present	33	3835.1
Notes						
1. Streamflow at this location is available 1948-1969 under gauge #12209500, then from 1993 to present under gauge # 12209490, Skookum Creek above diversion near Wickersham. These two records were merged						
2. Daily mean discharge is based on all the data available in the period 1 January 1944 to 31 December 2001.						

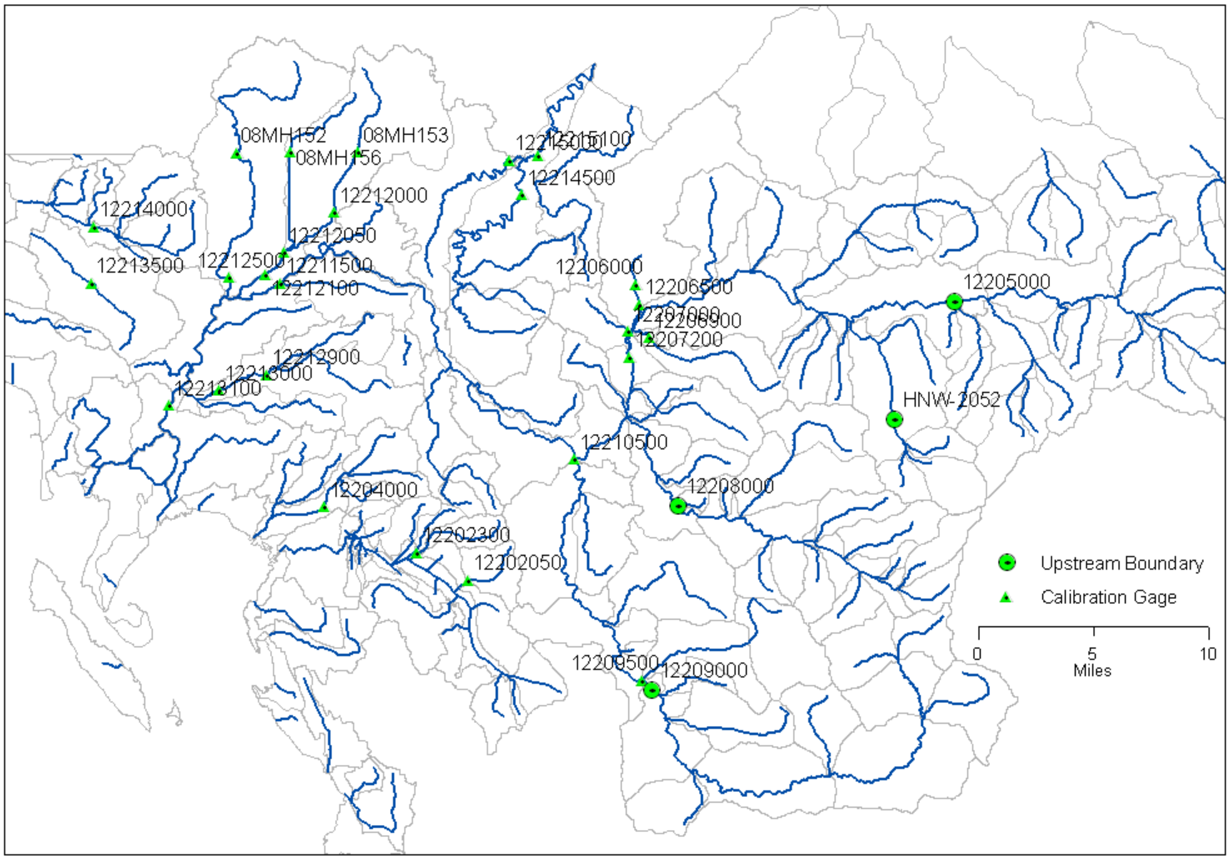

Figure 21. Streamflow gauges used in surface water quantity model for calibration and as upstream boundary inputs

Table 17 lists the four time periods chosen for calibration and three additional time periods chosen for model validation.

Table 17. Calibration and Validation Time Periods

	Calibration		Validation	
	Start	End	Start	End
1	10/1/1947	9/30/1950	10/1/1953	9/30/1954
2	10/1/1967	9/30/1971	10/1/1988	9/30/1989
3	10/1/1984	9/30/1988	10/1/1992	9/30/1993
4	10/1/1998	9/30/2001		

The calibration periods were chosen to represent extended periods of up to 4 years with good data availability. The validation periods were chosen to be single years with wet, average and dry conditions and good data availability so as to span the range of natural variability. The first calibration period is one where the availability of data for several lowland gauges overlap. The second calibration period captures much of the flow information for the reaches into Lake Whatcom (Smith Cr., Olsen Cr.). It also contains flow information on gauges at three lowland drainages including Sumas River, Tenmile and Fishtrap. The third period focuses on lowland areas in Canada, while the fourth and most recent period capitalizes on data available in Fishtrap and Lake Whatcom and includes recent data available on Racehorse Creek and Skookum Creek.

The first validation year (1954) was one with relatively wet conditions. The second validation year (1989) was relatively normal, while the third (1993) was dry.

Model Calibration

Calibration Using Parameter Multipliers

The section on input data preparation above gives the procedure whereby model parameters were estimated from soils, land use and other spatial information. This resulted in a set of a priori parameters for each drainage. It would be possible, in principle, to calibrate the model by adjusting parameters separately for each drainage; however, this would result in an unworkable number of parameters to adjust. It would also not be physically justifiable and would amount to over-fitting the model to the data available, and would reduce the justification and basis for extending the model to ungaged locations. The calibration procedure used applied multipliers to a subset of the parameters, limiting the number of adjustments to be made and retaining the spatial pattern obtained from the a priori parameter estimation based on spatial inputs. The calibration multipliers multiply the corresponding parameter in each drainage by the multiplier value thereby adjusting the parameters over the entire watershed in a similar way. Achieving a fit to streamflow at gaged locations in this manner results in a model where it is justifiable to interpret model results at ungaged locations as reasonable estimates of flow at these locations. Table 18 lists the parameters used in this procedure and the final set of multipliers at the end of calibration. This calibration was done by hand relying on the experience of the model developers (primarily Ross Woods of NIWA, New Zealand) as to the adjustments most appropriate to achieve a fit between model and observed flows. This hand calibration retains a maximum of the parameters at their a priori values enhancing the physical justification for the predictions at ungaged locations. Where the parameter multiplier is 1 the a priori parameter value was not changed.

Table 18. Parameter Multipliers after Calibration

Notation	Description	Multiplier
f (m^{-1})	Saturated store sensitivity	0.55
K (m/hr)	Vadose zone vertical saturated hydraulic conductivity	10
$\theta\Delta_1$	Drainable moisture content	1
$\theta\Delta_2$	Plant available moisture content	1
d (m)	Soil Store depth	1
c	Soil zone drainage sensitivity	1
ψ_{ϕ})μ(	Wetting front suction	1
V (m/hr)	Overland flow velocity	0.1
CC (m)	Canopy capacity	1
Cr	Intercepted evaporation enhancement	1
Albedo	Incident radiation reflectivity	1
T_o (m^2/hr)	Soil profile lateral conductivity	45
I_f (m^{-1})	Impervious fraction	0.5

In addition to adjustment of model parameters through multipliers we also compared the overall water balance comprised of precipitation, streamflow and evaporation losses over the calibration watersheds. We found that no matter how the parameters were adjusted there was insufficient rainfall at some of the rain gages to provide a realistic simulation of streamflow. This is a common problem in mountainous areas with sparse rain gage networks that do not provide good estimates of rainfall inputs. Here this was addressed by increasing the precipitation in the Eastern half of the catchment by a factor of 1.4 (i.e. 40%). This was achieved by changing the weighting factors associated with the following rain gages in modelspc.dat: 453160, 2131, 455663, 2132, 458715, 451679, 455840. The location of precipitation gages is shown in Figure 22.

The input files used for model calibration consisted of those for the existing conditions scenario being modeled. This means that land cover and artificial drainage were modeled as for existing conditions. However, during the process of model calibration, user withdrawals and diversions as specified in the water management input files were turned off. This is because we believe that the user withdrawals specified for existing conditions do not reflect the water management present for the calibration periods that extend as far back as 1947.

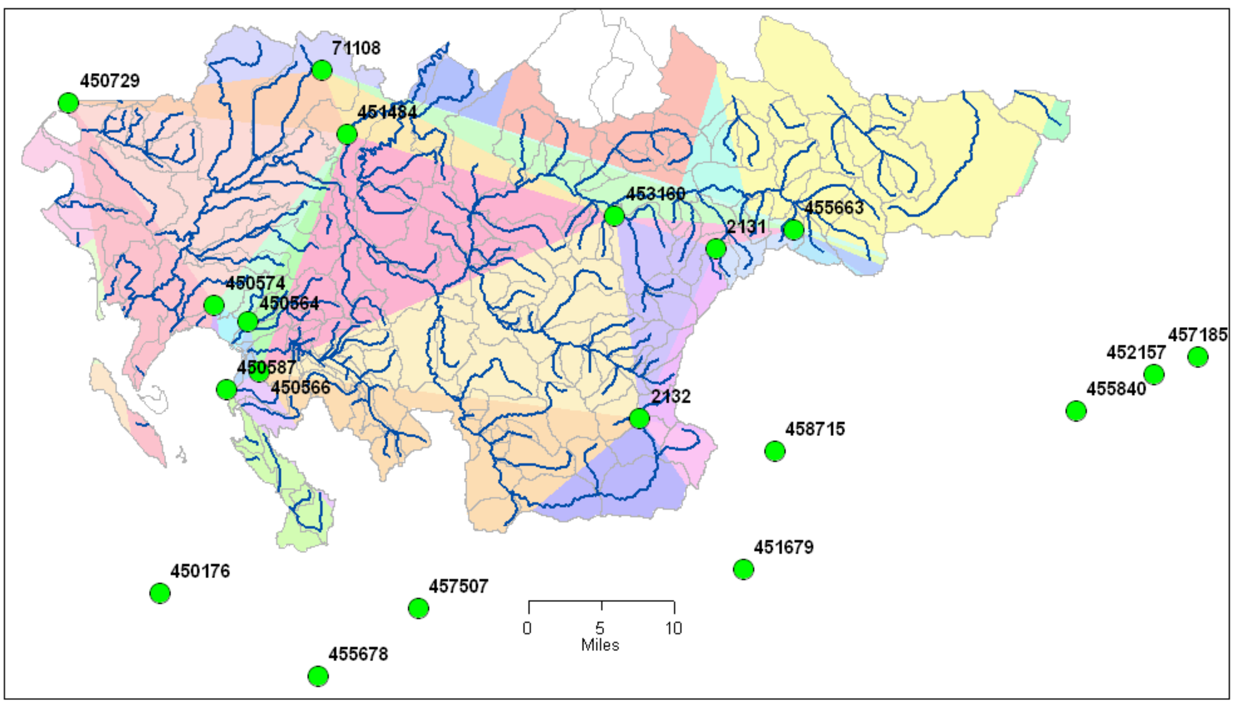

Figure 22. Precipitation gages and the Delauney triangles used for precipitation interpolation.

Appendix A.1 shows hydrograph comparison plots for all the calibration periods on all calibration sites. Table 19 gives a summary of model performance in terms of the ratio of measured to modeled flow averaged over the comparison periods.

Table 19. Calibration Performance Summary

Name	Node	Site	Ratio of modeled to observed streamflow			
			1947-1950	1967-1971	1984-1988	1998-2001
Fishtrap Creek at Lynden	3	12212000	1.5	1.31	0	0
Fishtrap Creek at Front Road at Lynden	4	12212050	0	0	0	1.19
Dakota Creek near Blaine	5	12214000	0.91	0	0	0
California Creek near Custer	6	12213500	0	0	0	0
Bertrand Creek near Lynden	7	12212500	1.02	0	0	0
Kendall Creek at Kendall	11	12206000	3.61	0	0	0
Coal Creek near Kendall	12	12207000	0.37	0	0	0
Racehorse Creek at North Fork Road near Kendall	13	12206900	0	0	0	0.89
NF Nooksack River near Deming	14	12207200	0	1.08	0	0
Kendall Creek at mouth at Kendall	15	12206500	0	0	0	0
Sumas River near Sumas	16	12214500	1.5	0	0	0
Nooksack River at Deming	23	12210500	0.99	0.96	1.05	1.04
Skookum Creek near Wickersham	25	12209000	1	1	1	1
Smith Creek near Bellingham	27	12209500	1.18	1.34	0	1.57
Olsen Creek near Bellingham	32	12202050	0	1.17	0	0
Squalicum Creek at Bellingham	34	12202300	0	1.29	0	0
Nooksack River at Ferndale	35	12204000	0.39	0	0	0
Tenmile Creek near Ferndale	38	12213100	0	0.99	1.03	1.05
Tenmile Creek near Laurel	39	12213000	0.77	0	0	0
Nooksack River near Lynden	40	12212900	0	0.85	0	0
Pepin Creek at International Boundary BC	42	12211500	0.97	0	0	0
Bertrand Creek at International Boundary BC	43	08MH156	0	0	0.3	0.25
Fishtrap Creek at International Boundary BC	44	08MH153	0	0	1.3	1.13
Johnson Creek at Sumas	45	08MH152	0	0	0.78	0.67
Sumas River near Huntington BC	46	12215000	0	0	0	0

Discussion of Calibration

The *f* parameter is the most sensitive parameter in Topnet. It is a measure of the sensitivity of lateral groundwater flow to changes in groundwater level. Its value greatly influences the responsiveness of simulated flow hydrographs and the shape of recession curves. *f* was set at 55% of the default value. This step was expected because no lookup values are available for *f*: the value was determined by hydrograph analysis. Care is required not to over-interpret the results of mathematical fitting of the *f* parameter to "noisy" recession data.

The *K* parameter was set to 10 times the default values for the various soil types in the catchment. The *K* parameter controls infiltration at the ground surface. Because infiltration has very large spatial variability at the drainage scale, and widespread overland flow caused by infiltration excess runoff is extremely rare in environments such as the Nooksack catchment, the effective drainage-scale value of *K* is expected to be larger than that measured at the scale of a soil core.

The *T* parameter was set to 45 times the default value from the various soil types in the catchment. The *T* parameter controls the lateral conductivity within the saturated zone and the extent of saturated area in each drainage based on the modeled saturation deficit. Similar to *K*, this is a drainage scale parameter related to hydraulic conductivity. Spatial variability results in the drainage scale parameter being larger than that estimated from soils and related to measurements at the scale of a soil core. A small value of *T* results in large saturated area and very flashy response due to large infiltration excess runoff. *T* was adjusted to in aggregate match the spikiness of modeled and observed hydrographs.

The overland flow velocity was set to 10% of the default value. Again, no lookup values were available: this value was set to provide the observed damping of small rainfalls which was apparent in the measured flow records.

The impervious fraction was set to 50% of the default values provided for each drainage. If this step was not carried out then unrealistically large responses to rainfall were generated by the model throughout the year. One possible cause for this is that the impervious areas in each drainage are not all connected to waterways, or are not completely impervious, so that rainfall that falls on them ends up infiltrating.

Overall in calibrating the model, we focused most on reproducing the streamflow in the mainstem gages, namely: North Fork Near Demming (Node 14), Nooksack at Demming (Node 23), Nooksack near Lynden (Node 42) and Nooksack at Ferndale (Node 38). A satisfactory calibration was achieved here with the overall ratio's showing less than 5% deviation. The adjustment of rainfall multipliers was the most significant factor in getting these flows right.

In the Fishtrap Bertrand and Pepin Creek area, (Nodes 3, 4, 7, 43, 44, 45) nodes 3, 4, 7 and 44 are satisfactorily modeled. Node 43 (Pepin at international boundary) has high baseflow that we are unable to model. Site 45 (Fishtrap at international boundary) is also undermodeled, but not to the same extent as site 43. Examining observed flow from Canada we find that the runoff expressed on a per unit area basis is high in Fishtrap and Pepin (39 in/yr at node 45 and 37 in/yr at node 43), but low in Bertrand (9 in/yr at node 44). Possible causes may be geology, precipitation, inaccurate basin outline delineation, artificial drainage impacts on flows or other unknowns. We do not have sufficient information to resolve these differences and believe that the observed flows at nodes 43 and 45 are unreasonably high given the precipitation in this region. Flows further South in Fishtrap Creek are around 24 in/yr (22 in/yr at node 3 and 26 in/yr at node 4). These are more consistent with the annual precipitation in this region of around 53 in/yr and ET around 29 in/yr. This ET value consistent with published pan evaporation values in this area (e.g. Dingman, 1994). There is no indication that precipitation is consistently underestimated in this area.

Dakota Creek (Node 5) is generally satisfactorily modeled. The model has some difficulty capturing the first runoff peak after a long dry period leading up to December 1950. This is due to the inherent difficulty models like this have in fully capturing the antecedent wetness. Perhaps the soils are such that they do not lose moisture the way the model represents the moisture loss. We do not have sufficient information to resolve this.

In the Sumas River (Nodes 16 and 47), the model does not fully capture summer sustained low flows and models too much winter runoff. This is most likely a groundwater/baseflow response that the model can not capture. The overmodeling of winter runoff is worse for station 16 than 47.

In Skookum Creek (Node 27), the model has some difficulty capturing the flashiness of this stream that may also be impacted by glacier flow.

In Tenmile Creek (Nodes 39 and 40), flow is adequately modeled. This is an area that is quite flat with considerable suspected groundwater interactions and contributions to baseflow. For example, the internally draining Fazon watershed is adjacent. Recharge in Fazon must appear as baseflow somewhere. The surface water model does not have the capability to accommodate these effects.

In Smith and Olsen Creeks (Nodes 32 and 34), the model is not as flashy as observed. The parameters could be adjusted to match this streamflow better, but the performance in other locations would then be worse.

In Kendall, Coal, and Racehorse Creeks (Nodes 11, 12, 13, and 15), the model performs poorly. In Kendall (Node 11), recessions are too fast and peaks are overestimated. In Racehorse and Coal Creeks (Nodes 12 and 13), modeled flow and baseflow is underestimated, especially in Coal creek. Racehorse and Coal Creek are underlain by bedrock geology. Kendall Creek is coarse grained glacial outwash. The inference is that rainfall in this region is higher than we have in the model. This would increase model flows in Racehorse and Coal. In Kendall, we surmise that much water infiltrates and perhaps passes beneath the gage. Racehorse and Coal Creek are primarily underlain by bedrock (see geology given in Figure 23) with runoff response dictated more by this geology than the soils information that the model used. The surface water quantity model is unable to incorporate this geologic information to better model streamflow in these drainages.

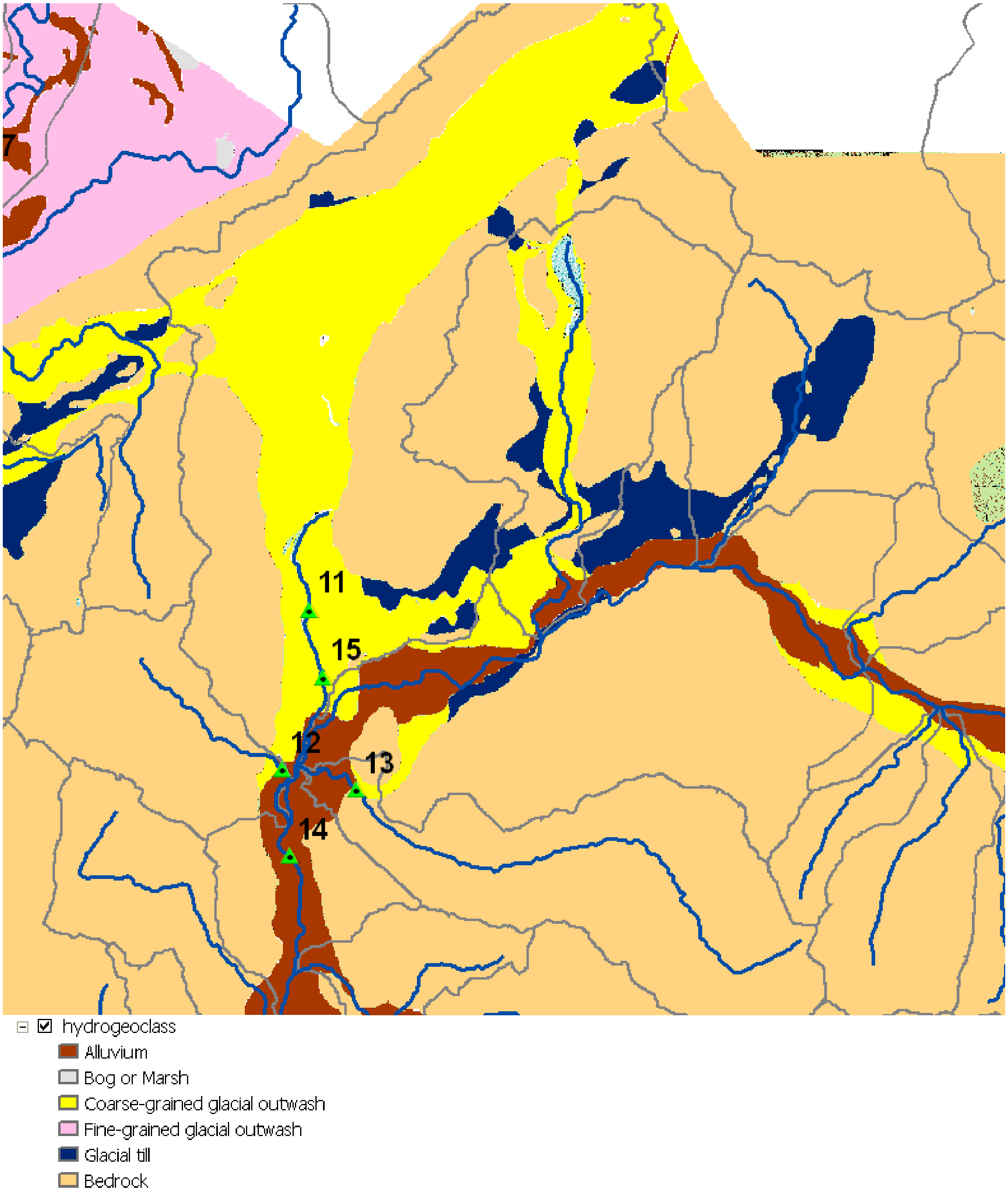

Figure 23. Hydrogeology in the vicinity of Kendal, Coal and Racehorse Creeks. Nodes 11 and 15 are on Kendall Creek. Node 12 is Coal Creek and Node 13 is Racehorse Creek. Node 14 is the North Fork of the Nooksack River

In summary, although the calibrations are poor in some cases, we believe that these are as good as can be obtained given the model and information available. The calibrated model is adequate for analyzing the relative impact of different water management options on streamflow in the WRIA 1 region.

References

Allen, R. G., (2001), "REF-ET: Reference Evapotranspiration Calculation Software for FAO and Standardized Equations," University of Idaho, http://www.kimberly.uidaho.edu/ref-et/.

Allen, R. G., L. S. Pereira, D. Raes and M. Smith, (1998), Crop evapotranspiration - Guidelines for computing crop water requirements - FAO Irrigation and Drainage Paper 56, FAO - Food and Agriculture Organization of the United Nations, Rome, http://www.fao.org/docrep/x0490e/x0490e00.htm.

Allen, R. G., I. A. Walter, R. L. Elliot and T. A. Howell, ed. (2005), ASCE Standardized Reference Evapotranspiration Equation, American Society of Civil Engineers, 216 p.

Anderson, E. A., (1976), "A Point Energy and Mass Balance Model of a Snow Cover," NOAA Technical Report NWS 19, U.S. Department of Commerce, 150 p.

Bandaragoda, C., D. G. Tarboton and R. Woods, (2004), "Application of TOPNET in the Distributed Model Intercomparison Project," Journal of Hydrology, 298: 178-201, doi:10.1016/j.jhydrol.2004.03.038.

Beven, K., R. Lamb, P. Quinn, R. Romanowicz and J. Freer, (1995a), "TOPMODEL," in Computer Models of Watershed Hydrology, Edited by V. P. Singh, Water Resources Publications, Highlands Ranch, Colorado, p.627-668.

Beven, K., P. Quinn, R. Romanowicz, J. Freer, J. Fisher and R. Lamb, (1995b), "TOPMODEL AND GRIDATB, A users guide to the distribution versions (95.02)," CRES technical Report TR110, Centre for Research on Environmentall Systems and Statistics, Institute of Environmental and Biological Sciences, Lancaster University, Lancaster LA 1 4YQ, UK.

Beven, K. J. and M. J. Kirkby, (1979), "A Physically Based Variable Contributing Area Model of Basin Hydrology," Hydrological Sciences Bulletin, 24(1): 43-69.

Bristow, K. L. and G. S. Campbell, (1984), "On the Relationship Between Incoming Solar Radiation and the Daily Maximum and Minimum Temperature," Agricultural and Forest Meteorology, 31: 159-166.

Brooks, R. H. and A. T. Corey, (1966), "Properties of Porous Media Affecting Fluid Flow," J. Irrig. and Drain. ASCE, 92(IR2): 61-88.

Daly, C., R. P. Neilson and D. L. Phillips, (1994), "A Statistical-Topographic Model for mapping Climatological Precipitation over Mountainous Terrain," Journal of Applied Meteorology, 33: 140-150.

Deardorff, J. W., (1968), "Dependence of Air-Sea Transfer Coefficients on Bulk Stability," Journal of Geophysical Research, 73(8): 2549-2557.

Deardorff, J. W., (1978), "Efficient prediction of ground surface temperature and moisture, with inclusion of a layer of vegetation," Journal of Geophysical Research, 83(C4): 1889-1903.

Dickinson, R. E., A. Henderson-Sellers and P. J. Kennedy, (1993), "Biosphere-Atmosphere Transfer Scheme (BATS) Version 1e as Coupled to the NCAR Community Climate Model," NCAR/TN-387+STR, National Center for Atmospheric Research, Boulder, CO, 71 p.

Dingman, S. L., (1994), Physical Hydrology, Macmillan, New York, 575 p.

Dyer, A. J. and B. B. Hicks, (1970), "Flux-gradient Relationships in the Constant Flux Layer," Quart. J. R. Met. Soc. 1970, 96: 715-721.

Hu, Z. and S. Islam, (1995), "Prediction of Ground Surface Temperature and Soil Moisture Content by the Force-Restore method," Water Resources Research, 31(10): 2531-2539.

Ibbitt, R., (1971), "Development of a Conceptual Model of Interception," Unpublished Hydrologic Research Progress Report No. 5, Ministry of Works, New Zealand.

Ibbitt, R. P. and R. Woods, (2004), "Re-scaling the topographic index to improve the representation of physical processes in catchment models," Journal of Hydrology, 293(1-4): 205-218, doi:10.1016/j.jhydrol.2004.01.016.

Jensen, M. E., R. D. Burman and R. G. Allen, ed. (1990), Evapotranspiration and Irrigation Water Requirements, ASCE Manuals and Reports on Engineering Practice No. 70, New York.

Jordan, R., (1991), "A one-dimensional temperature model for a snow cover," Technical documentation for SNTHERM.89, special technical report 91-16, US Army CRREL, 49 p.

Lowe, P. R., (1977), "An Approximating Polynomial for the Computation of Saturation Vapour Pressure," Journal of Applied Meteorology, 16: 100-103.

Luce, C. H., (2000), "Scale Influences on the Representation of Snowpack Processes," PhD Thesis, Civil and Environmental Engineering, Utah State University, 188 pp.

Luce, C. H. and D. G. Tarboton, (2001), "A Modified Force-Restore Approach to Modeling Snow-Surface Heat Fluxes," Proceedings of the 69th Annual Western Snow Conference, Sun Valley, Idaho, http://www.westernsnowconference.org/2001/2001papers.htm.

Luce, C. H., D. G. Tarboton and K. R. Cooley, (1998), "The Influence of the Spatial Distribution of Snow on Basin-Averaged Snowmelt," Hydrological Processes, 12(10-11): 1671-1683.

Luce, C. H., D. G. Tarboton and K. R. Cooley, (1999), "Subgrid Parameterization Of Snow Distribution For An Energy And Mass Balance Snow Cover Model," Hydrological Processes, 13: 1921-1933.

Price, A. G. and T. Dunne, (1976), "Energy balance computations of snowmelt in a subarctic area," Water Resources Research, 12(4): 686-694.

Rutter, A. J., K. A. Kershaw, P. C. Robins and A. J. Morton, (1972), "A predictive model of rainfall interception in forests, 1. Derivation of the model from observations in a plantation of Corsican Pine," Agricultural Meteorology, 9: 367-384.

Satterlund, D. R., (1979), "An Improved Equation for Estimating Long-wave Radiation From the Atmosphere," Water Resources Research, 15: 1643-1650.

Shuttleworth, W. J., (1993), "Evaporation," in Handbook of Hydrology, Chapter 4, Edited by D. R. Maidment, McGraw-Hill, New York.

Stewart, J. B., (1977), "Evaporation From the Wet Canopy of a Pine Forest," Water Resources Research, 13(6): 915-921.

Tarboton, D. G., (1997), "A New Method for the Determination of Flow Directions and Contributing Areas in Grid Digital Elevation Models," Water Resources Research, 33(2): 309-319.

Tarboton, D. G., T. G. Chowdhury and T. H. Jackson, (1995a), "A Spatially Distributed Energy Balance Snowmelt Model," ed. K. A. Tonnessen, M. W. Williams and M. Tranter, Proceedings of a Boulder Symposium, July 3-14, IAHS Publ. no. 228, p.141-155.

Tarboton, D. G., T. G. Chowdhury and T. H. Jackson, (1995b), "A Spatially Distributed Energy Balance Snowmelt Model," A Boulder Symposium, ed. K. A. Tonnessen, M. W. Williams and M. Tranter, Boulder, CO., July 3-14, IAHS Publ. no. 228, p.141-155.

Tarboton, D. G. and C. H. Luce, (1996a), "Utah Energy Balance Snow Accumulation and Melt Model (UEB)," Computer model technical description and users guide, Utah Water

Research Laboratory and USDA Forest Service Intermountain Research Station (http://www.engineering.usu.edu/dtarb/), 64 p.

Tarboton, D. G. and C. H. Luce, (1996b), "Utah Energy Balance Snow Accumulation and Melt Model (UEB)," Computer model technical description and users guide, Utah Water Research Laboratory and USDA Forest Service Intermountain Research Station (http://www.engineering.usu.edu/dtarb/).

U.S. Army Corps of Engineers, (1956), "Snow Hydrology, Summary report of the Snow Investigations," U.S. Army Corps of Engineers, North Pacific Division, Portland, Oregon, 142 p.

Walter, I. A., R. G. Allen, R. Elliott, M. E. Jensen, D. Itenfisu, B. Mecham, T. A. Howell, R. Snyder, P. Brown, S. Echings, T. Spofford, M. Hattendorf, R. H. Cuenca, J. L. Wright and D. Martin, (2000), "ASCE's Standardized Reference Evapotranspiration Equation," Proc. National Irrigation Symposium, ASAE, ed. E. RG, B. BL and T. TP, Phoenix, AZ., Nov. 14-16, 2000, p.209-215.

You, J., (2004), "Snow Hydrology: The Parameterization of Subgrid Processes within a Physically Based Snow Energy and Mass Balance Model," PhD Thesis, Civil and Environmental Engineering, Utah State University.

Appendix A.1 - Calibration Comparison Hydrograph Plots

The following figures show comparison hydrographs for all the calibration periods on all calibration sites. The plots are grouped according to the calibration period. Each plot has identifying information in the header or caption. Node refers to the Id field in Points_of_interest.shp giving the nodes where flow is modeled. Drainage refers to the WRIA 1 drainage containing the node. The average of the measured runoff for the period shown in the plot is given together with the ratio of modeled flow to measured flow expressed as a percentage. This comparison is made only for the dates in the period when measured data is available.

<u>Calibration Period 1 (10/1/1947-9/30/1950)</u>

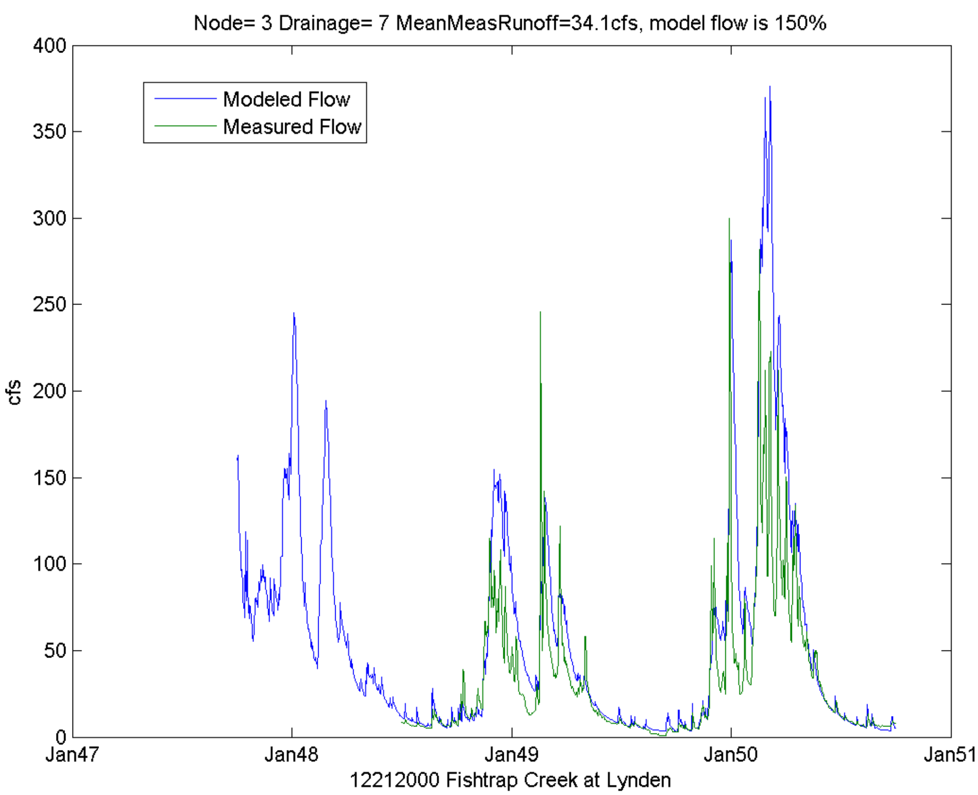

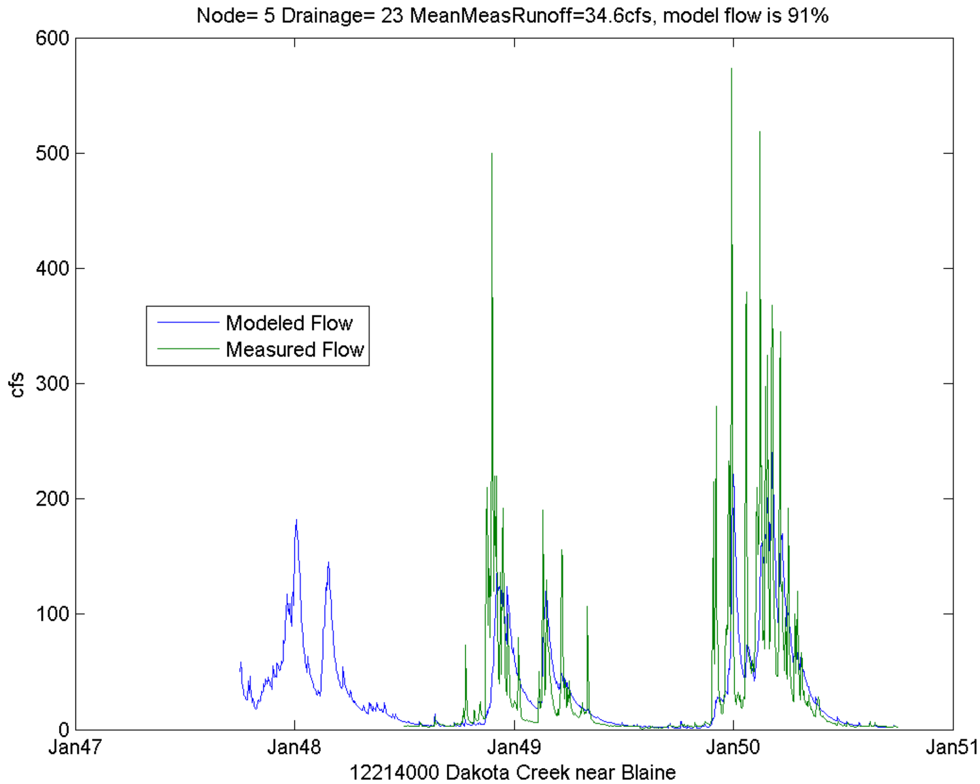
Node= 5 Drainage= 23 MeanMeasRunoff=34.6cfs, model flow is 91%
600
500
400
300
200
100
0
cfs
Modeled Flow
Measured Flow
Jan47
Jan48
Jan49
Jan50
Jan51
12214000 Dakota Creek near Blaine

1909

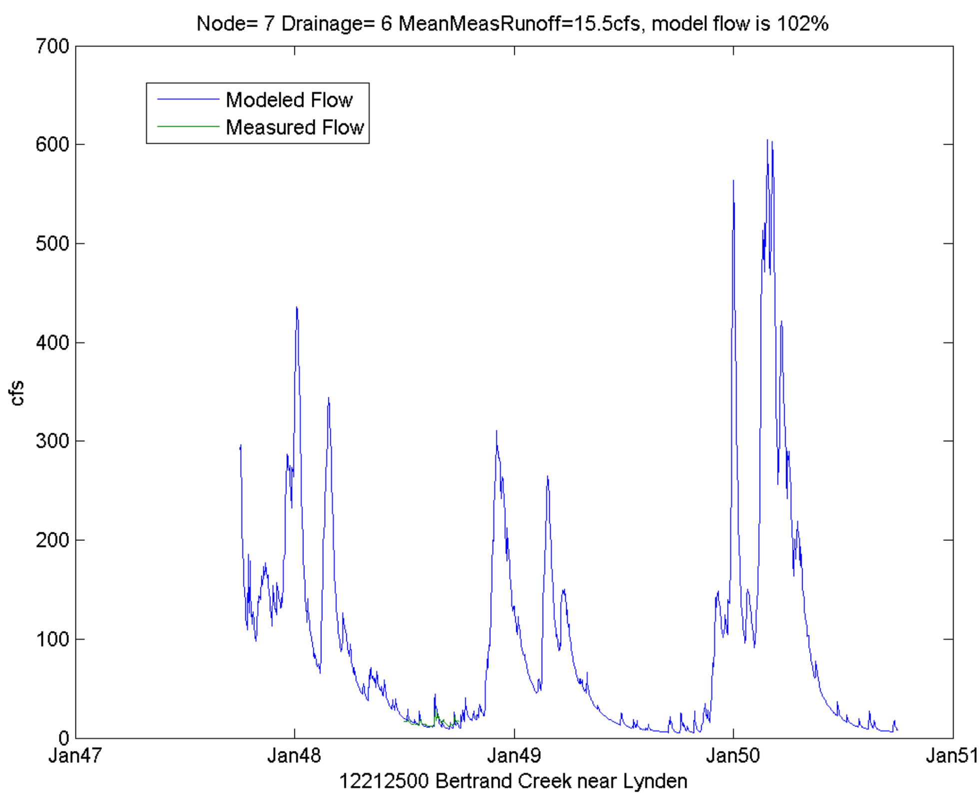
Node= 7 Drainage= 6 MeanMeasRunoff=15.5cfs, model flow is 102%
700
600
500
400
300
200
100
0
cfs
Modeled Flow
Measured Flow
Jan47
Jan48
Jan49
Jan50
Jan51
12212500 Bertrand Creek near Lynden

1910

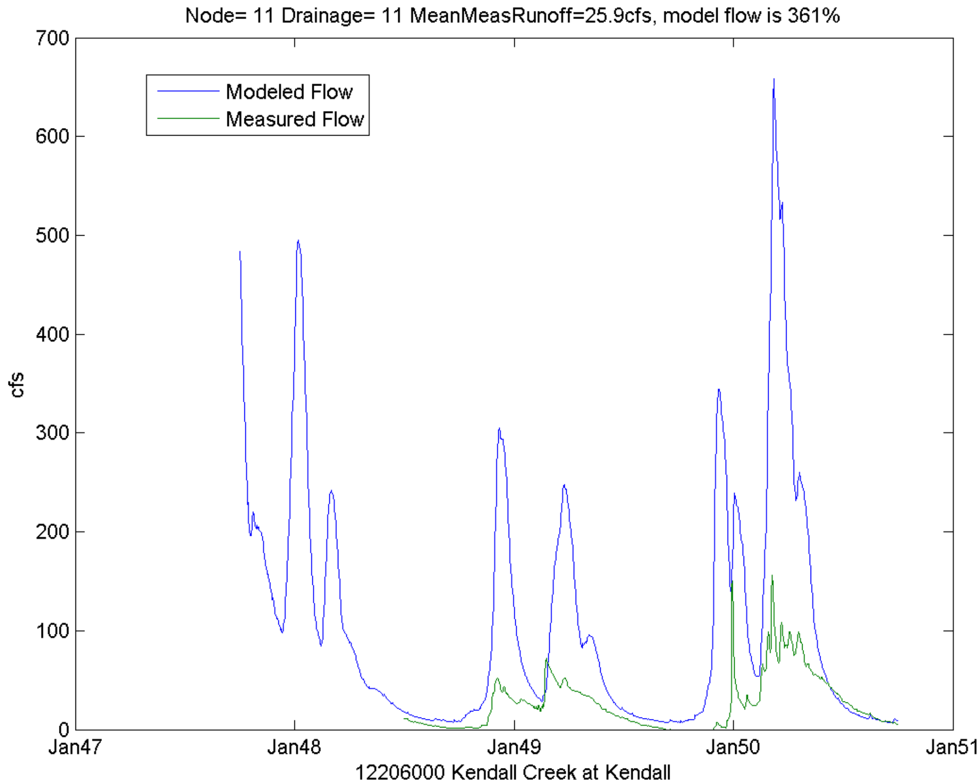
Node= 11 Drainage= 11 MeanMeasRunoff=25.9cfs, model flow is 361%
Modeled Flow
Measured Flow
cfs
700
600
500
400
300
200
100
0
Jan47
Jan48
Jan49
Jan50
Jan51
12206000 Kendall Creek at Kendall

1911

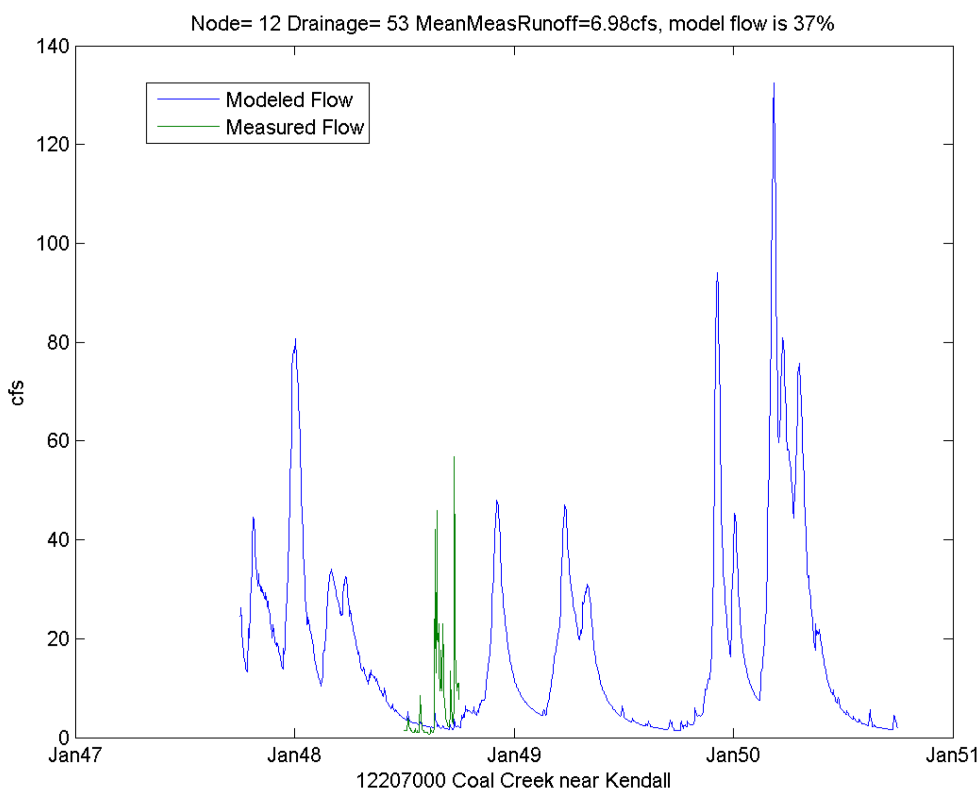
Node= 12 Drainage= 53 MeanMeasRunoff=6.98cfs, model flow is 37%
Modeled Flow
Measured Flow
cfs
140
120
100
80
60
40
20
0
Jan47
Jan48
Jan49
Jan50
Jan51
12207000 Coal Creek near Kendall

1912

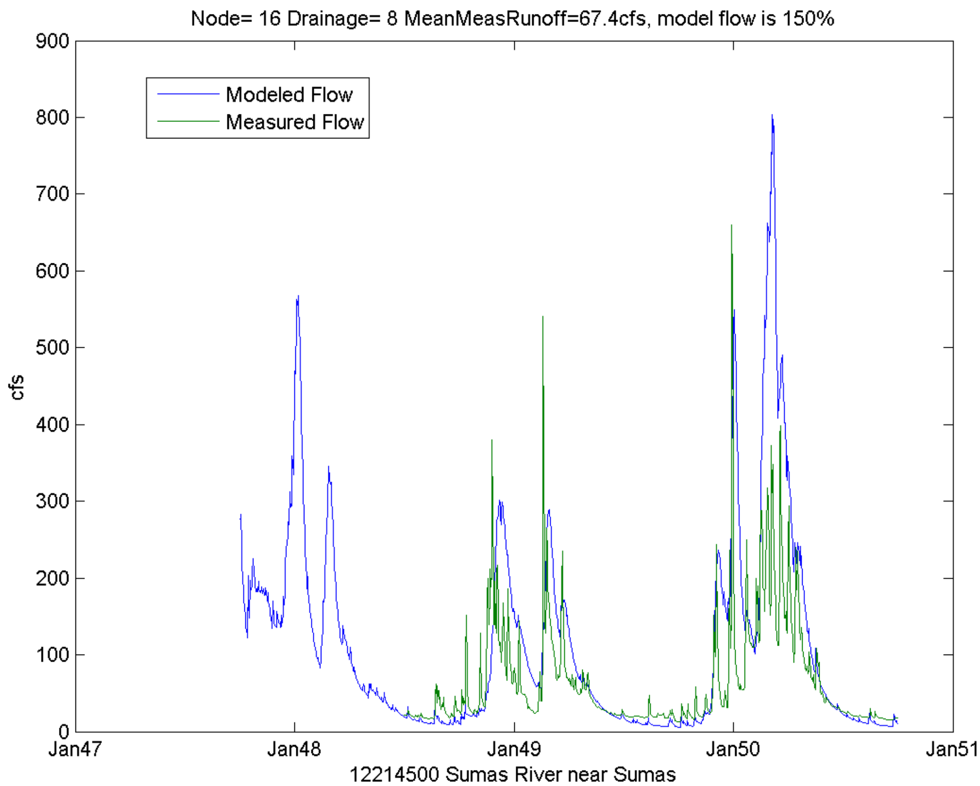
Node= 16 Drainage= 8 MeanMeasRunoff=67.4cfs, model flow is 150%
Modeled Flow
Measured Flow
cfs
900
800
700
600
500
400
300
200
100
0
Jan47
Jan48
Jan49
Jan50
Jan51
12214500 Sumas River near Sumas

1913

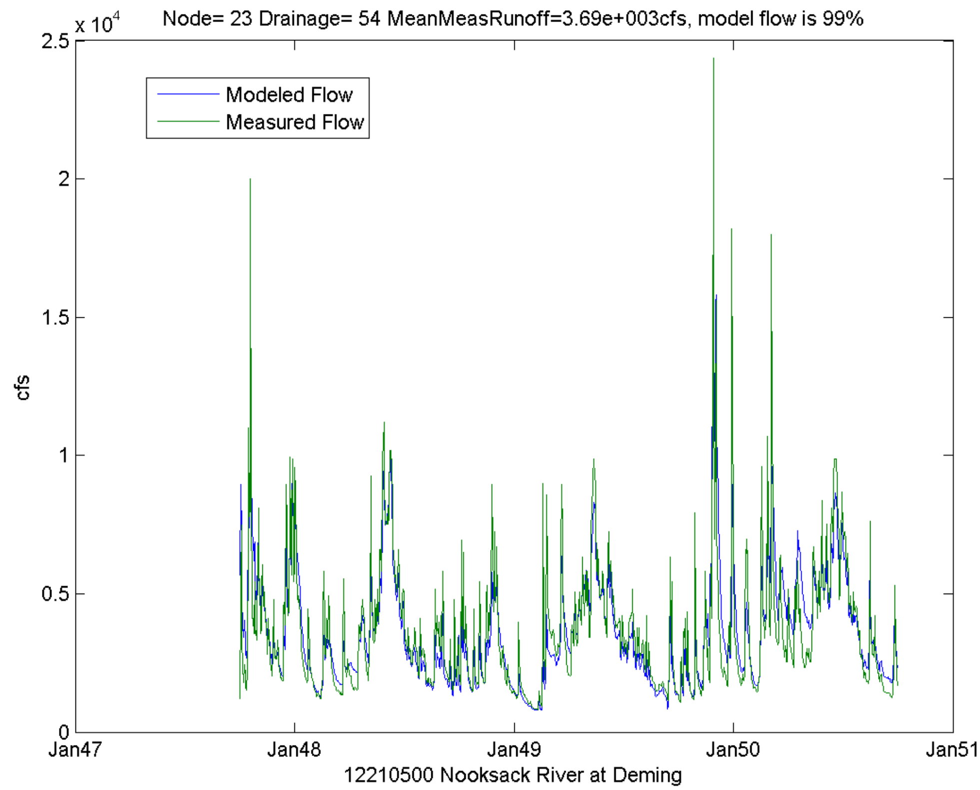
Node= 23 Drainage= 54 MeanMeasRunoff=3.69e+003cfs, model flow is 99%
x 10^4
Modeled Flow
Measured Flow
cfs
2.5
2
1.5
1
0.5
0
Jan47
Jan48
Jan49
Jan50
Jan51
12210500 Nooksack River at Deming

1914

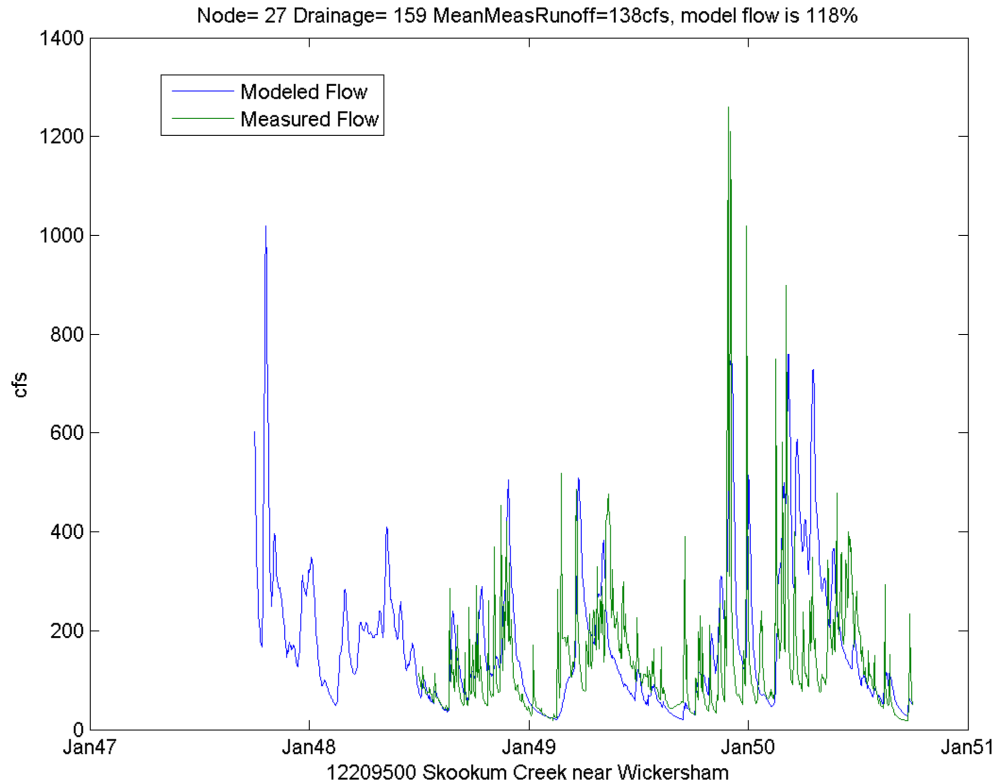
Node= 27 Drainage= 159 MeanMeasRunoff=138cfs, model flow is 118%
Modeled Flow
Measured Flow
cfs
1400
1200
1000
800
600
400
200
0
Jan47
Jan48
Jan49
Jan50
Jan51
12209500 Skookum Creek near Wickersham

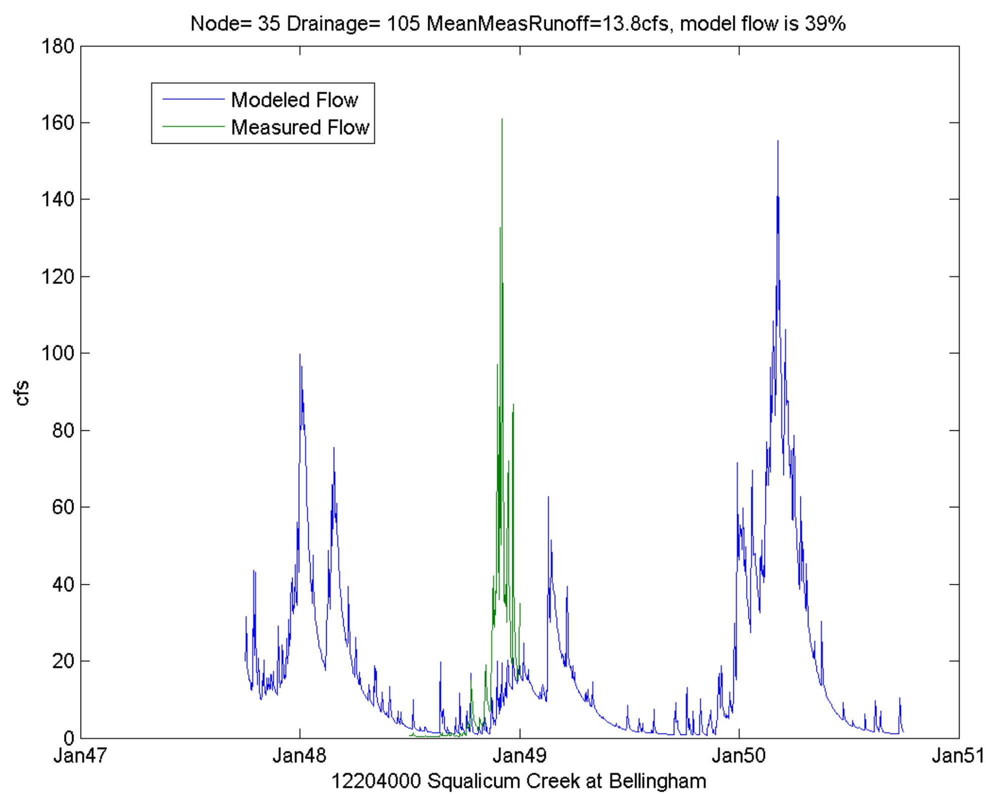
Node= 35 Drainage= 105 MeanMeasRunoff=13.8cfs, model flow is 39%
Modeled Flow
Measured Flow
cfs
180
160
140
120
100
80
60
40
20
0
Jan47
Jan48
Jan49
Jan50
Jan51
12204000 Squalicum Creek at Bellingham

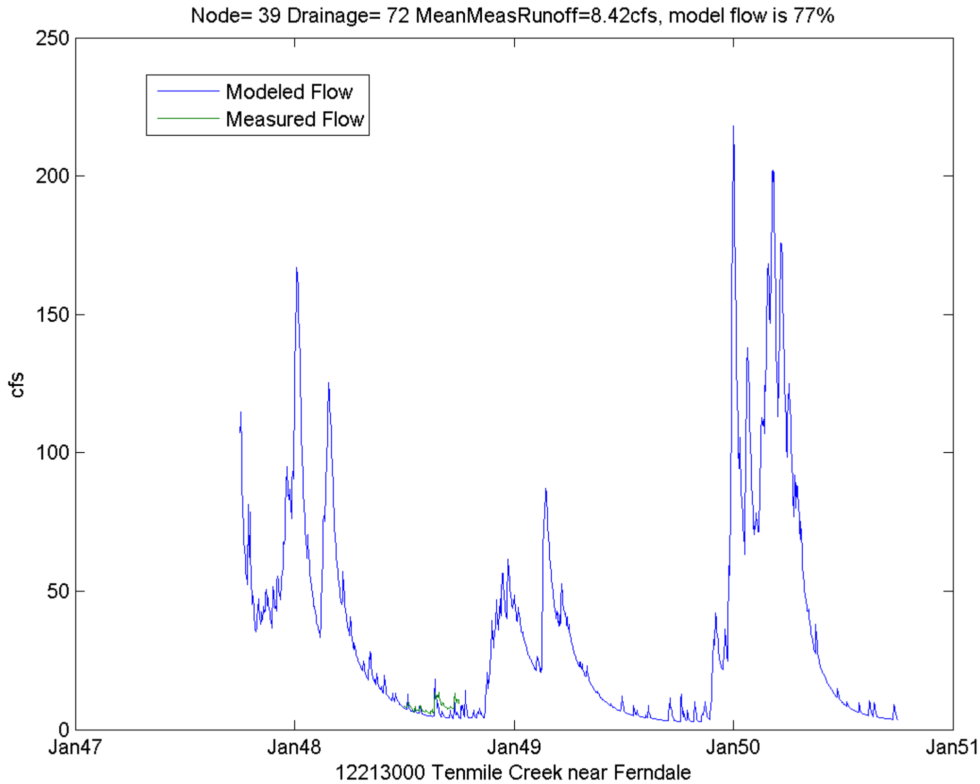
Node= 39 Drainage= 72 MeanMeasRunoff=8.42cfs, model flow is 77%
Modeled Flow
Measured Flow
cfs
250
200
150
100
50
0
Jan47
Jan48
Jan49
Jan50
Jan51
12213000 Tenmile Creek near Ferndale

1917

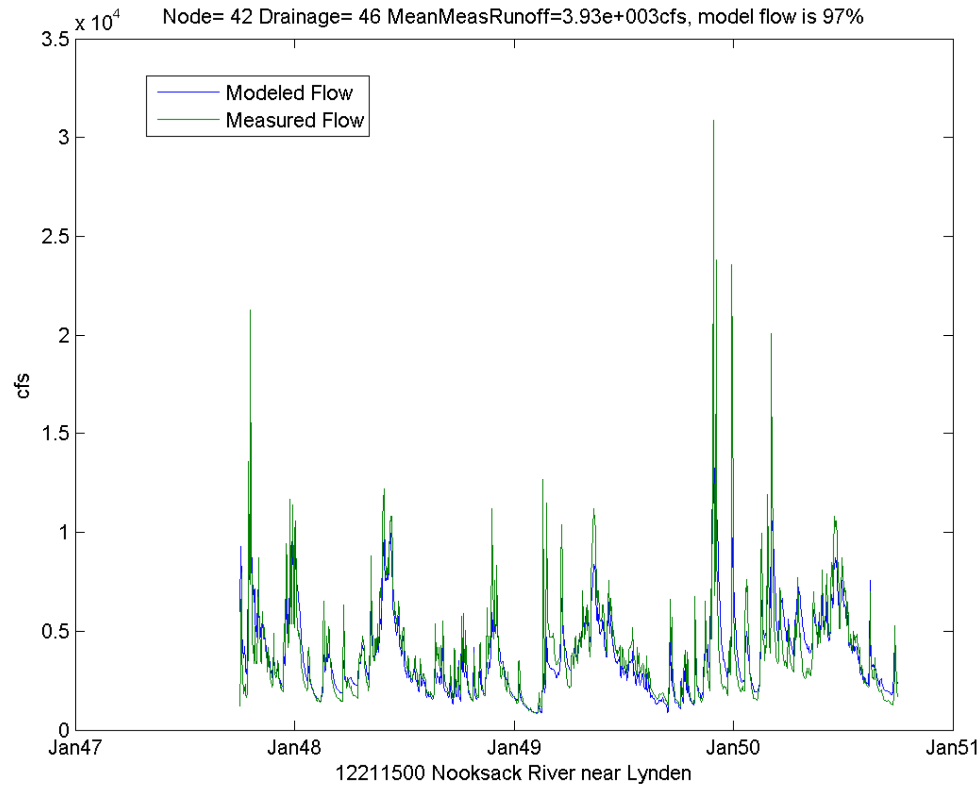
Node= 42 Drainage= 46 MeanMeasRunoff=3.93e+003cfs, model flow is 97%
x 10^4
Modeled Flow
Measured Flow
cfs
3.5
3
2.5
2
1.5
1
0.5
0
Jan47
Jan48
Jan49
Jan50
Jan51
12211500 Nooksack River near Lynden

1918

Calibration Period 2 (10/1/1967-9/30/1971)

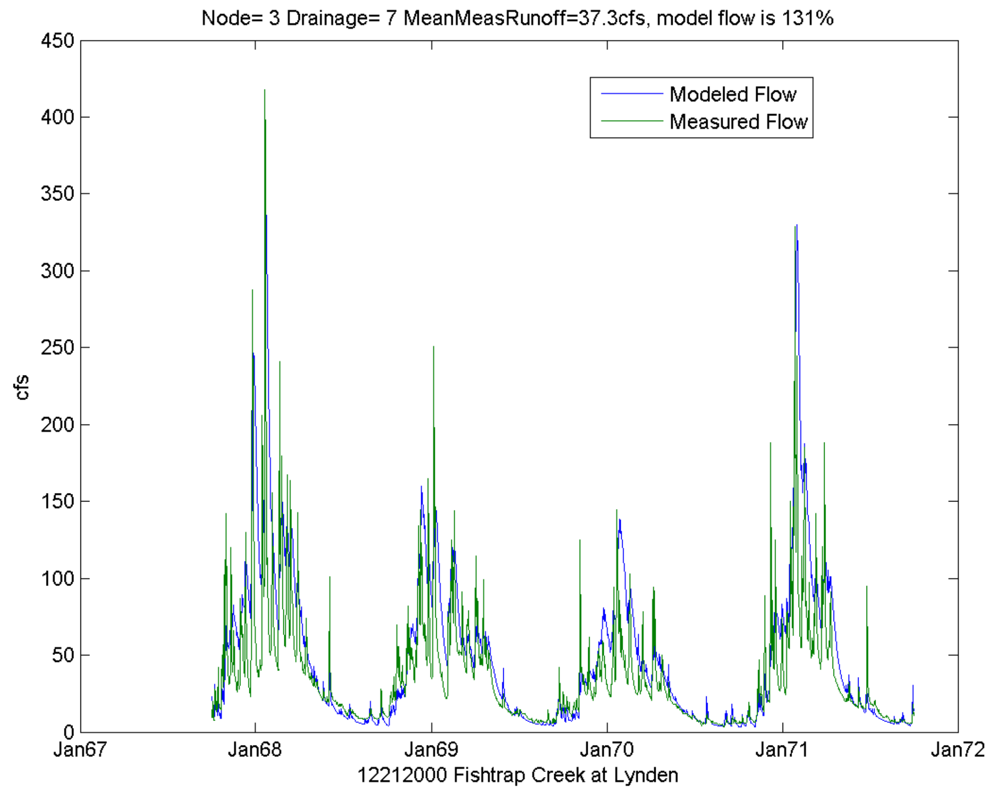

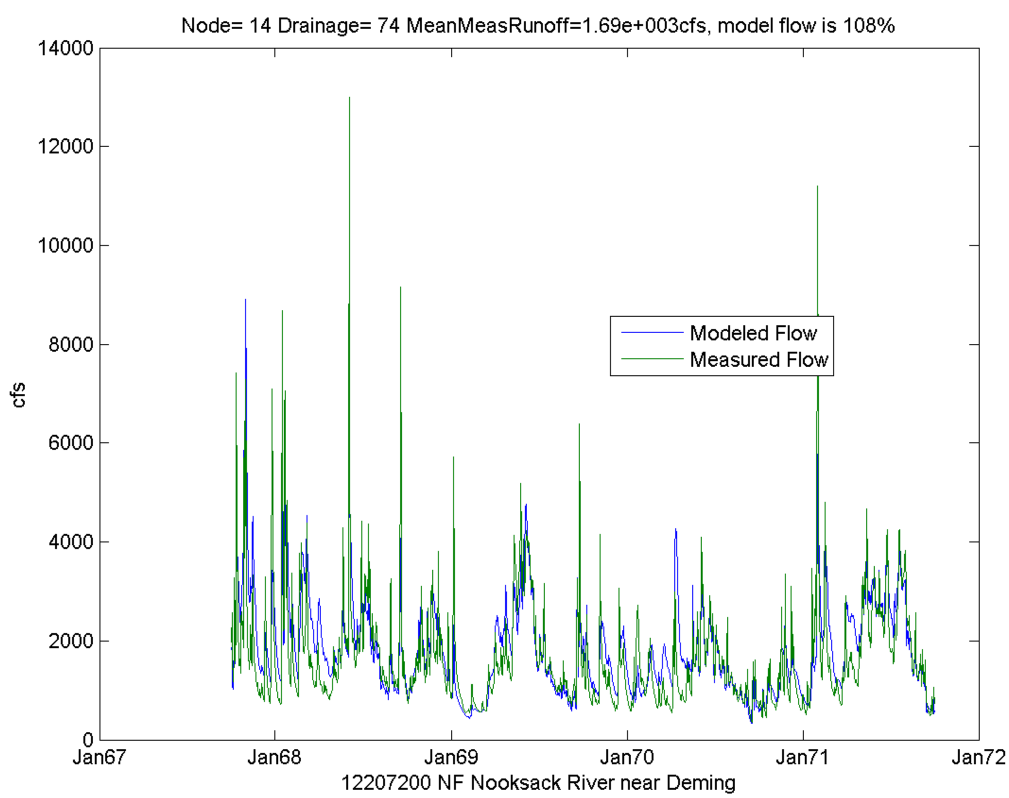

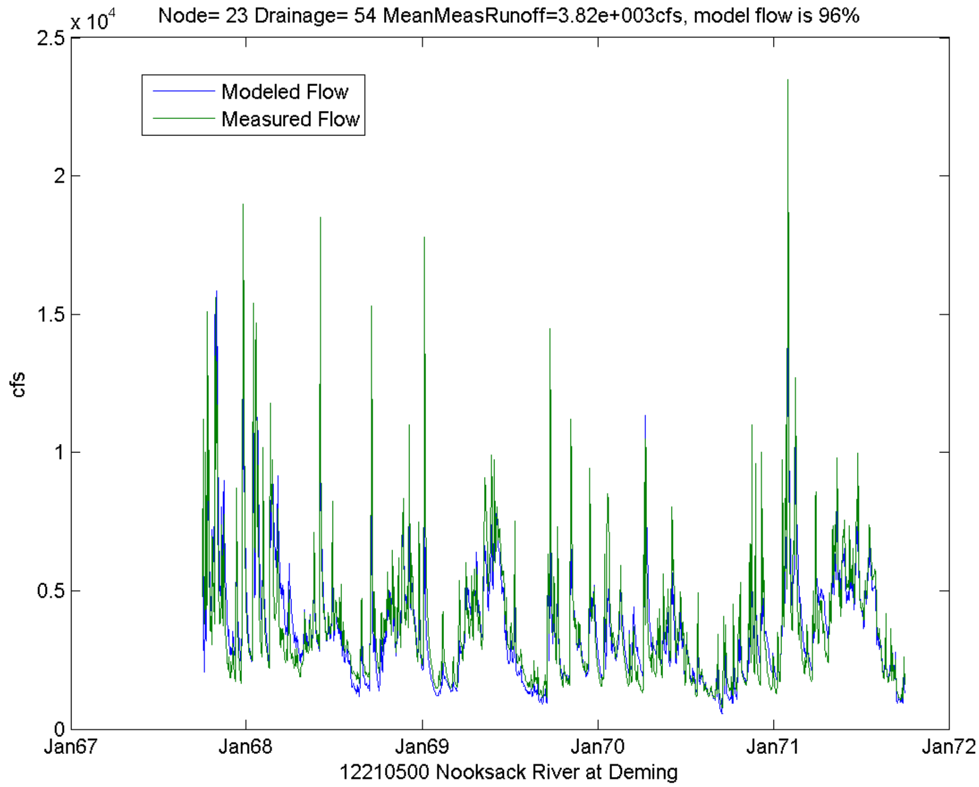
Node= 23 Drainage= 54 MeanMeasRunoff=3.82e+003cfs, model flow is 96%
x 10^4
2.5
2
1.5
1
0.5
0
cfs
Modeled Flow
Measured Flow
Jan67
Jan68
Jan69
Jan70
Jan71
Jan72
12210500 Nooksack River at Deming

1922

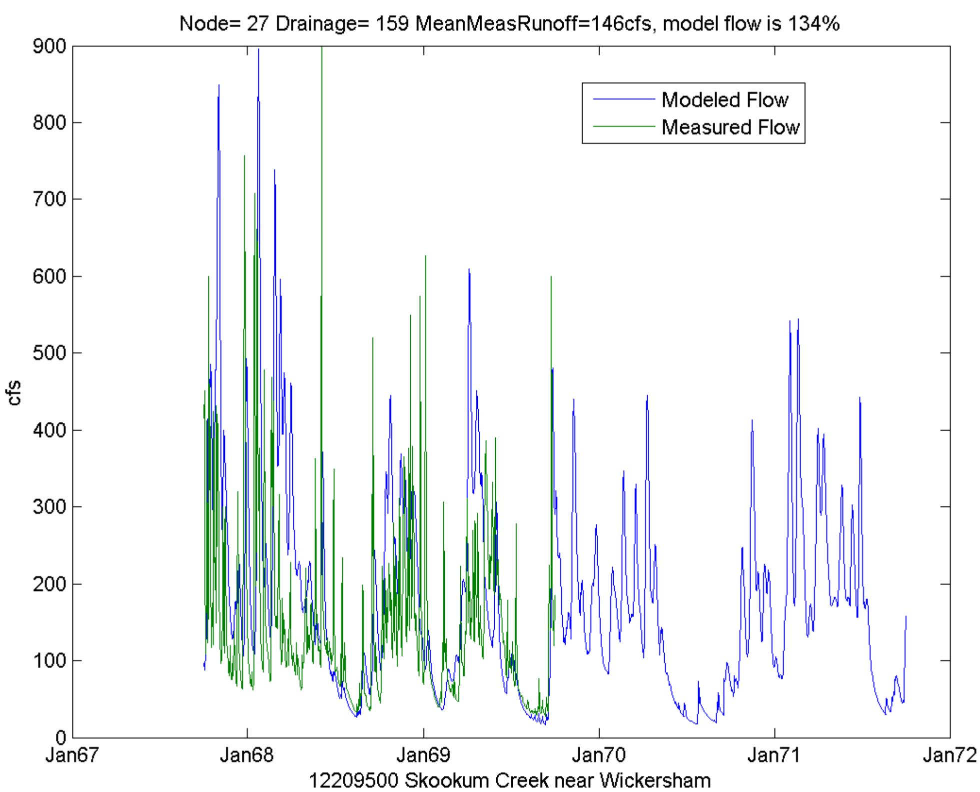
Node= 27 Drainage= 159 MeanMeasRunoff=146cfs, model flow is 134%
900
800
700
600
500
400
300
200
100
0
cfs
Modeled Flow
Measured Flow
Jan67
Jan68
Jan69
Jan70
Jan71
Jan72
12209500 Skookum Creek near Wickersham

1923

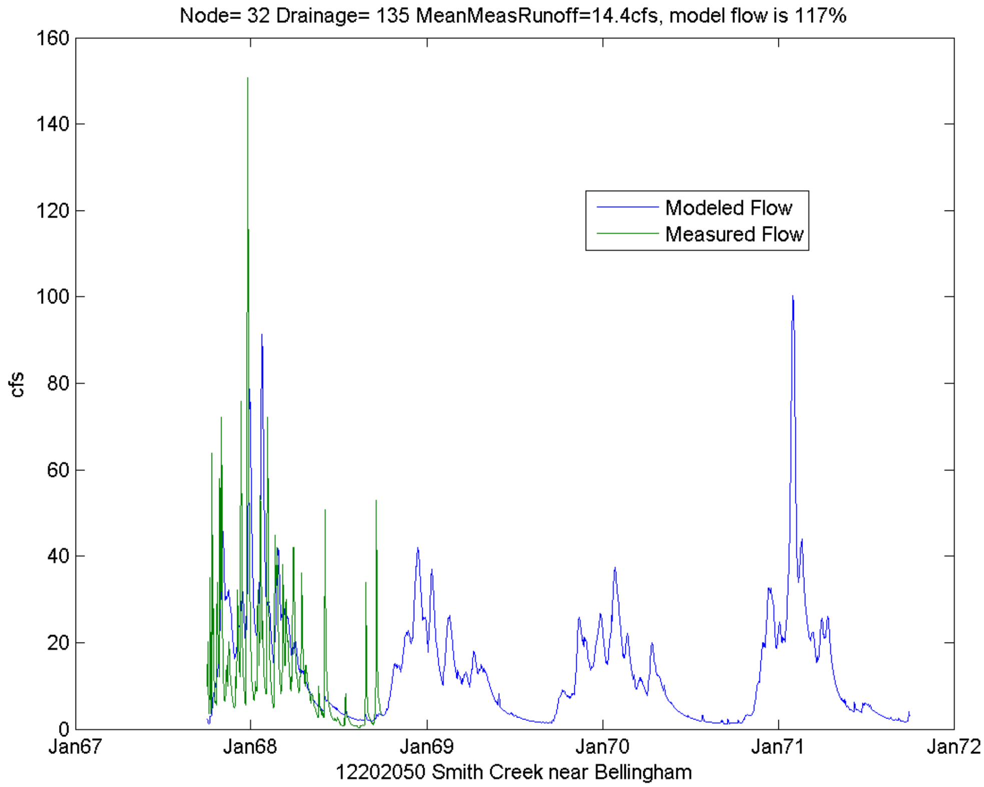
Node= 32 Drainage= 135 MeanMeasRunoff=14.4cfs, model flow is 117%
Modeled Flow
Measured Flow
cfs
0
20
40
60
80
100
120
140
160
Jan67
Jan68
Jan69
Jan70
Jan71
Jan72
12202050 Smith Creek near Bellingham

1924

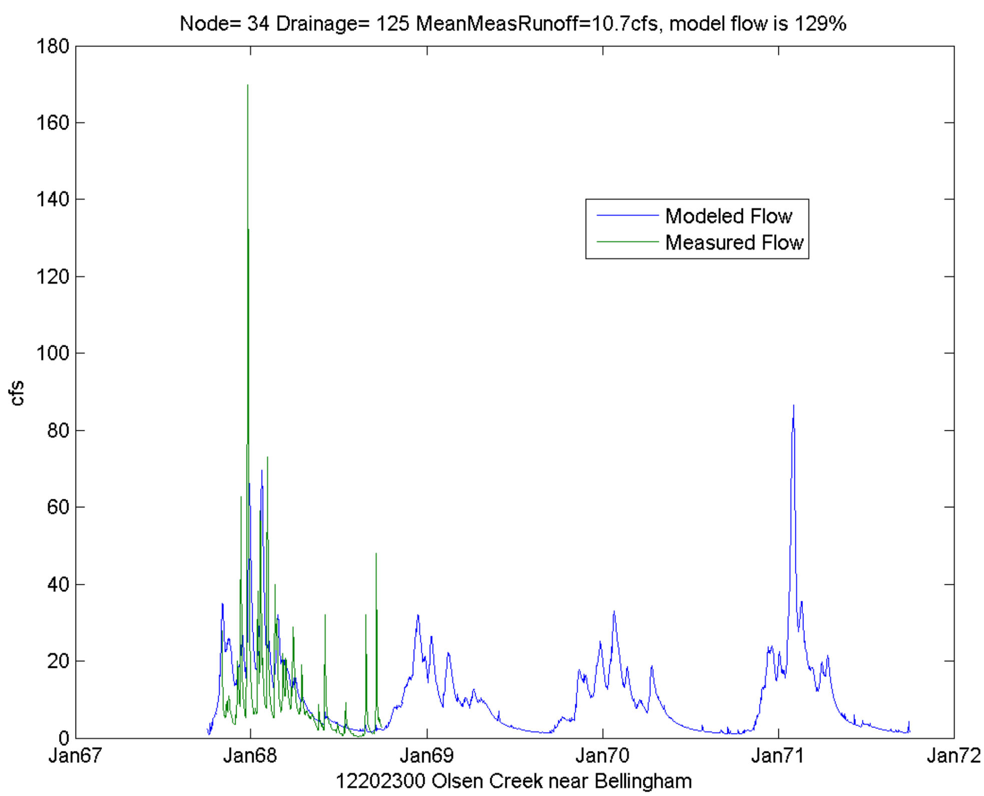
Node= 34 Drainage= 125 MeanMeasRunoff=10.7cfs, model flow is 129%
Modeled Flow
Measured Flow
cfs
0
20
40
60
80
100
120
140
160
180
Jan67
Jan68
Jan69
Jan70
Jan71
Jan72
12202300 Olsen Creek near Bellingham

1925

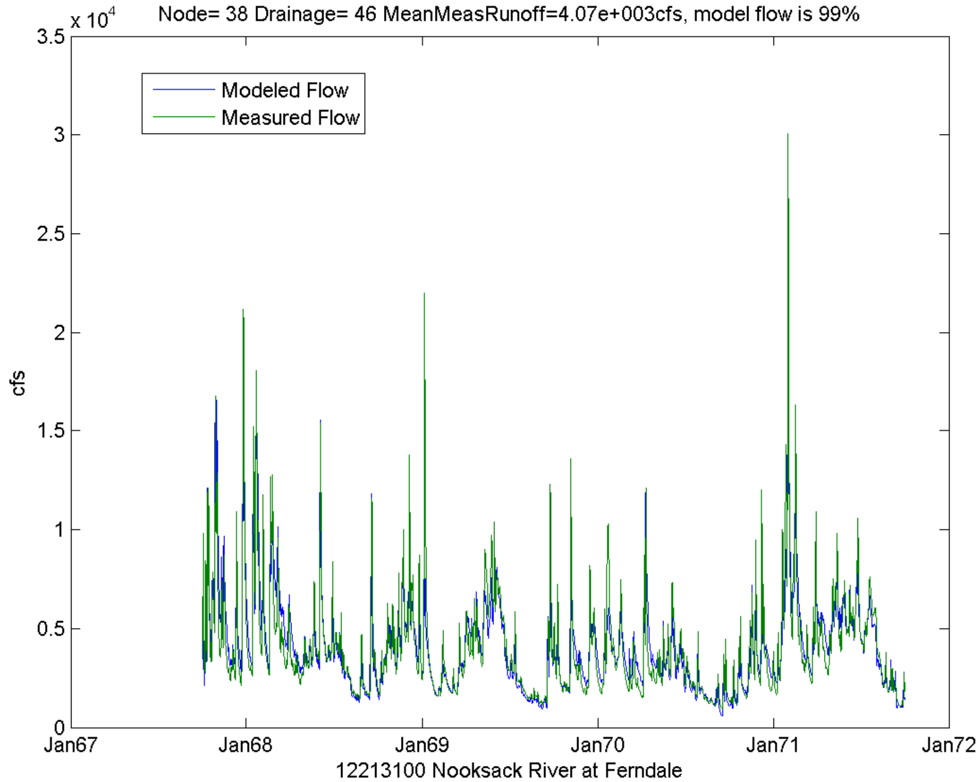
Node= 38 Drainage= 46 MeanMeasRunoff=4.07e+003cfs, model flow is 99%
x 10^4
3.5
3
2.5
2
1.5
1
0.5
0
cfs
Modeled Flow
Measured Flow
Jan67
Jan68
Jan69
Jan70
Jan71
Jan72
12213100 Nooksack River at Ferndale

1926

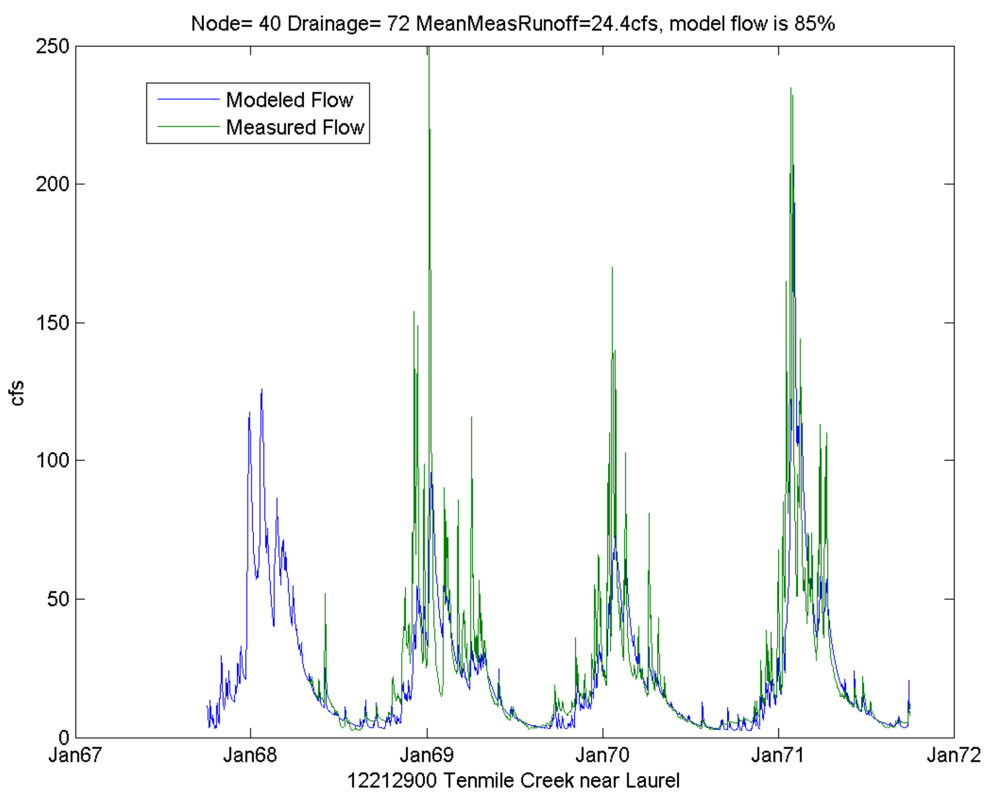
Node= 40 Drainage= 72 MeanMeasRunoff=24.4cfs, model flow is 85%
250
200
150
100
50
0
cfs
Modeled Flow
Measured Flow
Jan67
Jan68
Jan69
Jan70
Jan71
Jan72
12212900 Tenmile Creek near Laurel

1927

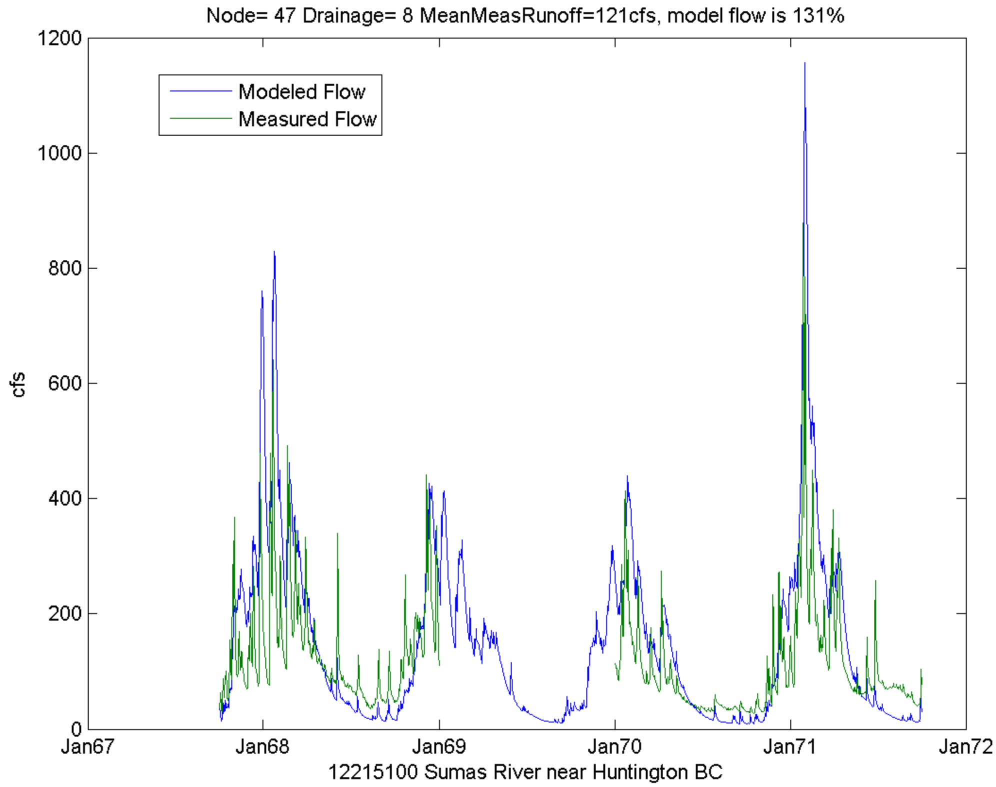

Node= 47 Drainage= 8 MeanMeasRunoff=121cfs, model flow is 131%
Modeled Flow
Measured Flow
cfs
1200
1000
800
600
400
200
0
Jan67
Jan68
Jan69
Jan70
Jan71
Jan72
12215100 Sumas River near Huntington BC

1928

Calibration Period 3 (10/1/1984-9/30/1988)

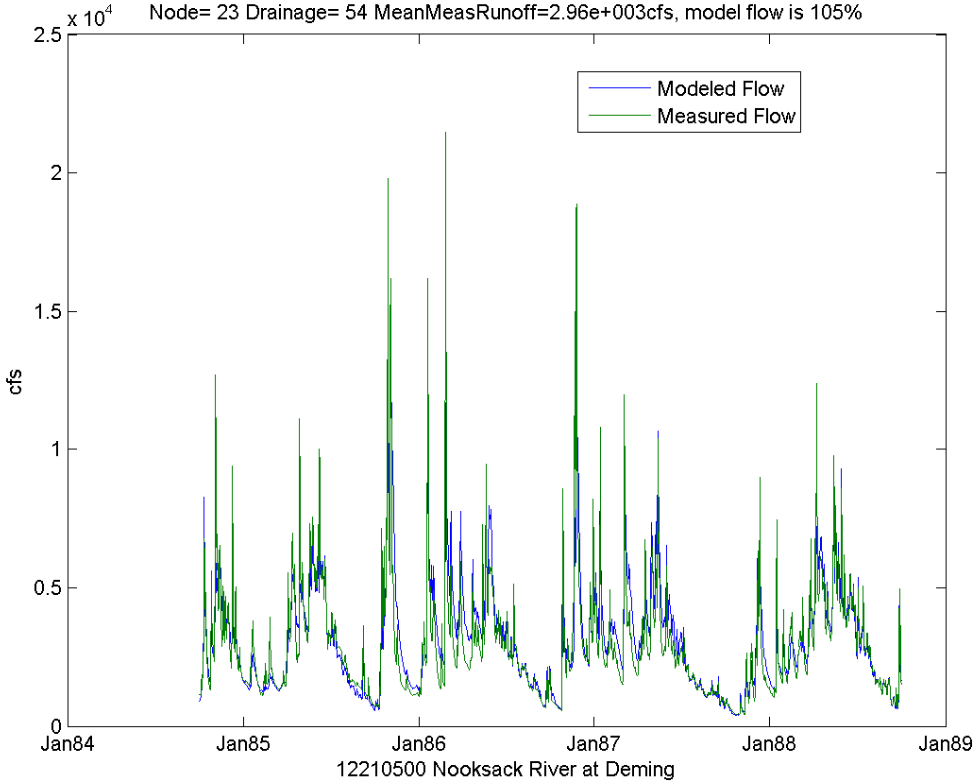

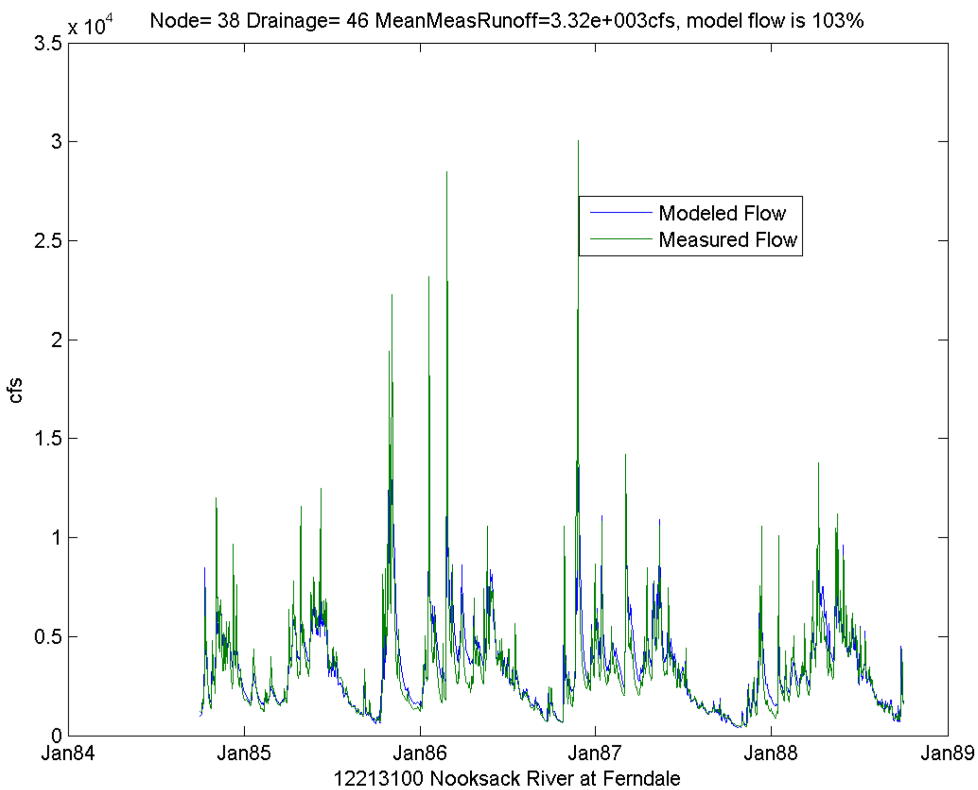

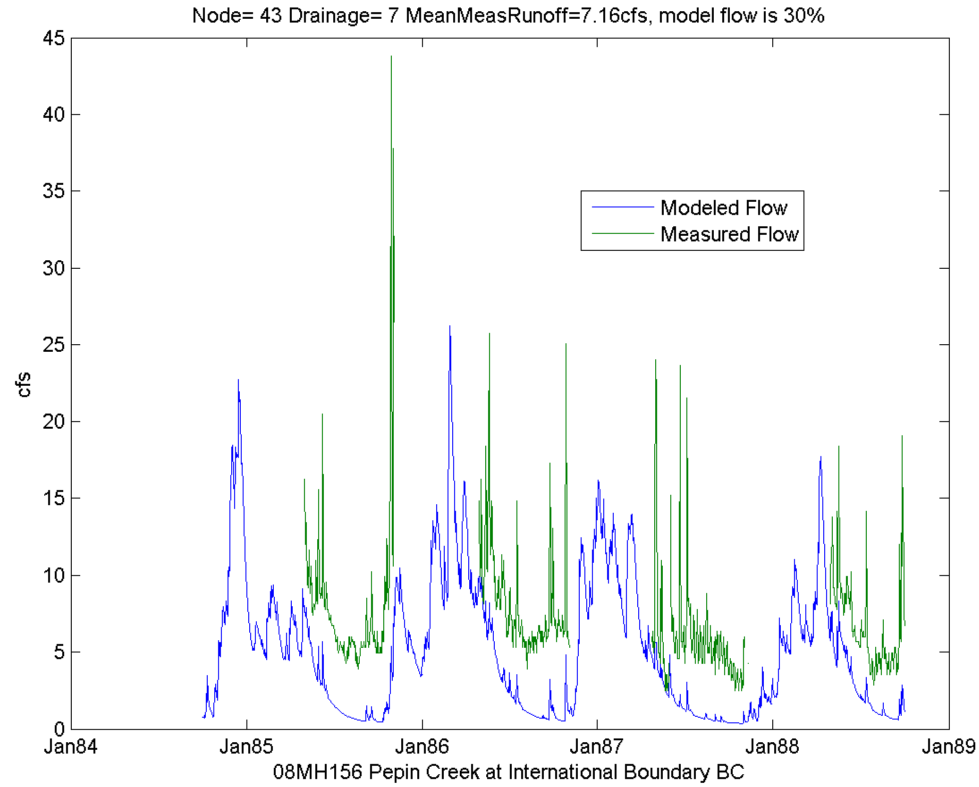

Node= 43 Drainage= 7 MeanMeasRunoff=7.16cfs, model flow is 30%
cfs
Modeled Flow
Measured Flow
Jan84
Jan85
Jan86
Jan87
Jan88
Jan89
08MH156 Pepin Creek at International Boundary BC

1932

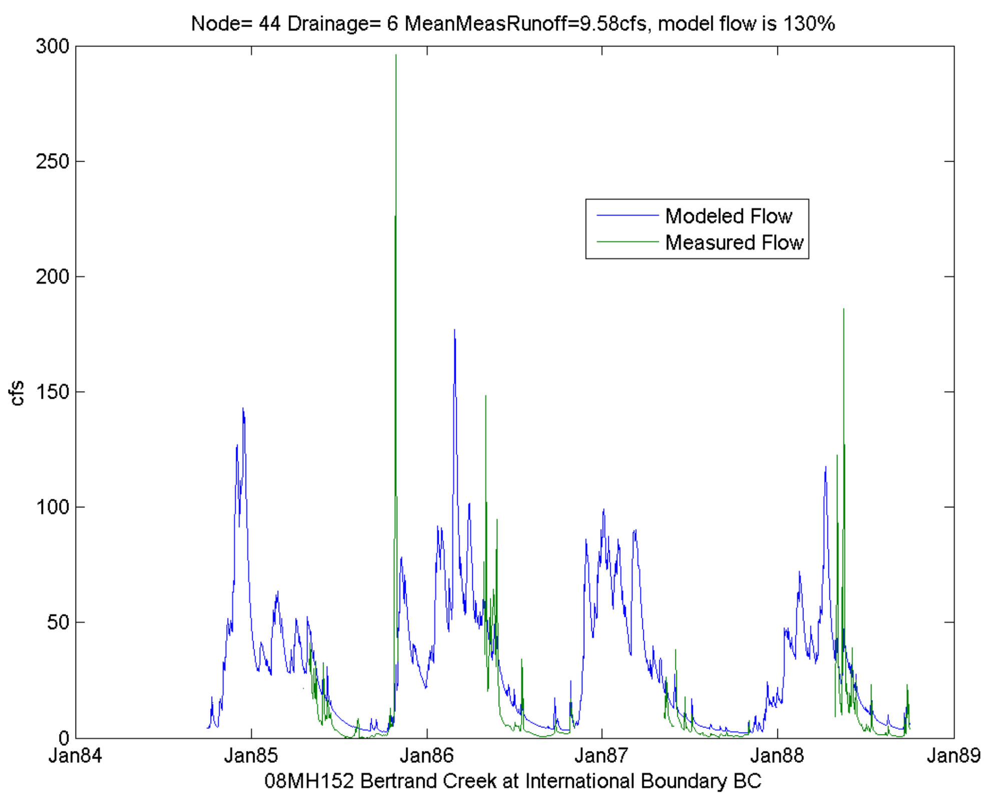

Node= 44 Drainage= 6 MeanMeasRunoff=9.58cfs, model flow is 130%
cfs
Modeled Flow
Measured Flow
Jan84
Jan85
Jan86
Jan87
Jan88
Jan89
08MH152 Bertrand Creek at International Boundary BC

1933

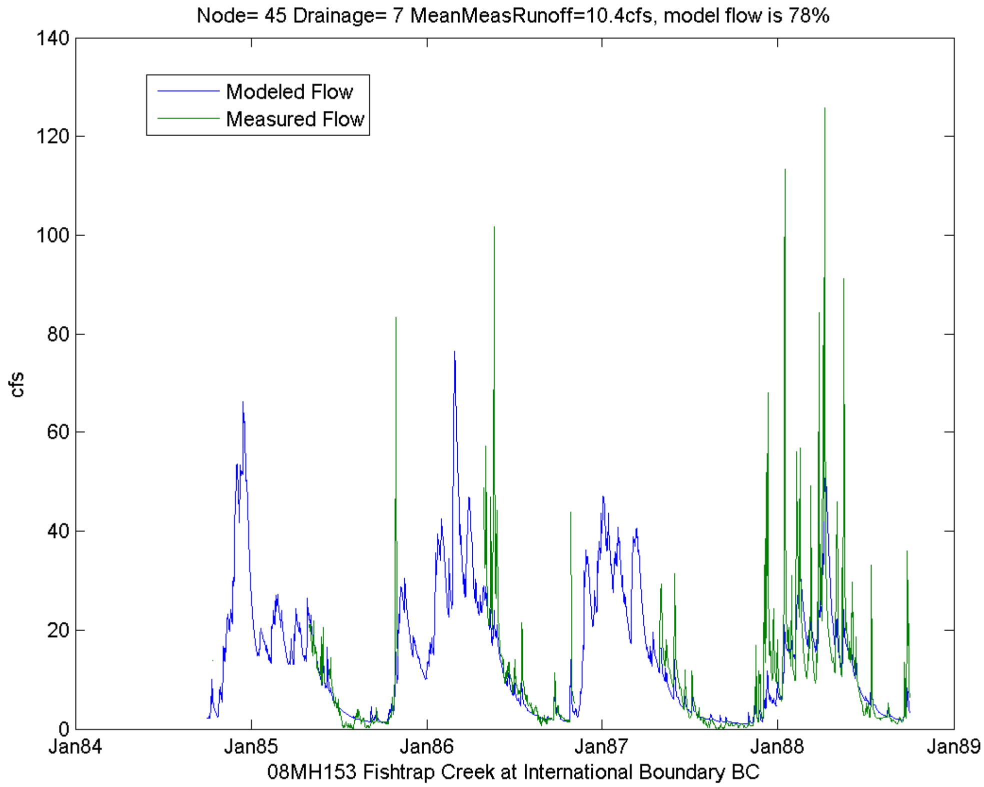
Node= 45 Drainage= 7 MeanMeasRunoff=10.4cfs, model flow is 78%
Modeled Flow
Measured Flow
cfs
0
20
40
60
80
100
120
140
Jan84
Jan85
Jan86
Jan87
Jan88
Jan89
08MH153 Fishtrap Creek at International Boundary BC

Calibration Period 4 (10/1/1998-9/30/2001)

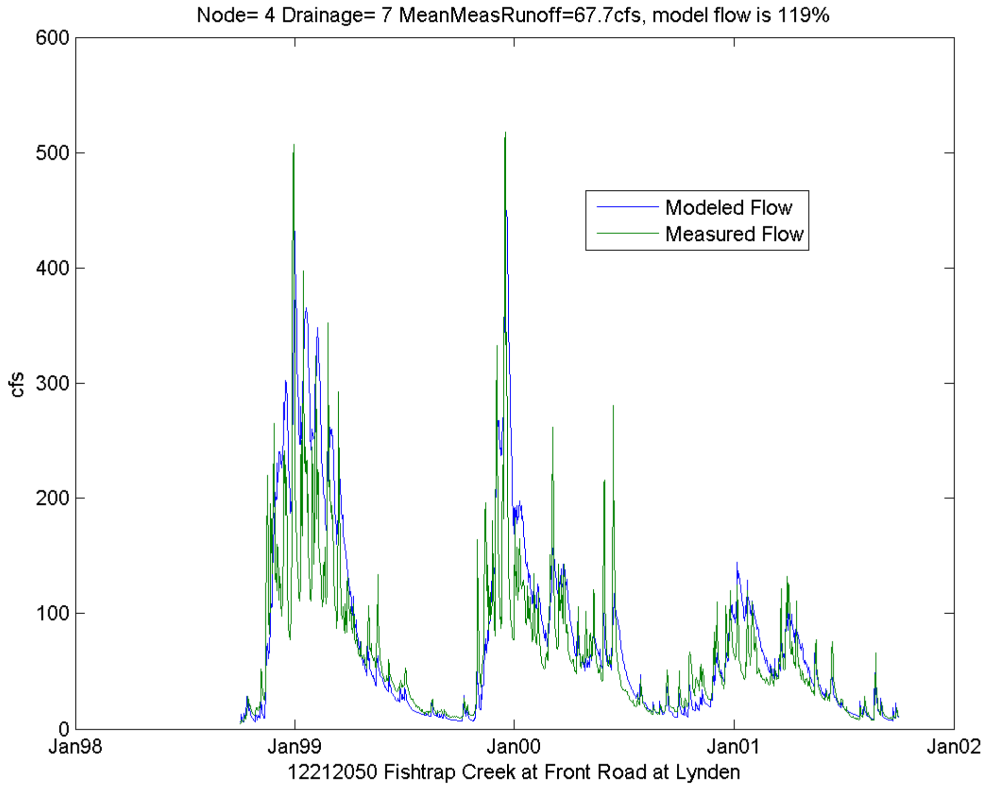

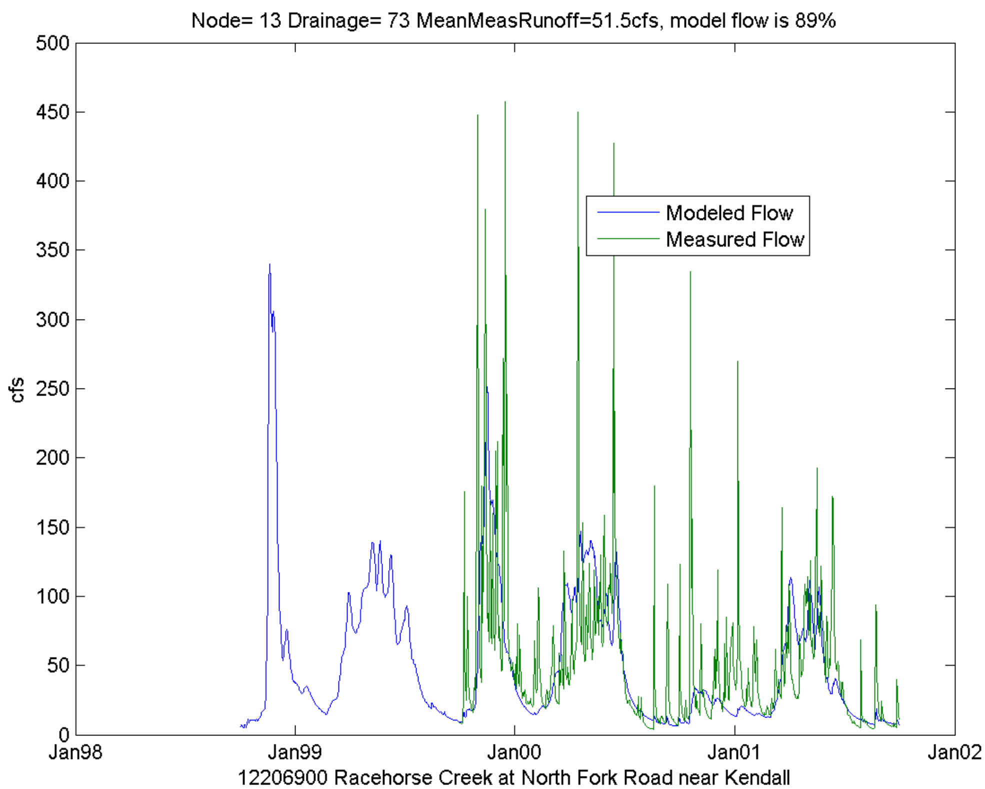

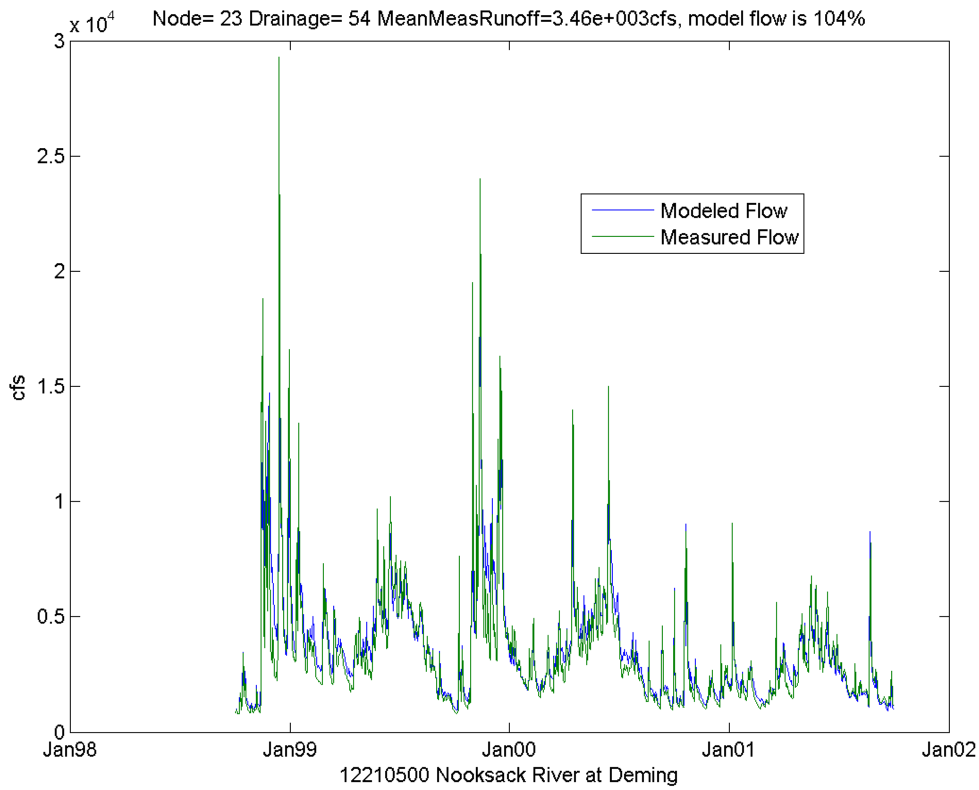
Node= 23 Drainage= 54 MeanMeasRunoff=3.46e+003cfs, model flow is 104%
x 10^4
3
2.5
2
1.5
1
0.5
0
cfs
Modeled Flow
Measured Flow
Jan98
Jan99
Jan00
Jan01
Jan02
12210500 Nooksack River at Deming

1939

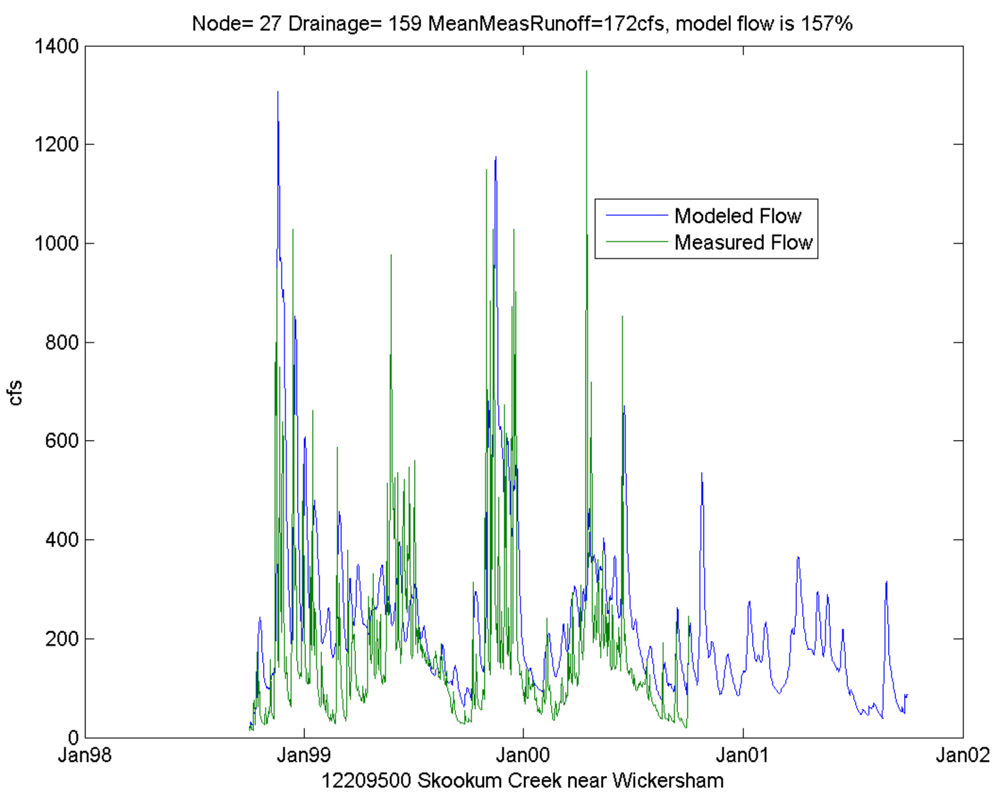
Node= 27 Drainage= 159 MeanMeasRunoff=172cfs, model flow is 157%
1400
1200
1000
800
600
400
200
0
cfs
Modeled Flow
Measured Flow
Jan98
Jan99
Jan00
Jan01
Jan02
12209500 Skookum Creek near Wickersham

1940

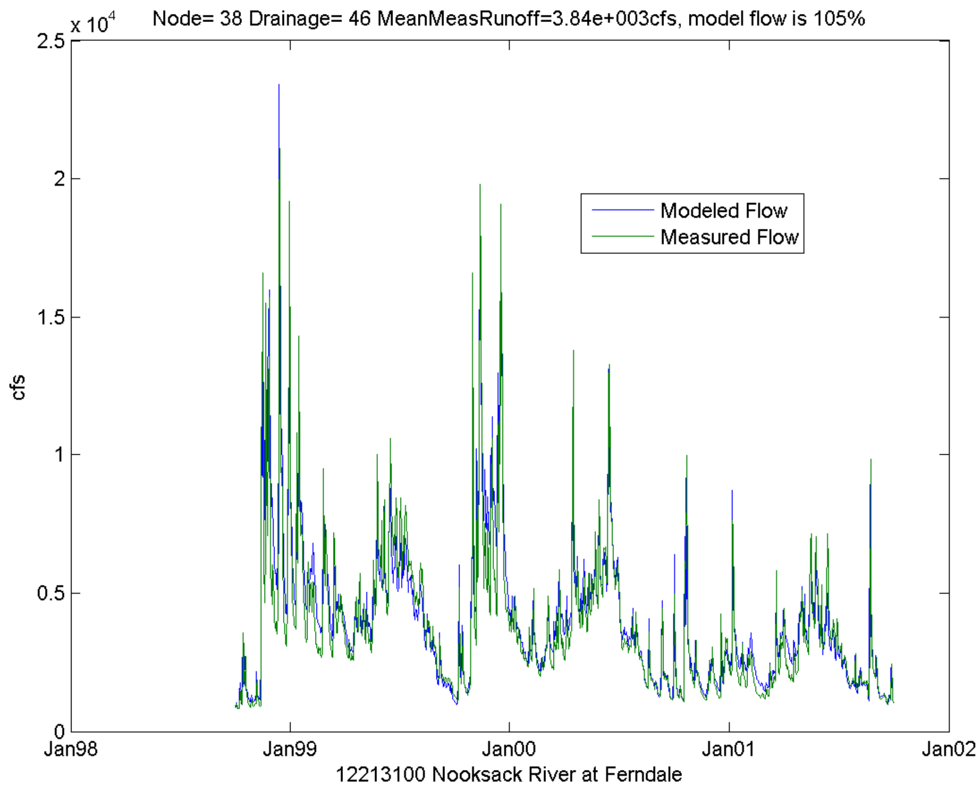
Node= 38 Drainage= 46 MeanMeasRunoff=3.84e+003cfs, model flow is 105%
x 10^4
2.5
2
1.5
1
0.5
0
cfs
Modeled Flow
Measured Flow
Jan98
Jan99
Jan00
Jan01
Jan02
12213100 Nooksack River at Ferndale

1941

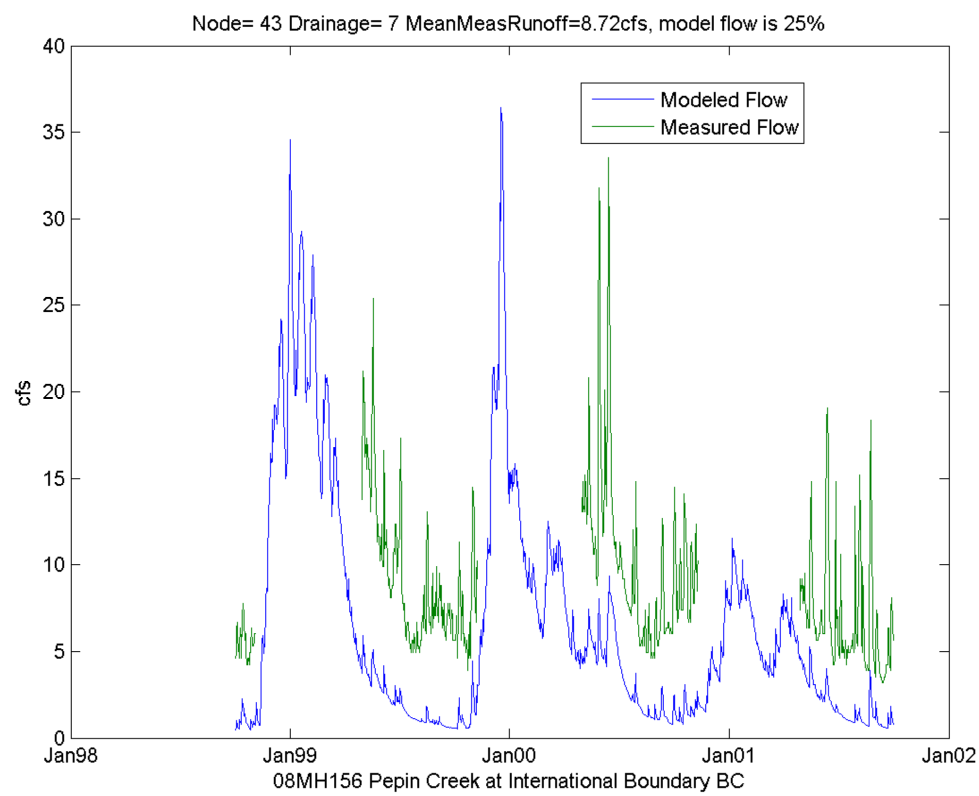
Node= 43 Drainage= 7 MeanMeasRunoff=8.72cfs, model flow is 25%
40
35
30
25
20
15
10
5
0
cfs
Modeled Flow
Measured Flow
Jan98
Jan99
Jan00
Jan01
Jan02
08MH156 Pepin Creek at International Boundary BC

1942

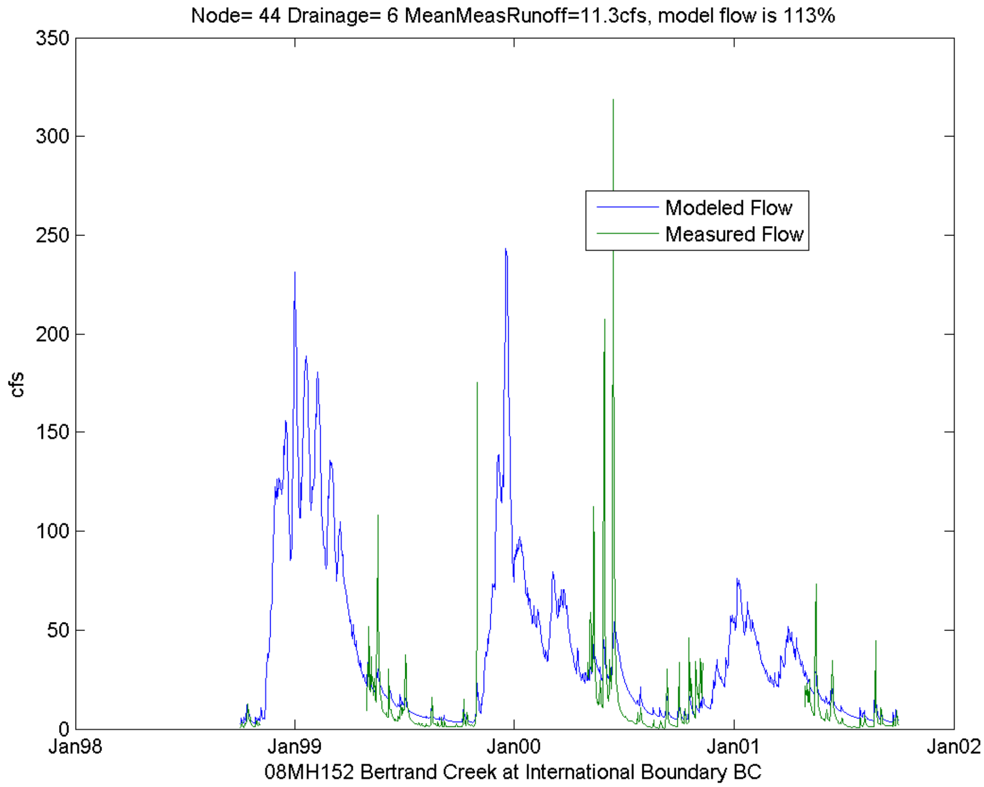
Node= 44 Drainage= 6 MeanMeasRunoff=11.3cfs, model flow is 113%
350
300
250
200
150
100
50
0
cfs
Modeled Flow
Measured Flow
Jan98
Jan99
Jan00
Jan01
Jan02
08MH152 Bertrand Creek at International Boundary BC

1943

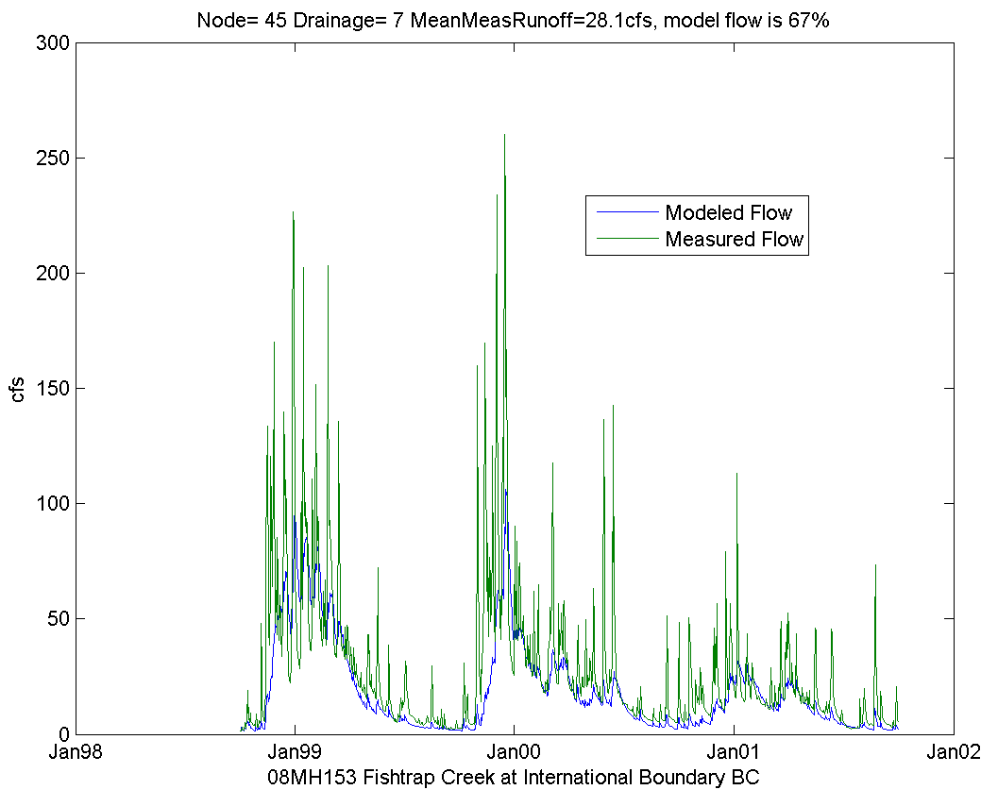
Node= 45 Drainage= 7 MeanMeasRunoff=28.1cfs, model flow is 67%
300
250
200
150
100
50
0
cfs
Modeled Flow
Measured Flow
Jan98
Jan99
Jan00
Jan01
Jan02
08MH153 Fishtrap Creek at International Boundary BC

1944

Validation Period 1 (10/1/1953-9/30/1954)

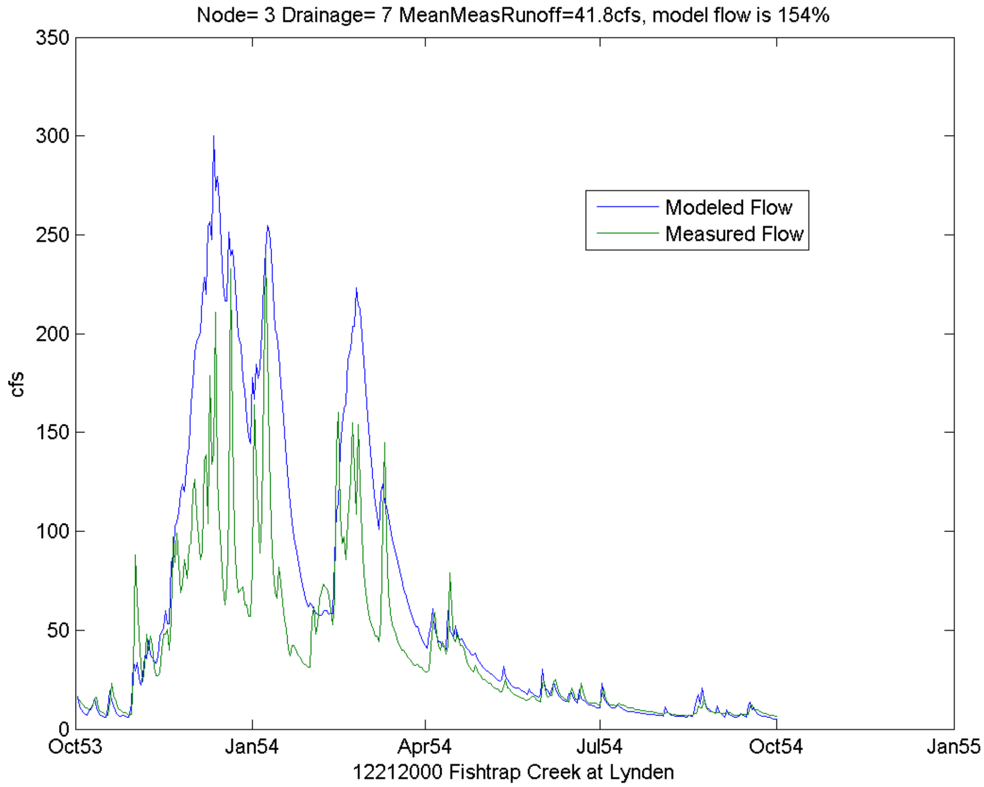

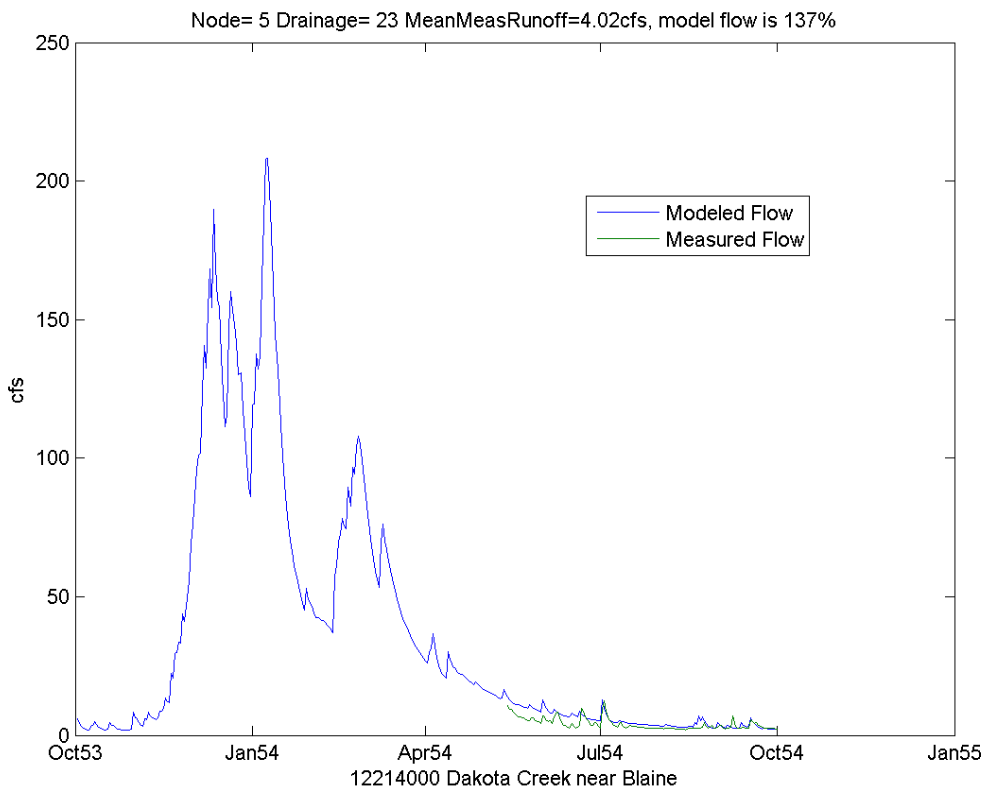

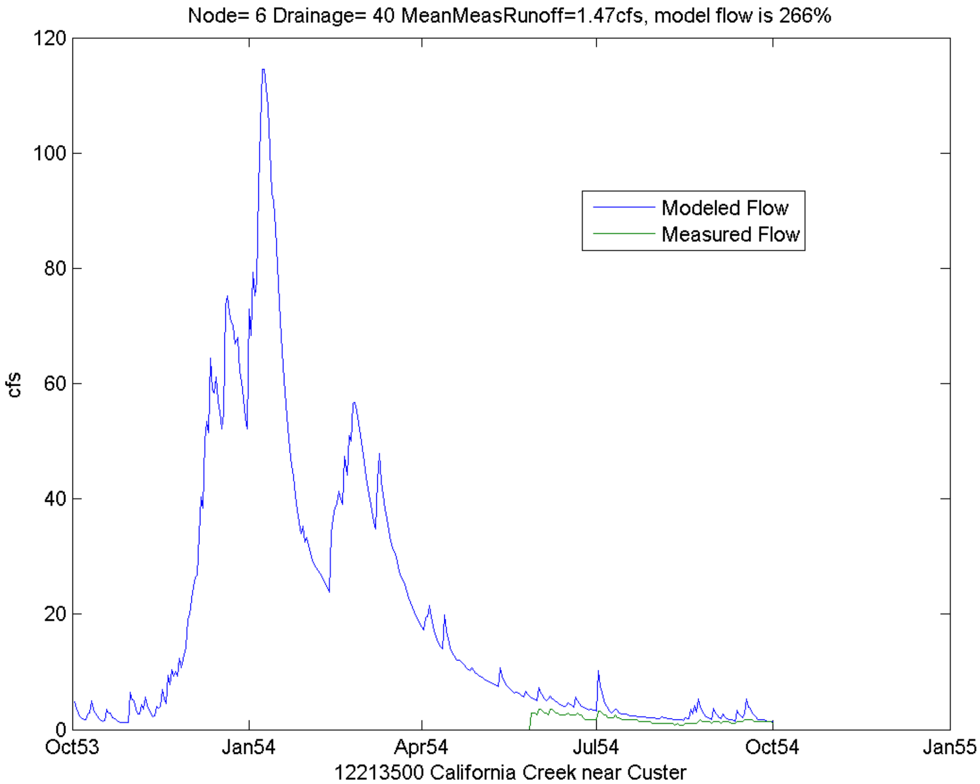
Node= 6 Drainage= 40 MeanMeasRunoff=1.47cfs, model flow is 266%
120
100
80
60
40
20
0
cfs
Modeled Flow
Measured Flow
Oct53
Jan54
Apr54
Jul54
Oct54
Jan55
12213500 California Creek near Custer

1948

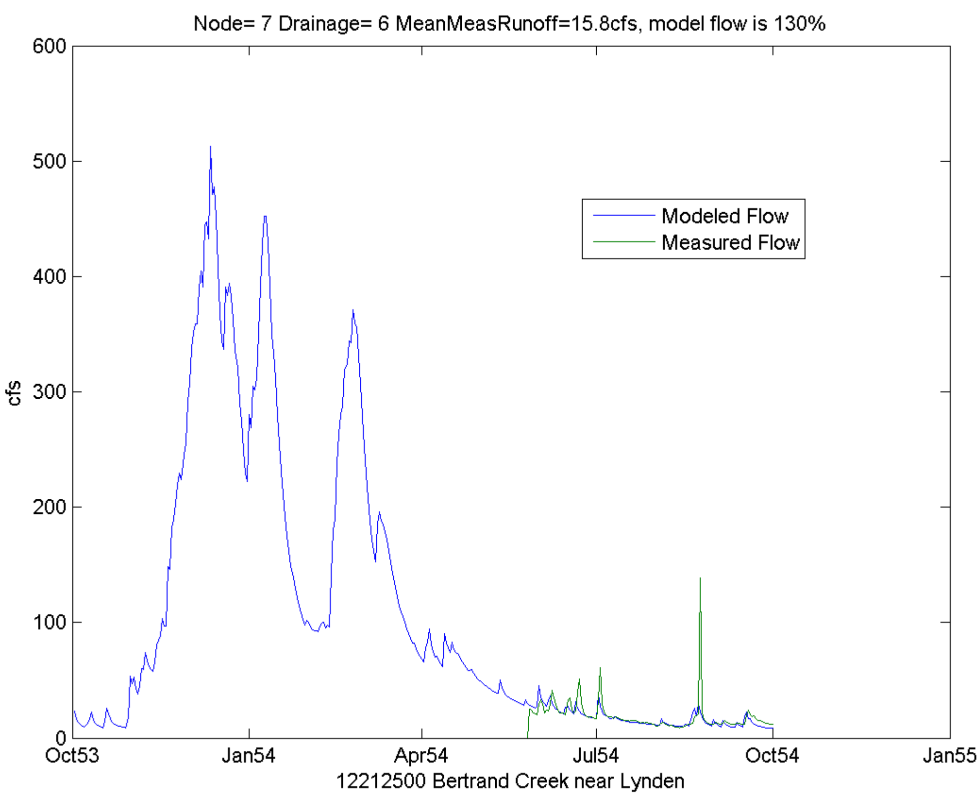
Node= 7 Drainage= 6 MeanMeasRunoff=15.8cfs, model flow is 130%
600
500
400
300
200
100
0
cfs
Modeled Flow
Measured Flow
Oct53
Jan54
Apr54
Jul54
Oct54
Jan55
12212500 Bertrand Creek near Lynden

1949

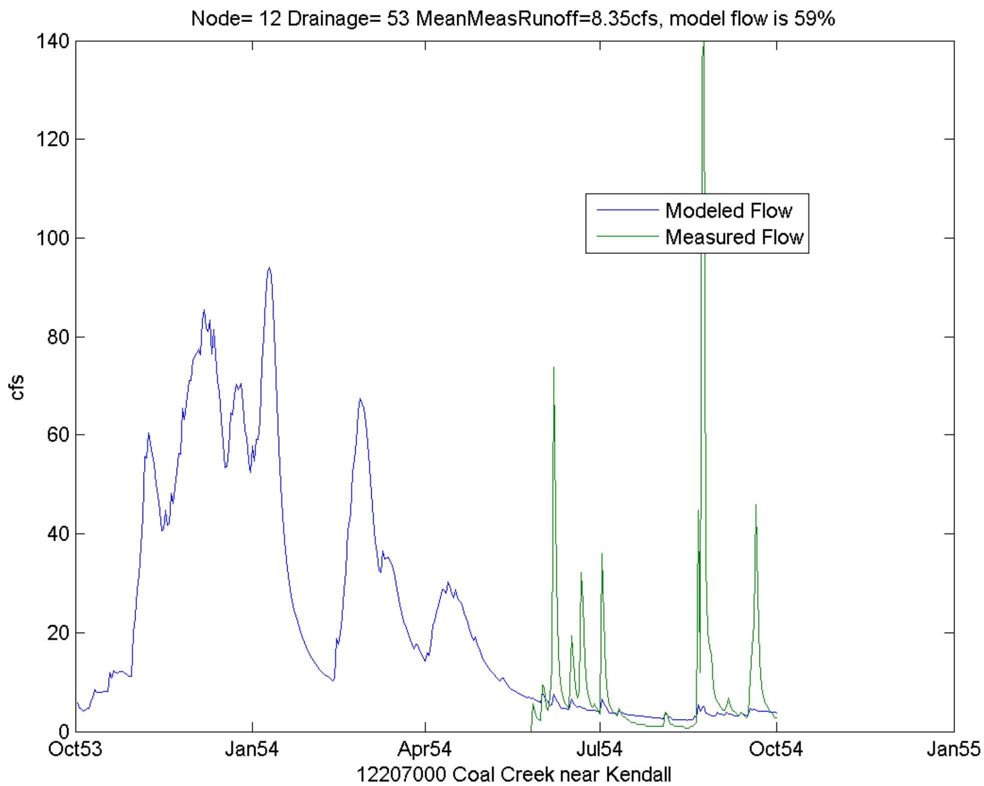
Node= 12 Drainage= 53 MeanMeasRunoff=8.35cfs, model flow is 59%
Modeled Flow
Measured Flow
cfs
0
20
40
60
80
100
120
140
Oct53
Jan54
Apr54
Jul54
Oct54
Jan55
12207000 Coal Creek near Kendall

1950

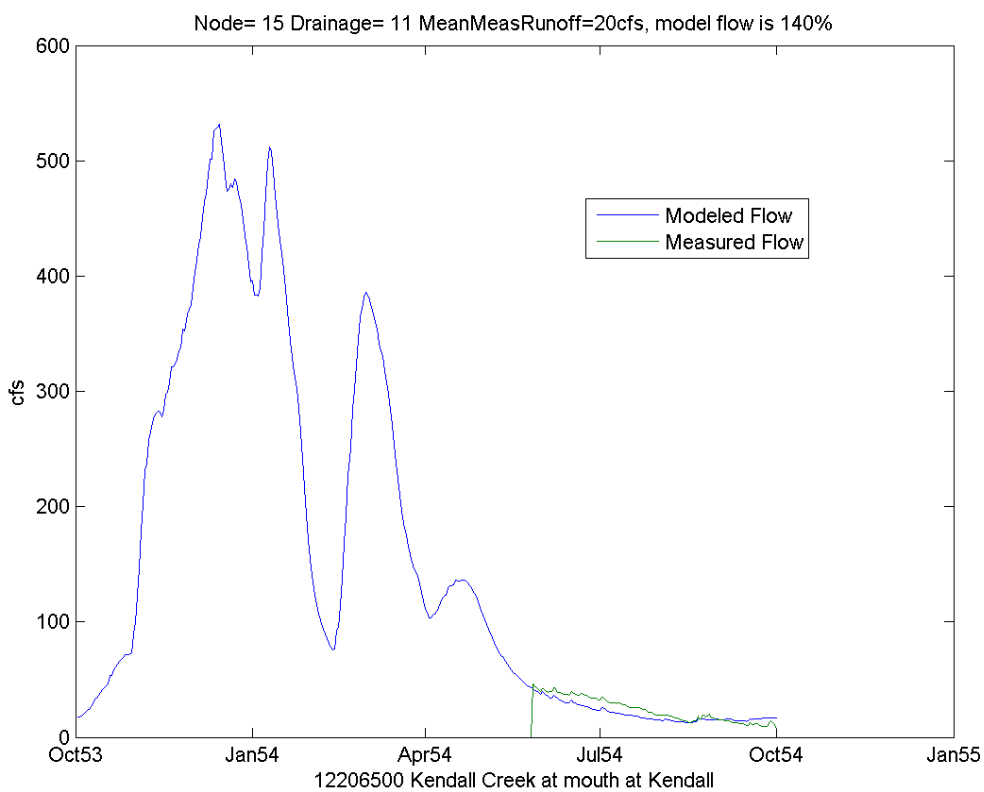
Node= 15 Drainage= 11 MeanMeasRunoff=20cfs, model flow is 140%
Modeled Flow
Measured Flow
cfs
0
100
200
300
400
500
600
Oct53
Jan54
Apr54
Jul54
Oct54
Jan55
12206500 Kendall Creek at mouth at Kendall

1951

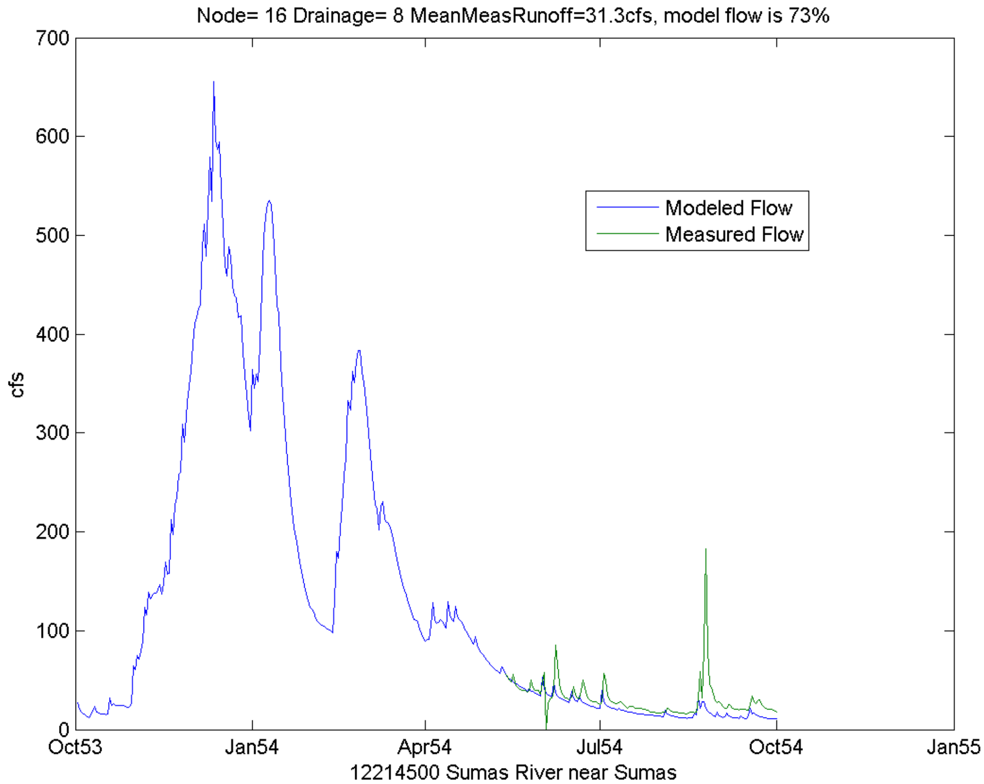
Node= 16 Drainage= 8 MeanMeasRunoff=31.3cfs, model flow is 73%
700
600
500
400
300
200
100
0
cfs
Modeled Flow
Measured Flow
Oct53
Jan54
Apr54
Jul54
Oct54
Jan55
12214500 Sumas River near Sumas

1952

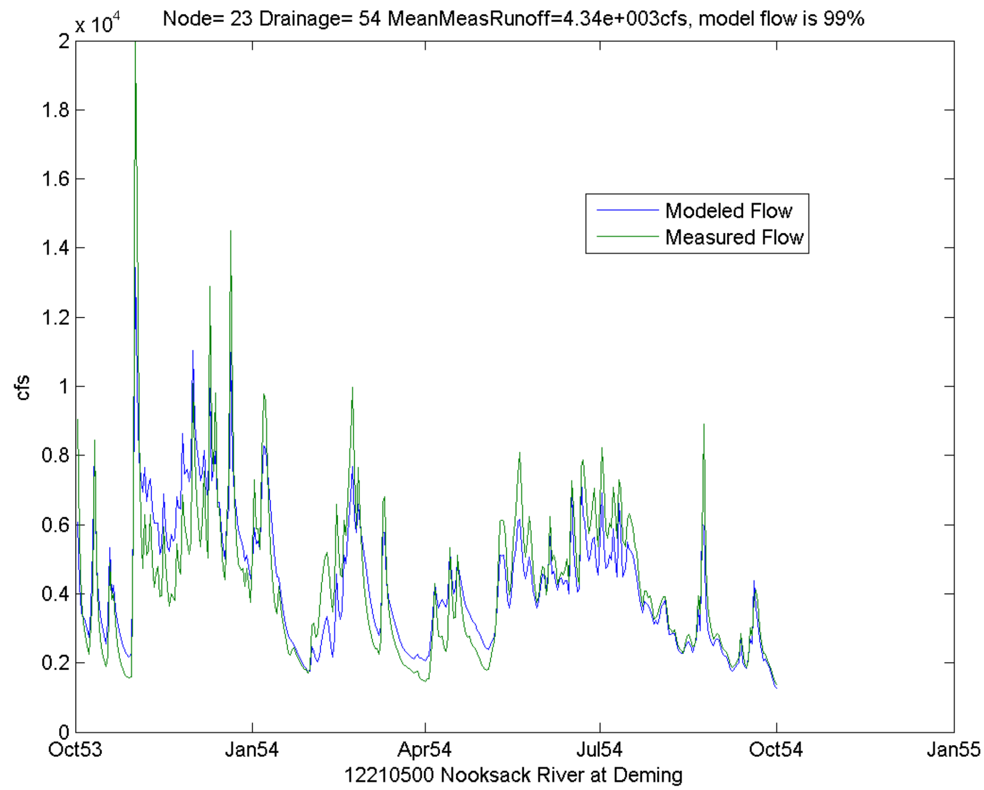
Node= 23 Drainage= 54 MeanMeasRunoff=4.34e+003cfs, model flow is 99%
x 10^4
2
1.8
1.6
1.4
1.2
1
0.8
0.6
0.4
0.2
0
cfs
Modeled Flow
Measured Flow
Oct53
Jan54
Apr54
Jul54
Oct54
Jan55
12210500 Nooksack River at Deming

1953

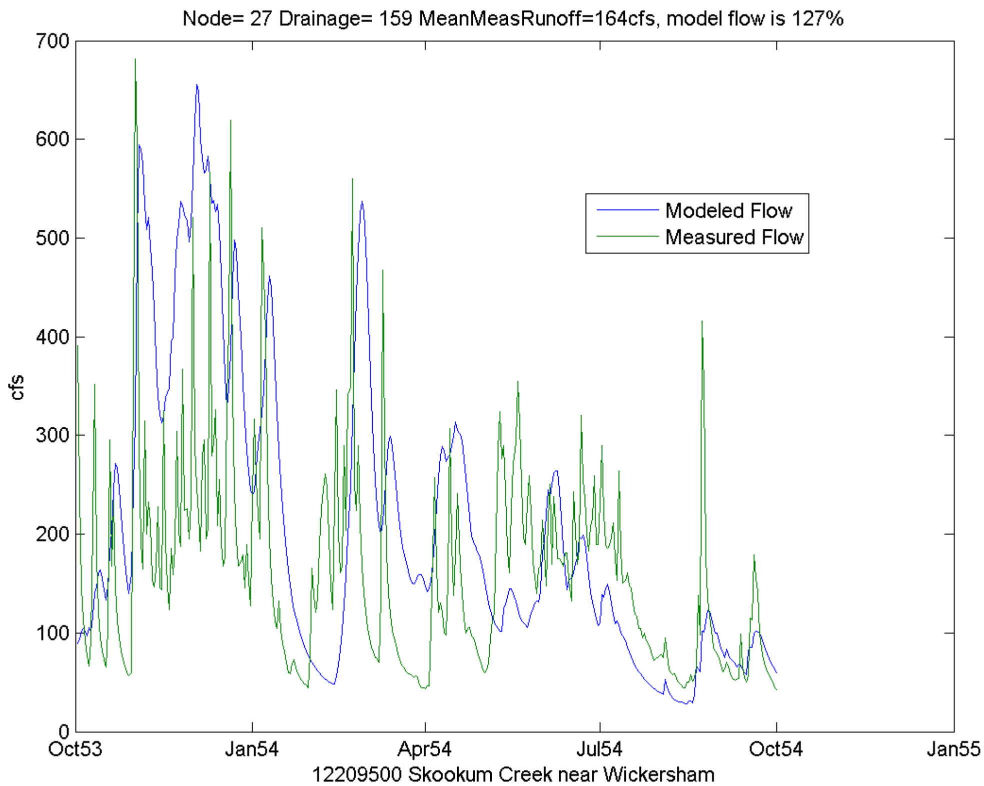
Node= 27 Drainage= 159 MeanMeasRunoff=164cfs, model flow is 127%
700
600
500
400
300
200
100
0
cfs
Modeled Flow
Measured Flow
Oct53
Jan54
Apr54
Jul54
Oct54
Jan55
12209500 Skookum Creek near Wickersham

1954

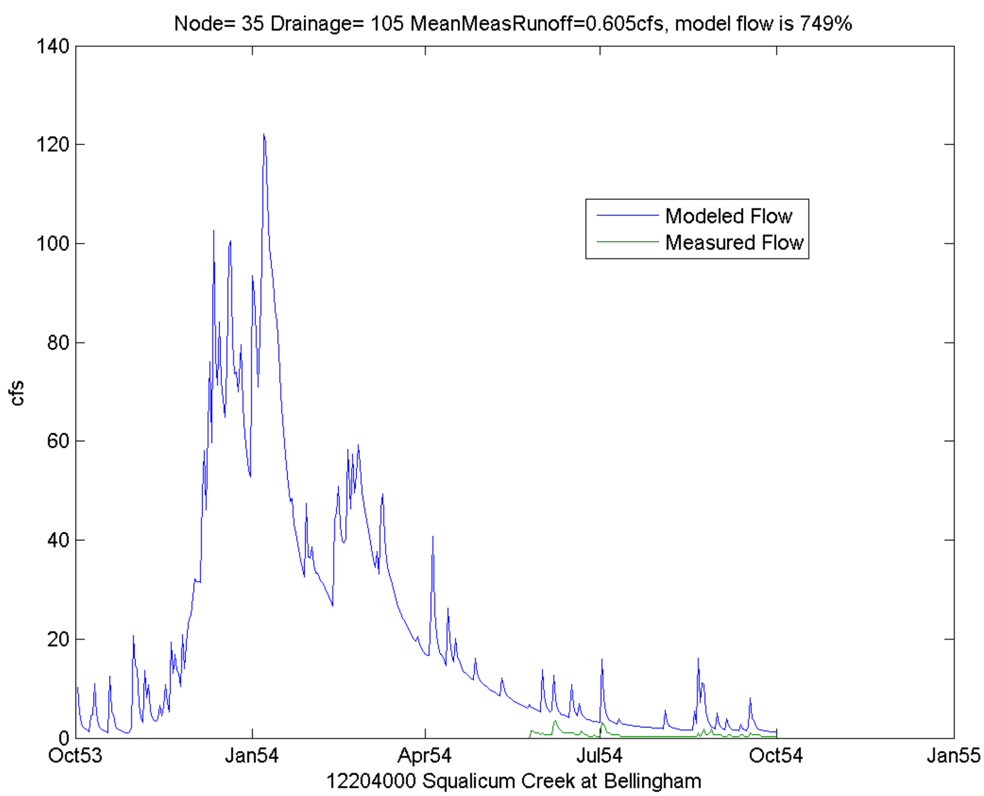
Node= 35 Drainage= 105 MeanMeasRunoff=0.605cfs, model flow is 749%
140
120
100
80
60
40
20
0
cfs
Modeled Flow
Measured Flow
Oct53
Jan54
Apr54
Jul54
Oct54
Jan55
12204000 Squalicum Creek at Bellingham

1955

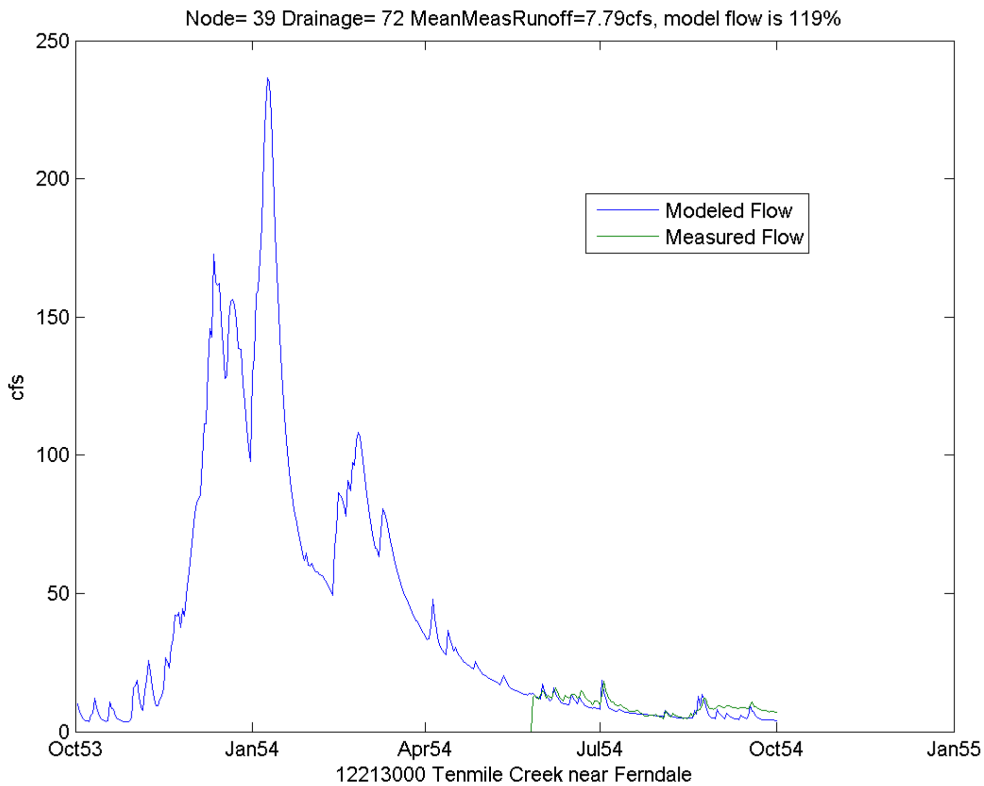
Node= 39 Drainage= 72 MeanMeasRunoff=7.79cfs, model flow is 119%
Modeled Flow
Measured Flow
cfs
250
200
150
100
50
0
Oct53
Jan54
Apr54
Jul54
Oct54
Jan55
12213000 Tenmile Creek near Ferndale

1956

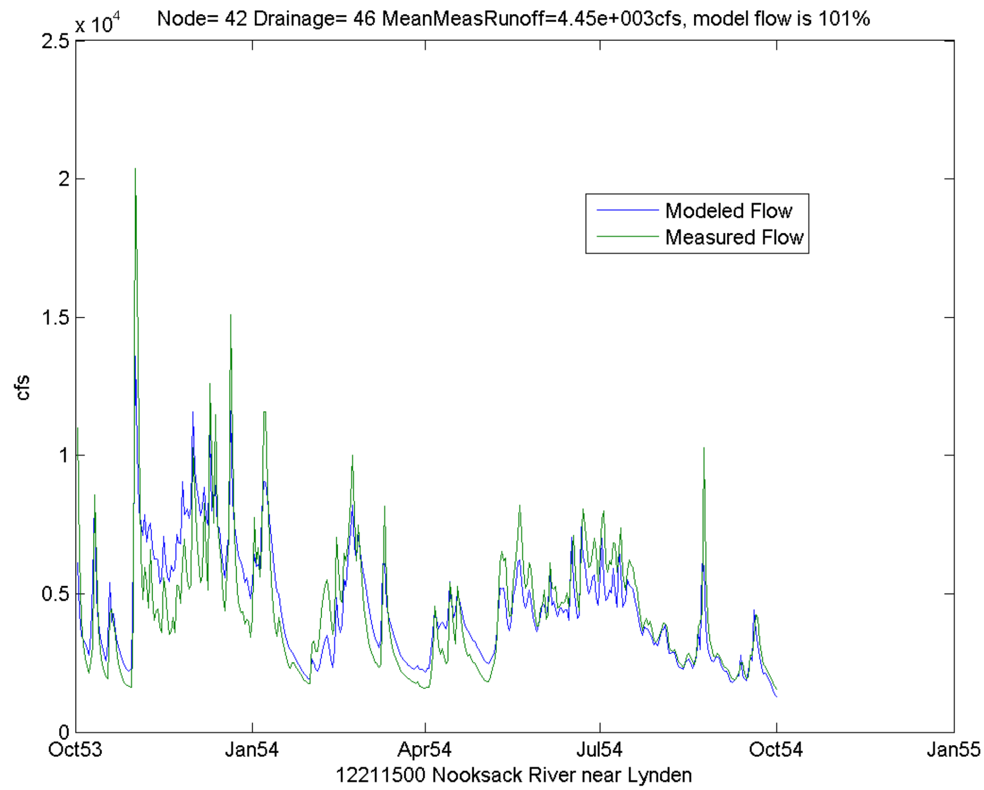
Node= 42 Drainage= 46 MeanMeasRunoff=4.45e+003cfs, model flow is 101%
x 10^4
Modeled Flow
Measured Flow
cfs
2.5
2
1.5
1
0.5
0
Oct53
Jan54
Apr54
Jul54
Oct54
Jan55
12211500 Nooksack River near Lynden

1957

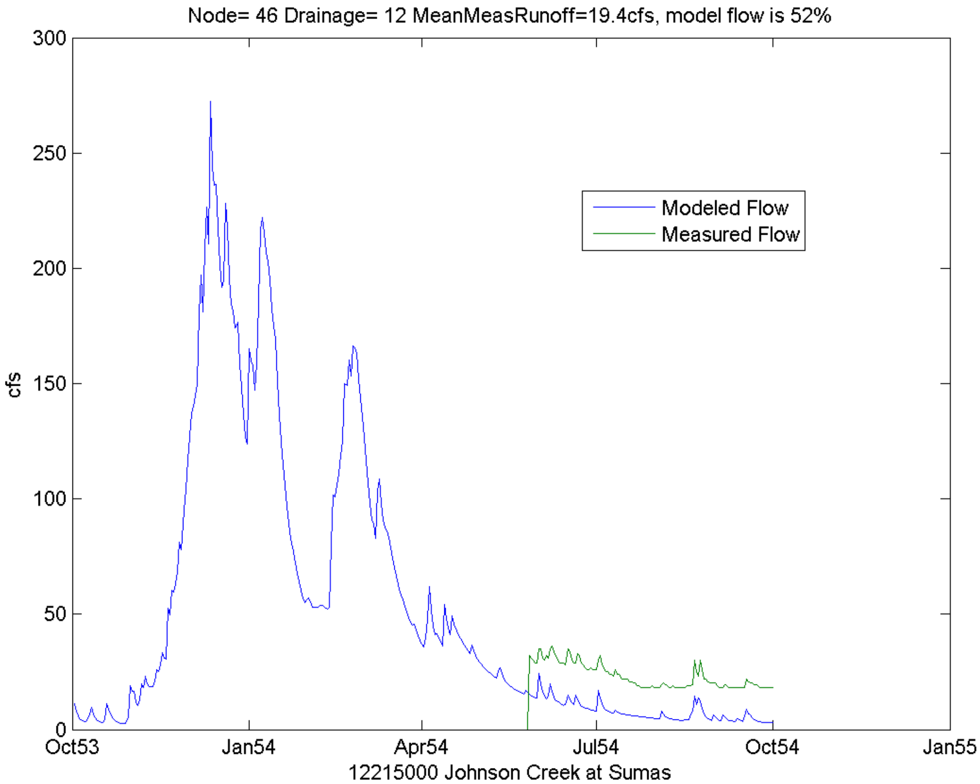
Node= 46 Drainage= 12 MeanMeasRunoff=19.4cfs, model flow is 52%
300
250
200
150
100
50
0
cfs
Modeled Flow
Measured Flow
Oct53
Jan54
Apr54
Jul54
Oct54
Jan55
12215000 Johnson Creek at Sumas

1958

Validation Period 2 (10/1/1988-9/30/1989)

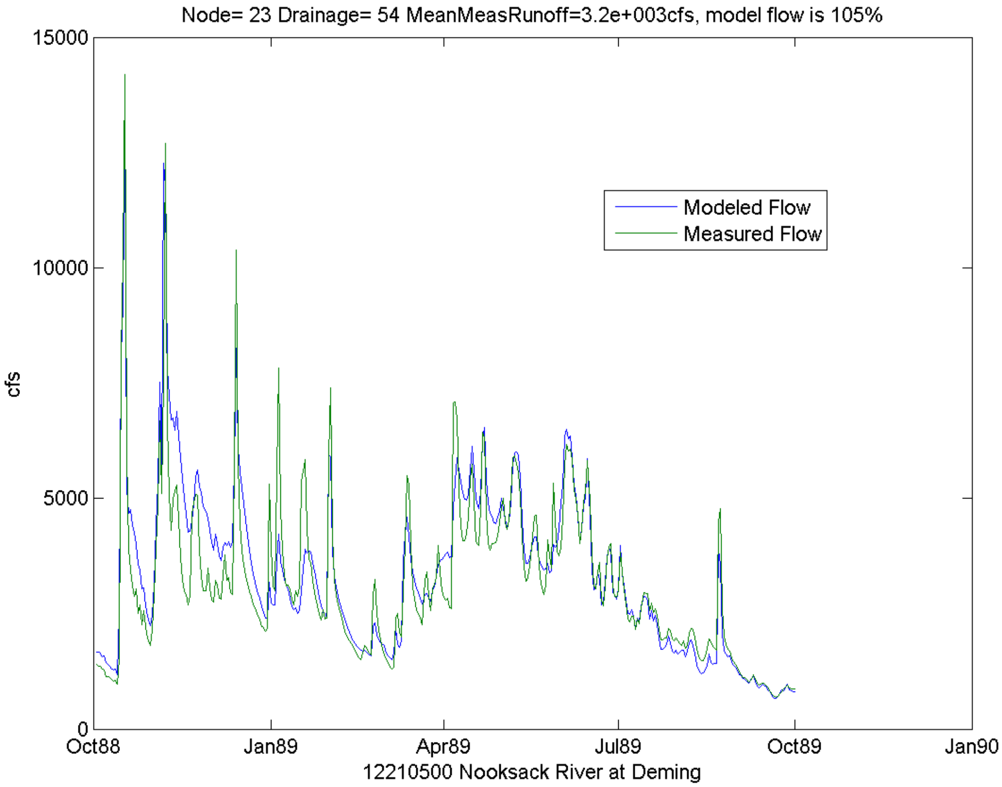

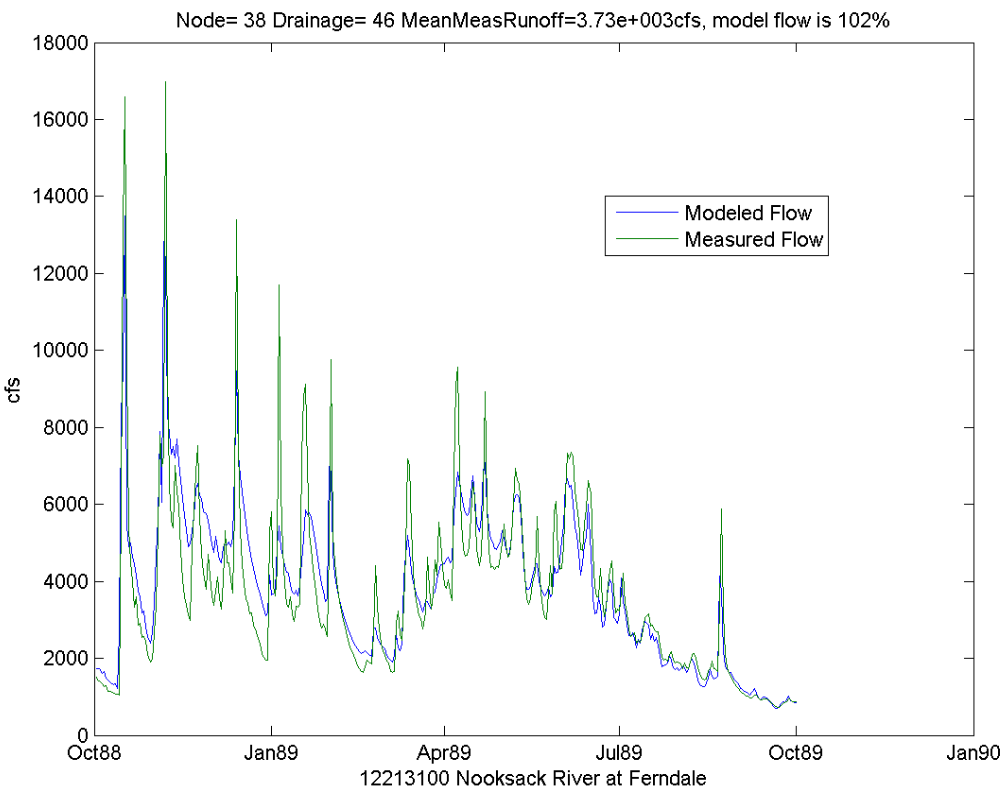

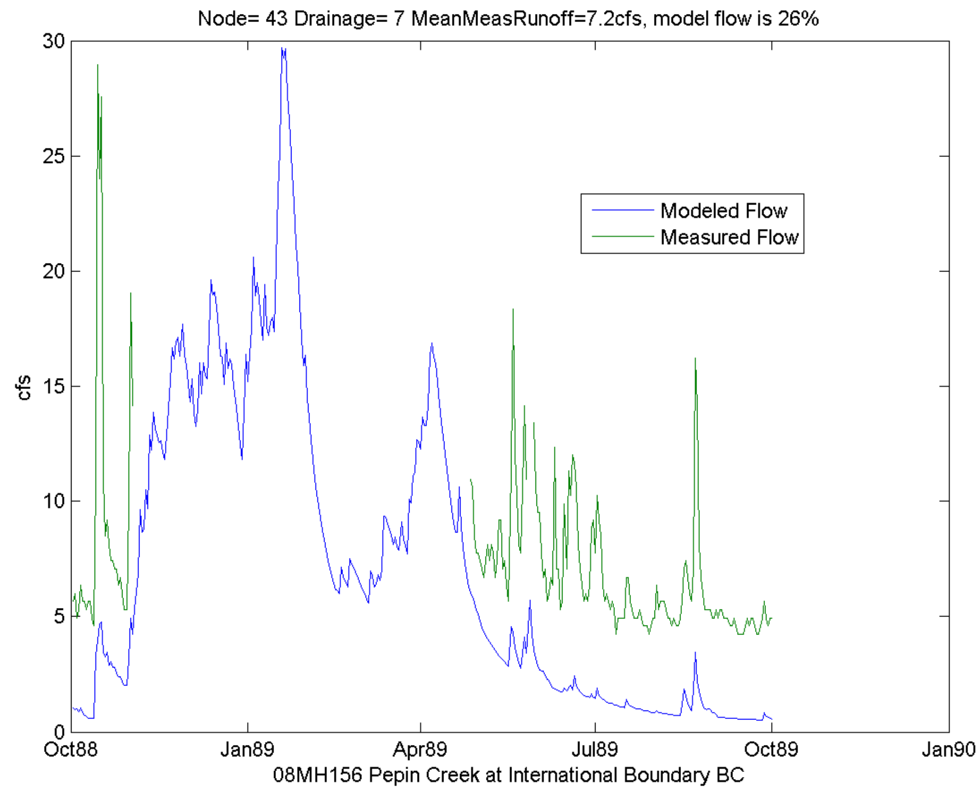
Node= 43 Drainage= 7 MeanMeasRunoff=7.2cfs, model flow is 26%
Modeled Flow
Measured Flow
cfs
30
25
20
15
10
5
0
Oct88
Jan89
Apr89
Jul89
Oct89
Jan90
08MH156 Pepin Creek at International Boundary BC

1962

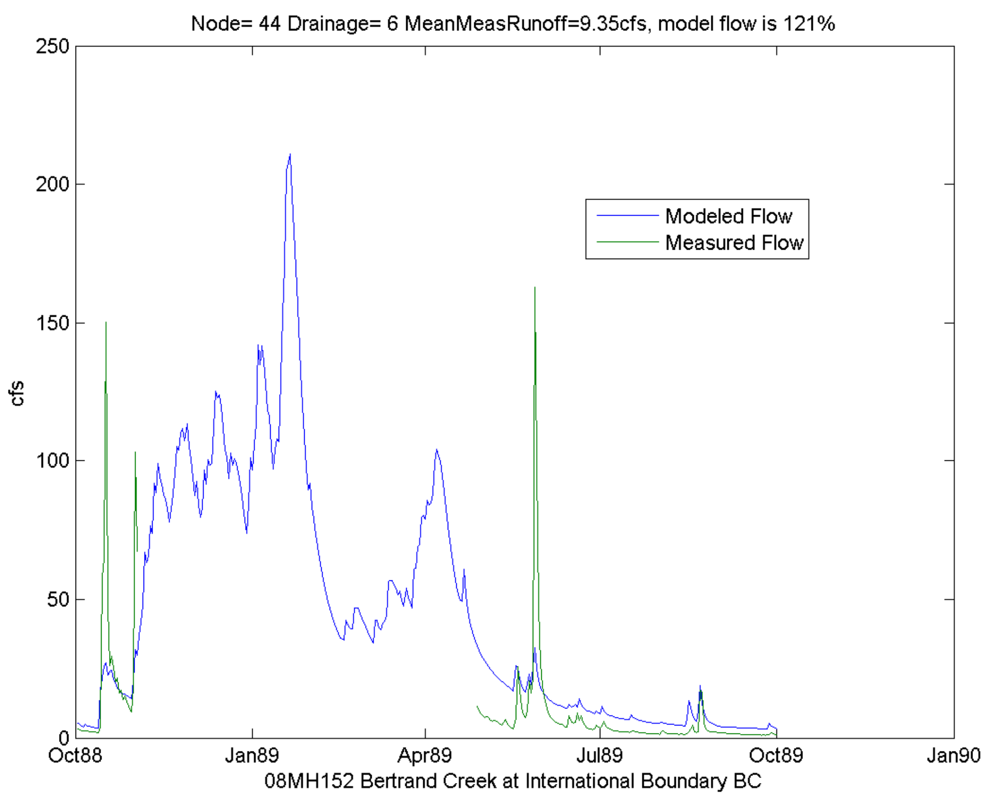
Node= 44 Drainage= 6 MeanMeasRunoff=9.35cfs, model flow is 121%
Modeled Flow
Measured Flow
cfs
250
200
150
100
50
0
Oct88
Jan89
Apr89
Jul89
Oct89
Jan90
08MH152 Bertrand Creek at International Boundary BC

1963

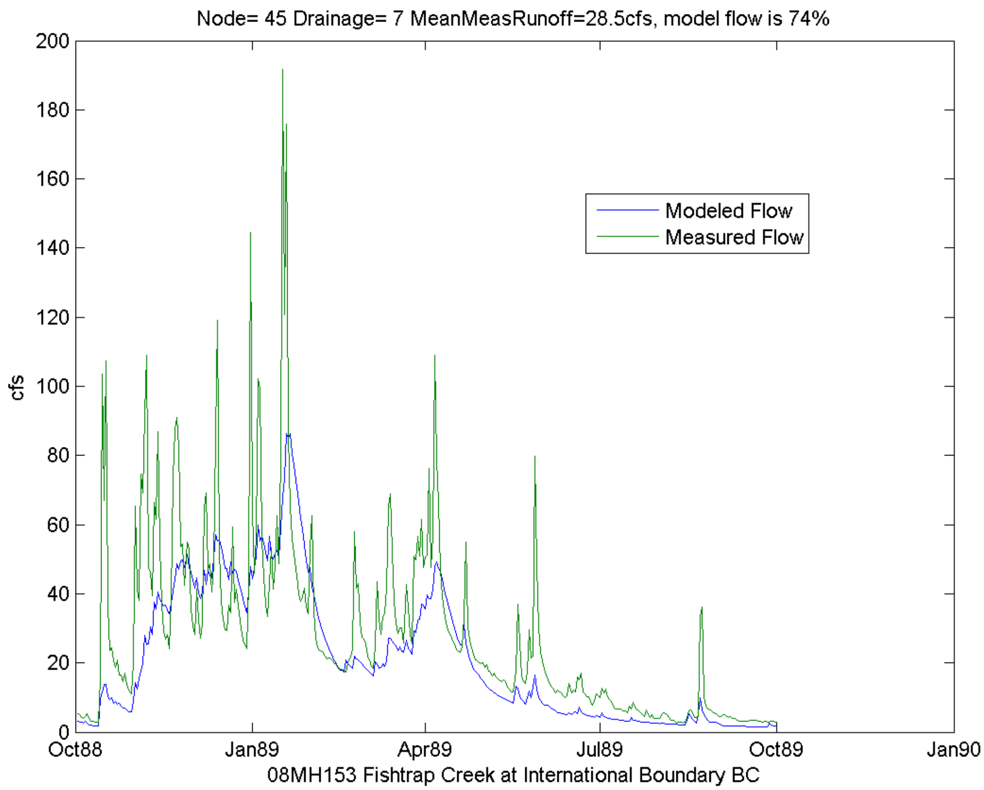
Node= 45 Drainage= 7 MeanMeasRunoff=28.5cfs, model flow is 74%
Modeled Flow
Measured Flow
cfs
200
180
160
140
120
100
80
60
40
20
0
Oct88
Jan89
Apr89
Jul89
Oct89
Jan90
08MH153 Fishtrap Creek at International Boundary BC

1964

Validation Period 3 (10/1/1992-9/30/1993)

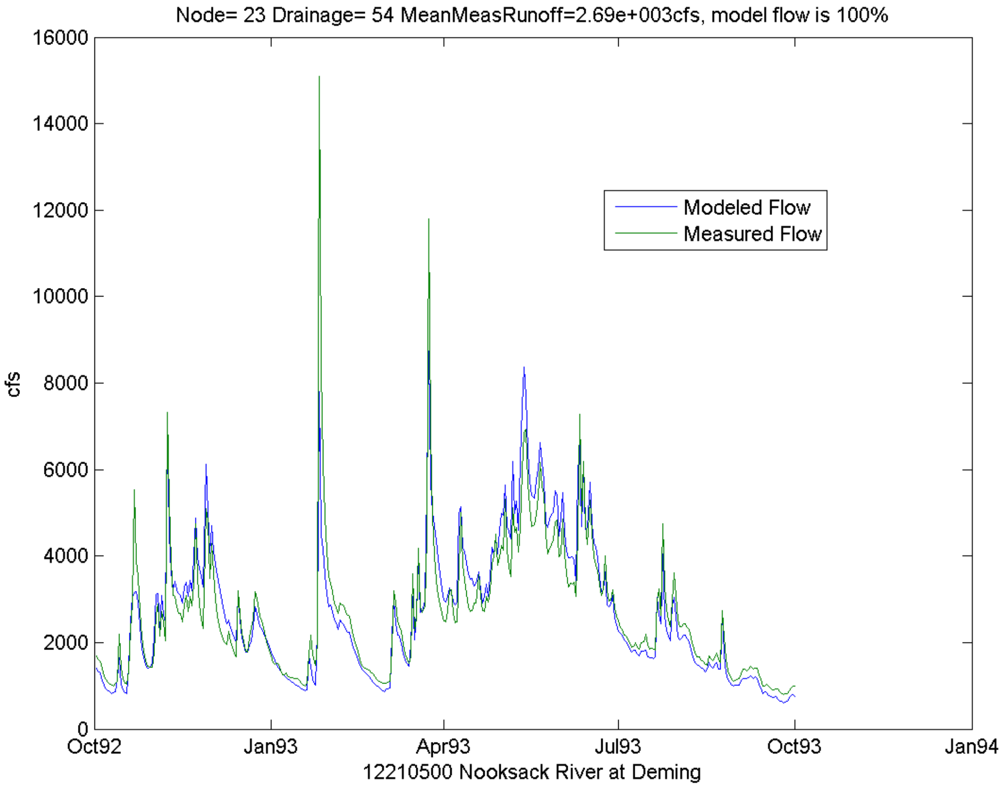

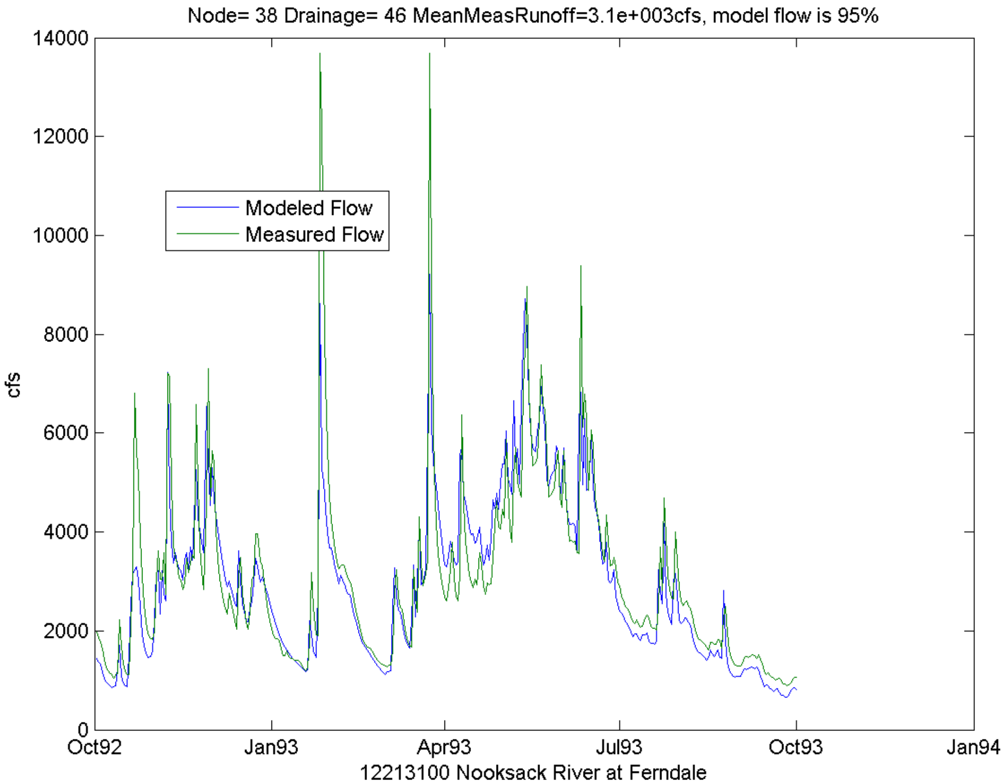

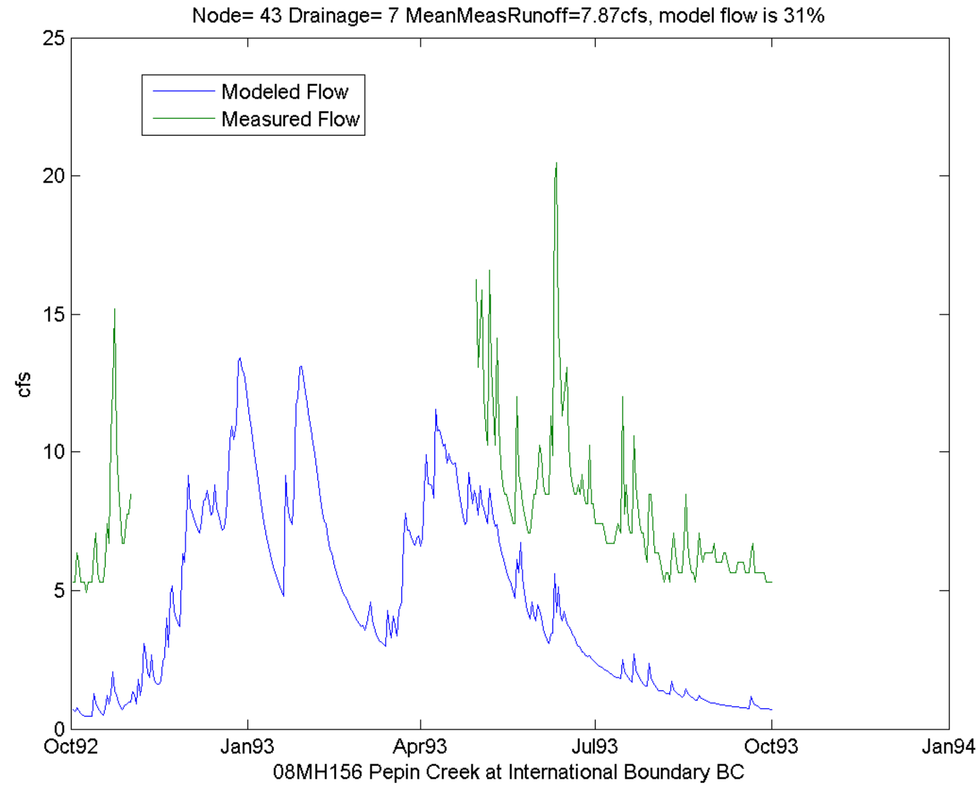
Node= 43 Drainage= 7 MeanMeasRunoff=7.87cfs, model flow is 31%
Modeled Flow
Measured Flow
cfs
25
20
15
10
5
0
Oct92
Jan93
Apr93
Jul93
Oct93
Jan94
08MH156 Pepin Creek at International Boundary BC

1968

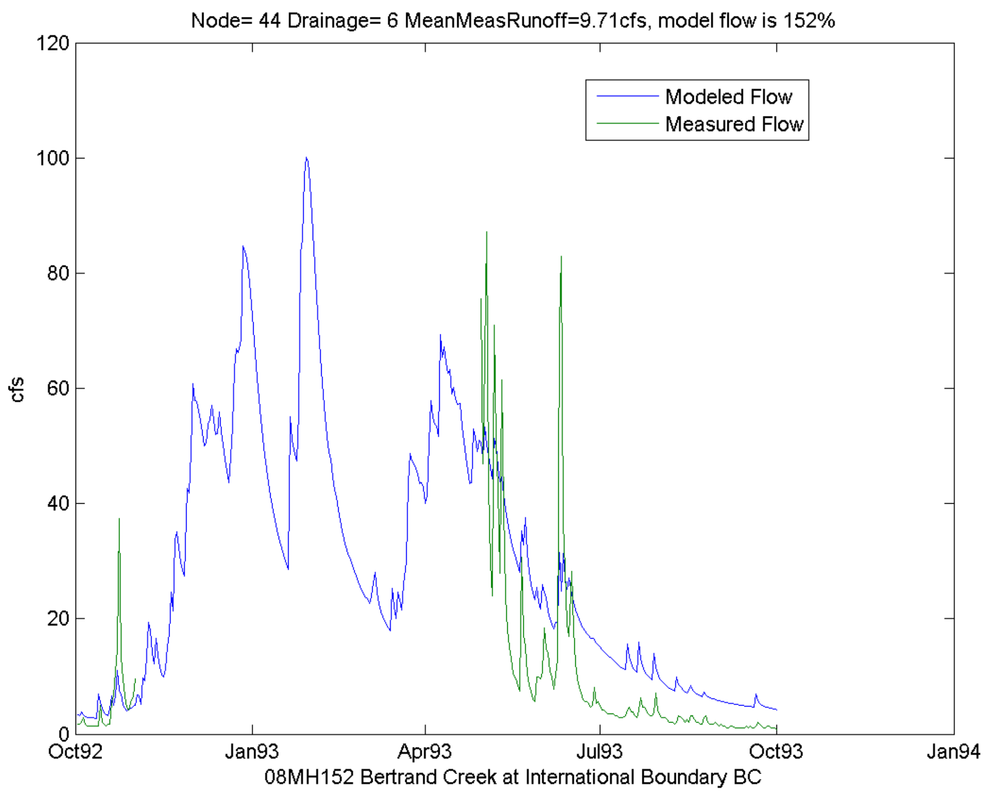
Node= 44 Drainage= 6 MeanMeasRunoff=9.71cfs, model flow is 152%
Modeled Flow
Measured Flow
cfs
120
100
80
60
40
20
0
Oct92
Jan93
Apr93
Jul93
Oct93
Jan94
08MH152 Bertrand Creek at International Boundary BC

1969

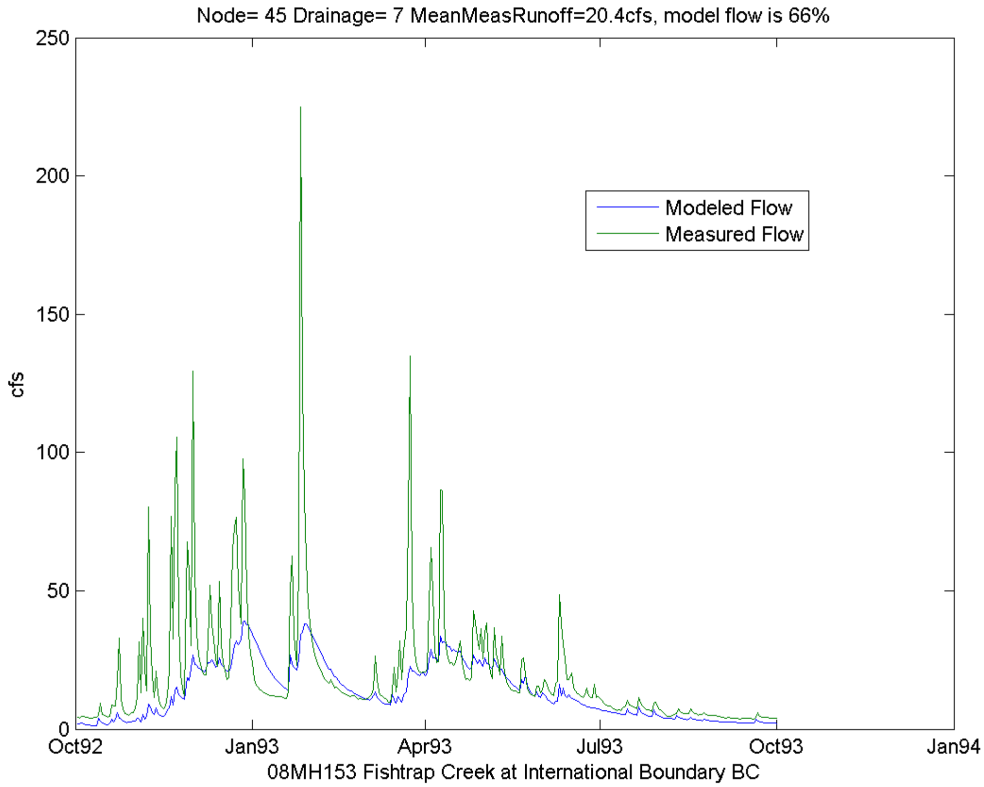
Node= 45 Drainage= 7 MeanMeasRunoff=20.4cfs, model flow is 66%
250
200
150
100
50
0
cfs
Modeled Flow
Measured Flow
Oct92
Jan93
Apr93
Jul93
Oct93
Jan94
08MH153 Fishtrap Creek at International Boundary BC

1970

Contents of Electronic Appendix

File	Description
<u>Spreadsheets related to spatial inputs</u>	
lut_impervious.xls	Lookup table for impervious fraction by land use and land cover
lut_irrigation.xls	Lookup table for irrigation parameters by land use and land cover
lut_kc.xls	Lookup table for crop coefficients
lut_lulc.xls	Lookup table for land use and land cover parameters
lut_soils.xls	Lookup table for soils parameters
lut_tile_drained.xls	Lookup table for tile drainage coefficients
lut_ditch_drained.xls	Lookup table for ditch drainage coefficients
AsciiGrids.zip	Zipped Folder with ASCII grid files used in preparing TOPNET spatial input
<u>Model input files specifying spatial parameters for each drainage</u>	
basinpars_existing.txt	Basin parameters file for existing conditions
basinpars_fbo.txt	Basin parameters file for full buildout conditions
basinpars_historic.txt	Basin parameters file for historic buildout conditions
<u>Spreadsheets related to management inputs</u>	
user_existing.xls	Spreadsheet with users created for the existing conditions scenario
additional_users.xls	Spreadsheet with additional users created manually (Dairies and diversions)
MonthlyDemandFraction_with_additional_information.xls	Spreadsheet with monthly demand information
population_data.xls	Spreadsheet with population data used to set up users.
PWS_existing_sources.xls	Spreadsheet with public water supply information for existing sources
ReturnFlow.xls	Spreadsheet with return flow information
SourceMixing_with_additional_information.xls	Spreadsheet with source mixing information
GISSWQ.zip	Zipped Folder with GIS information used in the Surface Water Quality Work including ArcGIS map document to display this information.
TopNetModel	Folder with complete source code and executable for TOPNET model
<u>Input files needed to run the model</u>	
ModelInputFilesExisting.zip	Zipped Folder with complete set of input files needed to run existing conditions scenario
ModelInputFilesFBO.zip	Zipped Folder with complete set of input files needed to run full build out conditions scenario
ModelInputFilesHistoric.zip	Zipped Folder with complete set of input files needed to run historic conditions scenario

ModelFilesDescriptions	Folder with detailed description of the format of each model input and output file. The spreadsheet Model_files_summary.xls in this folder includes hyperlinks to each file and summarizes the purpose for each file